9-1-2013

The Role of YKL-40 in the Progression of Glioblastoma

Ralph Anthony Francescone
University of Massachusetts - Amherst, ralph.francescone@gmail.com

THE ROLE OF YKL-40 IN THE PROGRESSION OF GLIOBLASTOMA

A Dissertation Presented

by

RALPH A. FRANCESCONE III

Submitted to the Graduate School of the
University of Massachusetts Amherst in partial fulfillment
of the requirements for the degree of

DOCTOR OF PHILOSOPHY

September 2013

Molecular and Cellular Biology Program

The Role of YKL-40 in the Progression of Glioblastoma

A Dissertation Presented

by

RALPH A. FRANCESCONE III

Approved as to style and content by:

_____
Rong Shao, Chair

_____
Sallie Smith Schneider, Member

_____
Kathleen Arcaro, Member

_____
Neil Forbes, Member

_____
Barbara Osborne, director
Molecular and Cellular Biology Program

DEDICATION

To my parents: Ralph and Cyndy
Without your loving support and care, I would not be the person I am today! You are the best!

To my amazing brother: David
Your drive and intelligence have always motivated me to strive to work hard and try my best.
And the late night talks and video games always reminded me what is important in life.

To my wonderful Yady:
For always accepting me for who I am and loving me unconditionally.

To all my friends and family:
You all have been a part of my life in some way and I thank you so much!

To my lost loved ones:
You are the reason I will fight every day to cure cancer

ACKNOWLEDGMENTS

Special thanks to:

My advisor
Dr. Rong Shao
I appreciate all your hard work and willingness to teach a young scientist like me. I cannot thank you enough and I think we made a great team!

Thanks to the Shao Lab former and current members!
You always made lab such a fun experience and work never really felt like work.

Thanks to my dissertation committee
All your support and suggestions helped shape me as a researcher and a person. Thank you for everything!

MCB Program and Students
You guys were my mental health holiday! The community was a major reason I came to UMASS in the first place, and I had a blast with all of you.

My Friends
You were my escape from the daily grind. I can't thank you enough for the years of friendship that have stood the test of time!

My family
My foundation. Thanks for always being there for me, whether that was driving me to a fall league baseball game at 7 am, dressing me up for the prom, or defending me in the schoolyard. You guys are the best!

Yady
I am so blessed to have met you! We have had a great beginning, and I hope our journey together lasts forever!

My New Family
The Puerto Rican Crew has become my new family and accepted me with open arms! I look forward to many more visits, delicious food, and hockey games together.

ABSTRACT

THE ROLE OF YKL-40 IN THE PROGRESSION OF GLIOBLASTOMA
September 2013

RALPH A. FRANCESCONE, B.S., MERRIMACK COLLEGE

Ph.D., UNIVERSITY OF MASSACHUSETTS AMHERST

Directed by: Professor Rong Shao

Glioblastoma Multiforme (GBM) is the most common brain cancer and one of the most fatal forms of cancer overall. The average survival time is 10-14 months, and less than 10% of patients survive more than 5 years after diagnosis. It is characterized by extreme vasculature, chemo/radioresistance, and invasiveness into the normal brain. The current standard of care, which includes surgical removal of tumor, radiation, and the chemotherapeutic agent temozolomide, initially stunt tumor growth. Nevertheless, the tumor invariably rebounds and the patient succumbs to the disease. Therefore, there is an urgent need to develop new therapies for this devastating disease.

YKL-40 is one of the most over-expressed proteins by GBM cells, and is elevated in the serum of patients with GBM. YKL-40 is implicated in a host of inflammatory diseases and has been shown to play a major role in the maturation of some cells of the immune system, especially macrophages. Thus, it has been suggested that YKL-40 may act as a prognostic biomarker for cancer and inflammatory disease. However, little is known about the role of YKL-40 in relation to cancer development and progression, and more work needs to be done to validate it as a biomarker or as a therapeutic target.

It was the goal of the work described herein to uncover some of the key molecular mechanisms of GBM development and progression in the hopes of offering new therapeutic targets. Using a wide variety of *in vitro* and *in vivo* techniques, the role of a secreted glycoprotein YKL-40 in

GBM was probed. It was demonstrated that YKL-40 enhanced angiogenesis, radioresistance, and progression of GBM cells. Moreover, inhibition of YKL-40 in mouse models markedly arrested tumor growth and vascularization, lending support to the idea of YKL-40 as a therapeutic target. Finally, YKL-40 drove GBM cells into a mesenchymal phenotype, where the tumor cells act as mural-like cells, supporting tumor vasculature networks. Hopefully, the results from these studies will offer the rationale to develop drugs against YKL-40 and potentially extend the lives of patients with this terrible disease.

TABLE OF CONTENTS

Page

LIST OF FIGURES

CHAPTER 1

INTRODUCTION: GLIOBLASTOMA AND YKL-40

1.1 YKL-40

YKL-40 is a secreted glycoprotein that was first discovered in the medium of a human osteosarcoma cell line, MG-63 (Johansen, Williamson, et al. 1992). It is a 40 kDa protein named after its first three amino acids; tyrosine, lysine, and leucine. YKL-40 has a 53% sequence homology to a member of the family 18 chitinases, which bind to and catabolize chitin (Fusetti, et al. 2003). While YKL-40 can directly bind to chitin, it lacks the glycosyl hydrolase activity to break down chitin (Fusetti, et al. 2003, Renkema, et al. 1998). Therefore, YKL-40 is deemed a "chitinase-like protein" and its gene product is known as chitinase 3 like 1 protein (CHI3L1).

With respect to normal physiology, YKL-40 is expressed by activated neutrophils, macrophages, vascular smooth muscle cells, and chondrocytes (Junker, Johansen and Andersen, et al. 2005, Johansen, Baslund, et al. 1999, Volck, Ostergaard, et al. 1999, Volck, Price, et al. 1998, Recklies, White and Ling 2002, Shackelton, Mann and Millis 1995). Moreover, it is expressed at all stages of early human muscle and skeletal development (Johansen, Høyer, et al. 2007). YKL-40 has been shown to play a role in extracellular matrix remodeling, macrophage induced inflammation, and T-cell function (Junker, Johansen and Andersen, et al. 2005, Johansen, Baslund, et al. 1999, Shackelton, Mann and Millis 1995, Lee, Hartl, et al. 2009, Rathcke, Johansen and Vestergaard 2006). It has been demonstrated that YKL-40 is more highly expressed in cells that are more metabolically active, and at sites of high cell turnover (mammary involution, for example) (Ringsholt, et al. 2007). Therefore, YKL-40 is considered a growth factor and this has been shown for fibroblasts, bone cells, and vascular smooth muscle

cells (Schultz and Johansen 2010, Recklies, White and Ling 2002, Shackelton, Mann and Millis 1995, Ringsholt, et al. 2007).

It has been demonstrated that YKL-40 is over-expressed in the serum of patients with a wide variety of inflammatory diseases, diabetes, and cardiovascular diseases (Matsuura, et al. 2011, Lee and Elias, Role of breast regression protein-39/YKL-40 in asthma and allergic responses 2010, Rathcke, Raymond, et al. 2010). Additionally, YKL-40 serum levels have been positively correlated with shorter survival and tumor aggressiveness in many types of cancer, including glioblastoma (Pelloski, Mahajan, et al. 2005, Cintin, Johansen, et al. 2002, Hogdall, et al. 2003, Johansen, Christensen, et al. 2003, Jensen, Johansen and Price 2003, Bergmann, et al. 2005). The actual function of YKL-40 in the progression of cancer is unknown. It is suggested that it can act as a survival factor/growth factor for the cancer cells. Also, due to the link between YKL-40 and inflammation, tumor associated macrophages that express high levels of YKL-40 have been implicated in the development of cancer. No known mechanisms have been elucidated to confirm these suggestions.

1.2 Glioblastoma Multiforme

Glioblastoma Multiforme (GBM), commonly referred to as glioblastoma, is the most lethal cancer, and the most common malignancy of the brain and central nervous system. It is classified as a World Health Organization (WHO) grade IV tumor that carries an average survival time of approximately 10-14 months (Van Meir, et al. 2010).

These tumors are extremely difficult to treat due to a wide variety of factors. First, they are often heterogeneous in nature, made up of neurons, oligodendrocytes (insulates neurons), and astrocytes (supporting glial cells). Thus, it is a complicated process to pinpoint one particular mechanism for tumorigenesis or therapy. Second, these tumors are characterized by

extreme vascularization, proliferation, radioresistance, and DNA repair (Van Meir, et al. 2010, Wen and Kesari 2008).

Because of the complex nature of these tumors, GBM is often classified into distinct subtypes in an attempt to guide research to develop targeted therapies. In general, there are four subtypes that have been determined through extensive genomic analysis (Verhaak, et al. 2010, Sottoriva, et al. 2013, Phillips, et al. 2006). They are listed in order of best prognosis; Neural, Pro-neural, Classical, and Mesenchymal. The neural and pro-neural subgroups most closely mirror normal brain cells. These cases of GBM often contain the differentiation markers of all three major brain cell types, which are neurons, oligodendrocytes, and astrocytes. They also often have the best response to therapy (Verhaak, et al. 2010, Sottoriva, et al. 2013, Phillips, et al. 2006). In contrast to the neural and pro-neural groups, classical and mesenchymal tumors have a much worse prognosis and are much less differentiated (Carro, et al. 2010, Verhaak, et al. 2010). Classical GBM tumors contain the most common mutations, such as overamplification of EGFR, and deregulation of the cell cycle through the Ink4a/ARF gene locus. The Mesenchymal subtype is the most aggressive and invasive form of GBM, and also carries a considerable inflammatory component. YKL-40 has emerged as a key marker for the mesenchymal phenotype, and is also correlated with the worst overall survival of GBM patients (Pelloski, Mahajan, et al. 2005, Nigro, et al. 2005, Verhaak, et al. 2010).

In the past, the standard of care for glioblastoma has been surgical resection, radiation therapy, and a frontline chemotherapeutic, such as a temozolomide (Van Meir, et al. 2010, Wen and Kesari 2008). Recent discoveries have demonstrated the heterogeneity of GBM tumors and the need for targeted therapies, such as anti-angiogenic agents. Additionally, a mono-therapeutic approach will not succeed because these tumors will overcome the treatment by overcompensating through another molecular mechanism. For example, there

have been multiple studies showing the tumors treated with a humanized monoclonal antibody against VEGF (bevacizumab or avastin) or small molecules against its receptor will initially inhibit angiogenesis and tumor volume (Keunen, et al. 2011, de Groot, et al. 2010, Pàez-Ribes, et al. 2009, di Tomaso, Snuderl, et al. 2011). Nevertheless, the tumor becomes more invasive and spreads further into the normal brain tissue. GBM cells seem to maintain this phenotype even after treatment ceases and continue to invade into the normal brain, detrimental to overall patient survival (Pàez-Ribes, et al. 2009, di Tomaso, Snuderl, et al. 2011). Therefore, new molecular targets specific to GBM need to be identified, as well as a multipronged treatment regimen that will not allow the tumors to overcome a single targeted therapy.

1.3 GBM and YKL-40: A potential therapeutic target

YKL-40 is one of the most over-expressed proteins in the serum of glioblastoma patients and in genome wide microarray data of GBM tumor tissue (Hormigo, et al. 2006, Nigro, et al. 2005). It has been associated with GBM tumor radioresistance and overall poor patient prognosis (Pelloski, Mahajan, et al. 2005). Additionally, a siRNA knockdown of the VEGF gene in the U87 GBM cell line up-regulated YKL-40 protein levels (Saidi, et al. 2008). Consequently, YKL-40 is under heavy consideration as a tumor biomarker for all cancers, especially for glioblastoma (Schultz and Johansen 2010). Despite these facts, almost nothing is known about the mechanisms associated with YKL-40 and glioblastoma tumor progression. For that reason, further study of YKL-40 at the molecular level is highly warranted.

1.4 Blood Vessel Architecture

Vasculature of the human body provides tissues with oxygen, nutrients and secreted protein messages, while also moving toxic waste products away from those cells (Hofman and Chen 2010). Vasculature contains three major entities: endothelial cells, basement membrane

glycoproteins, and pericytes (Kalluri 2003, Bergers and Benjamin 2003). First, vasculature consists of an inner sheet of endothelial cells that is folded upon itself to create a long tube like structure known as the vessel. Lining the outside of this vessel is a complex mixture of extracellular matrix components, such as laminin, heparan sulfate proteoglycans, and collagen (Kalluri 2003). This is known as the basement membrane of a blood vessel, and differs slightly depending on the function of the tissue. The last major component of vasculature is the pericyte, which is a type of cell that supports blood vessel stability and growth. These cells line the outside of the vessel, making contact with the endothelial cells and the basement membrane. The basic cellular organization of a vessel is illustrated in Figure 1.1.

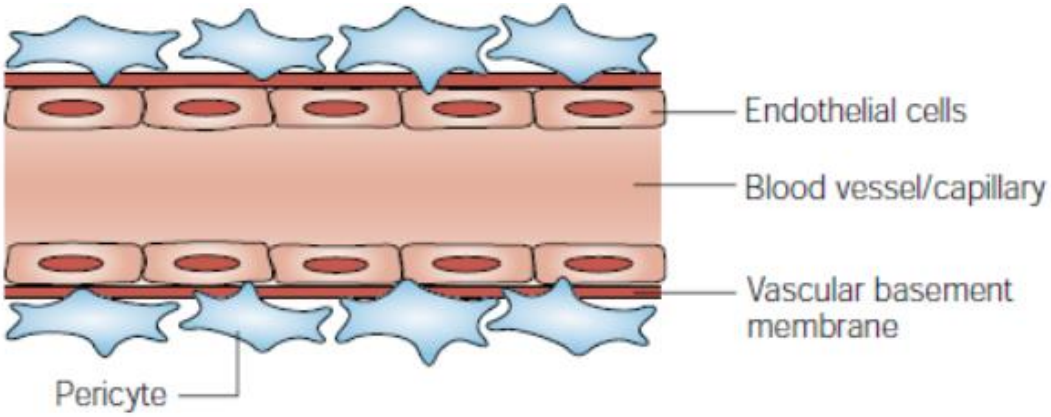

Figure 1.1. Basic Structure of a Vessel.

Vasculature comprises three major components: endothelial cells, basement membrane, and pericytes. [Reproduced with permission from (Kalluri 2003)]

1.5 The Vasculature of Glioblastoma

GBM is one of the most vascularized tumors and, as a result, there are many different types of vasculature that exist within brain tumors (Furnari, et al. 2007, Wen and Kesari 2008, Hardee and Zagzag 2012, Brem, Cotran and Folkman 1972). The five distinct types of vasculature that are present in GBM are as follows:

1.) Vascular co-option; 2.) Angiogenesis; 3.) Vasculogenesis; 4.) Vasculogenic Mimicry 5.) Tumor Derived Endothelial Vessels

Vascular co-option is the process where tumor cells migrate toward pre-existing vessels in the normal brain and grow around them to gain an initial blood supply (Holash, et al. 1999, Hardee and Zagzag 2012). Chronologically, this is the first step for GBM tumors to become vascularized. Next, once the tumor cells begin to proliferate, hypoxic and necrotic areas develop in the expanding tumor. GBM cells respond by stimulating angiogenesis, the manner by which cancerous cells recruit blood vessels to the tumor, and this becomes the predominant form of vasculature in the growing GBM tumor (Bergers and Benjamin 2003, Carmeliet and Jain 2011, Hardee and Zagzag 2012). At this stage, it is unclear if the other three forms of vasculature contribute significantly to the evolving GBM tumor. Nevertheless, new blood vessels can be created by bone marrow stem cells, the process termed vasculogenesis, or from the tumor cells themselves independent of endothelial cells, which is known as vasculogenic mimicry (Hardee and Zagzag 2012, El Hallani, et al. 2010, Hendrix, et al. 2003). Lastly, glioblastoma stem cells can differentiate into endothelial cells and create vessels as well (Ricci-Vitiani, et al. 2010, Wang, et al. 2010). The five major types of vasculature are illustrated in Figure 1.2. For the studies described in this thesis, I will focus mostly on angiogenesis and vasculogenic mimicry and these will be discussed in further detail in the following sections.

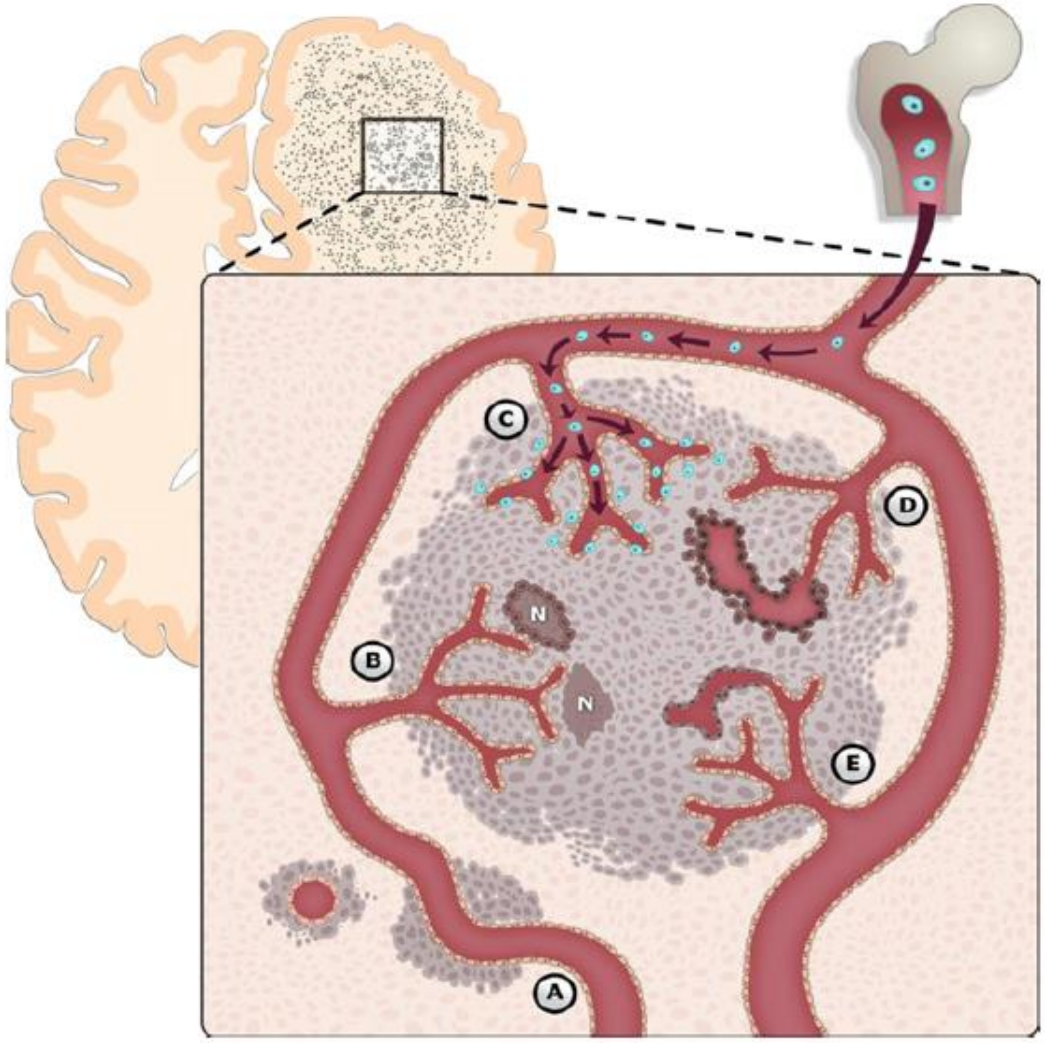

Figure 1.2 Types of Vasculature Present in Glioblastoma

A.) Vascular Co-option: The process where tumor cells hijack pre-existing brain vessels.
B.) Angiogenesis: Tumor cells stimulate pre-existing vessels to grow and expand within tumors
C.) Vasculogenesis: *De novo* formation of blood vessels from bone marrow derived progenitor cells
D.) Vasculogenic Mimicry: Tumor cells act as vascular cells and form their own functional vessels, independent of endothelial cells.
E.) GBM Stem Cell Endothelial Transdifferentiation: Glioma stem cells transdifferentiate into endothelial cells and form vessels.
[Reproduced with permission from (Hardee and Zagzag 2012)]

1.6 Tumor Vasculature: Angiogenesis

Angiogenesis is the process in which new blood vessels are generated. This is a normal event that occurs during embryonic development, growth during puberty, wound healing, and female reproductive organ maintenance (Bergers and Benjamin 2003). In general, endothelial vessels are quiescent and these cells live for hundreds of days before being replaced (Carmeliet, Mechanisms of angiogenesis and arteriogenesis 2000). However, in the occurrence of an injury that disrupts these stable blood vessels, angiogenesis will be initiated. Vascular endothelial growth factor A, VEGF-A, (will be referred to as VEGF in this writing) is one of the main angiogenic factors that can promote blood vessel sprouting and formation (Pettersson, et al. 2000). It binds to its main receptor, VEGFR-2, and sparks a signaling cascade that leads to proliferation and survival of endothelial cells. The basic mechanism of physiological angiogenesis is as follows (Kalluri 2003, Hofman and Chen 2010 , Bergers and Benjamin 2003, Carmeliet 2000, Pettersson, et al. 2000):

1) Vasodilation (blood vessels swell)

2) Pericytes become loose and disconnect from the endothelial cells

3) Endothelial cells loosely connect to one another

4) Extracellular matrix is degraded by MMPs (metalloproteinases)

5.) Endothelial cells proliferate due to VEGF, basic fibroblast growth factor, epidermal growth factor, or other angiogenic proteins

6.) Endothelial cells migrate towards angiogenic factors

7.) Blood vessels are formed and pericytes are recruited for vessel stability

Tumor angiogenesis is the process where host vasculature is recruited to the tumor and stimulates the sprouting and development of those vessels within the tumor. Tumor angiogenesis is essential for tumor growth, and appears to be the rate limiting step in tumor

development (Kalluri 2003, Bergers and Benjamin, Tumorigenesis and the Angiogenic Switch 2003). The process is very similar to physiological angiogenesis, but is much more dynamic and new vessels are always evolving due to the hypoxic nature of a highly proliferating tumor (Kalluri 2003, Hofman and Chen 2010 , Bergers and Benjamin 2003, Carmeliet 2000, Pettersson, et al. 2000). Hypoxia induces the secretion of large amounts of VEGF, other angiogenic factors, and MMPs which leads to the development of new blood vessels. This process is summarized in Figure 1.3.

Tumor vessels do differ from normal tissue vessels in a few key ways (Kalluri 2003, Hofman and Chen 2010 , Bergers and Benjamin 2003, Carmeliet 2000, Pettersson, et al. 2000). First, these vessels are often over-dilated and thus much leakier than the normal vessels. Second, tumor vessels are disorganized and do not have a well-structured morphology. Lastly, the endothelial cells of tumors multiply and migrate at a high rate, which is very different from the low turnover seen with normal endothelial cells.

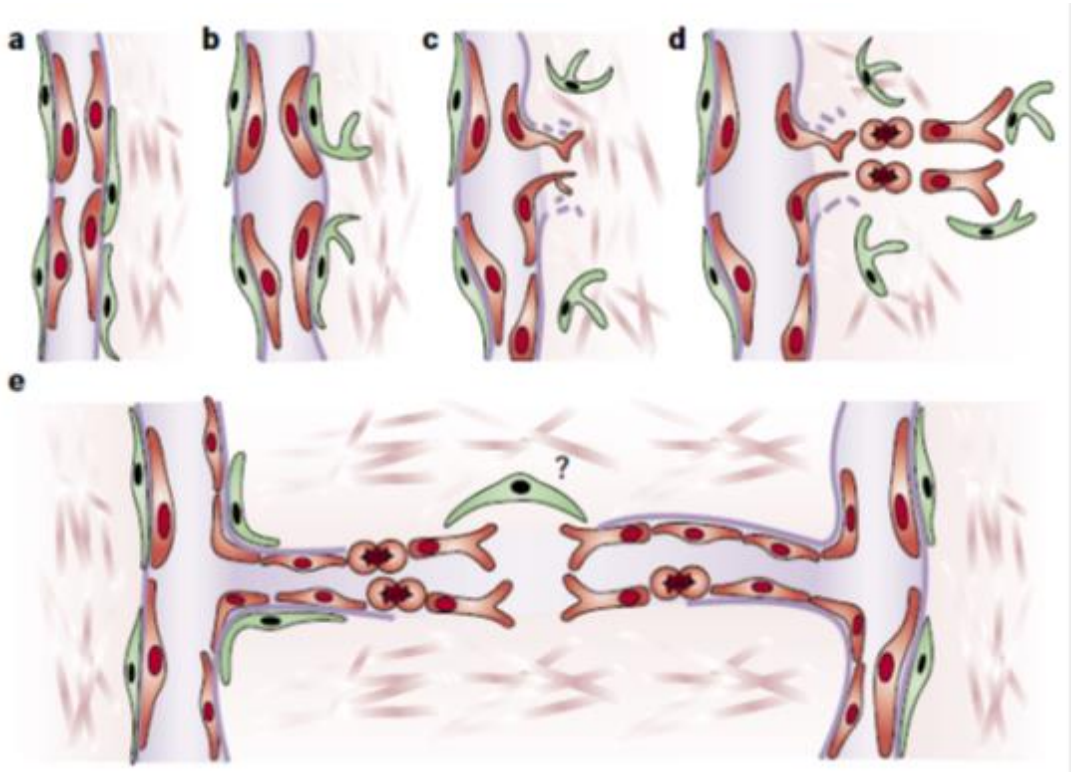

Figure 1.3 Tumor Angiogenesis

A) Quiescent Vessel. **B)** Pericytes detach and basement membrane is degraded. **C)** Endothelial cells move toward angiogenic signal. **D)** Endothelial cells begin to divide in the direction of the signal. **E)** Endothelial cells reach each other at both ends and bind to each other to create a vessel. Pericytes may help guide the endothelial cells as well. [Reproduced with permission from (Bergers and Benjamin 2003)]

1.7 Tumor Vasculature: Vasculogenic Mimicry

Another phenomenon that is abundant in cancer, especially in glioblastoma, is a process known as vasculogenic mimicry (VM). VM refers to the ability of tumor cells themselves to create vasculature that can carry blood and nutrients throughout a tumor, independent of endothelial cell angiogenesis (Maniotis, et al. 1999). VM was first discovered in 1999 in melanoma, and was later found in breast, prostate, lung, ovarian, as well as many other cancers (Maniotis, et al. 1999, Hendrix, et al. 2003). Last year, vasculogenic mimicry was also identified in glioblastoma (El Hallani, et al. 2010).

VM shares various characteristics with vasculogenesis, a primitive, immature form of angiogenesis (Maniotis, et al. 1999, Hendrix, et al. 2003). These vessels or "tumor cell lined channels" are characterized by a tube like network consisting of many smaller vessels that are perfused with red blood cells (Hendrix, et al. 2003). In angiogenesis, it is thought that there is a progenitor cell that can differentiate into a more mature vascular cell. In relation to cancer, this event is known as transdifferentiation, whereby a tumor cell differentiates into a type of cell that is not of the cancer cell's origin, in this case some type of vascular cell (Dong, et al. 2011, Ricci-Vitiani, et al. 2010, Wang, et al. 2010). It has been shown that these tumor derived channels express both tumor markers and some vascular (endothelial or pericyte) cell markers (Hendrix, et al. 2003, El Hallani, et al. 2010, Ricci-Vitiani, et al. 2010, Wang, et al. 2010). A synopsis of VM can be seen in Figure 1.4.

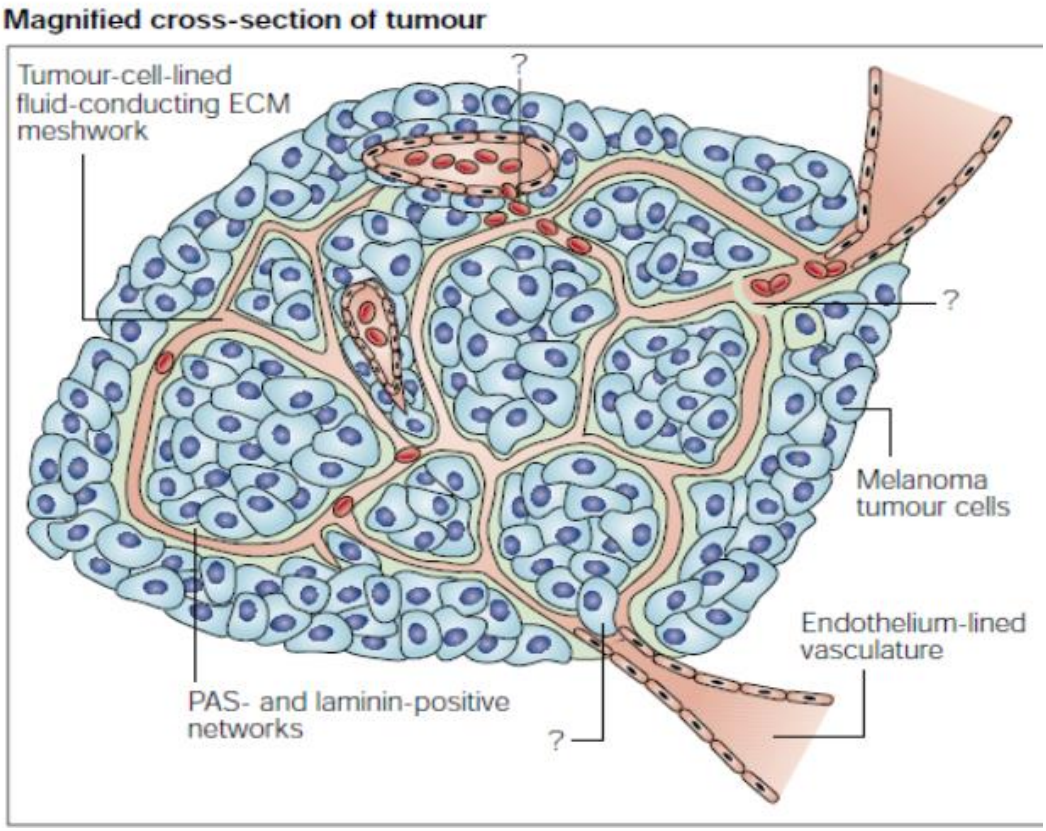

Figure 1.4 Vascular Networks in Melanoma.

This is a cross section of a tumor depicting the complex network of channels and vessels that persist throughout the tumor. The circular channels are endothelial derived vasculature, and the orange and green channels together comprise the tumor derived vasculature. Blue cells are tumor cells and red circles throughout the channels are red blood cells. [Reproduced with permission from (Hendrix, et al. 2003)]

1.8 Molecular Mechanisms Controlling Endothelial Cell Junctions

As previously mentioned, blood vessels consist of two major cell types; endothelial cells and pericytes. These cells must form stable connections that allow the transport of blood to the various tissues of the body. Simultaneously, these bonds between the cells also must be flexible in order for the body to respond to certain stresses, such as wound healing or inflammation [35-38]. Thus, the connections, or cell-cell junctions, must be tightly controlled by molecular cues to allow vessel growth and permeability.

There are two important kinds of contact involved with endothelial cells; endothelial to endothelial cell binding and endothelial to pericyte binding. The first is mediated by tight junctions and adherens junctions (Figure 1.5) [35]. These contacts allow endothelial cells to bind together and pass ions and signals laterally to one another. Additionally, the space between the contacts can allow other cell types to pass through, such as leukocytes during inflammation (Dejana 2004, Bazzoni and Dejana 2004, Dejana, Tournier-Lasserve and Weinstein 2009, Vestweber 2008).

Vascular endothelial cadherin, or VE-cadherin, is a vital adhesion molecule that is specific to endothelial cells and helps maintain and regulate these junctions (Dejana 2004, Bazzoni and Dejana 2004, Dejana, Tournier-Lasserve and Weinstein 2009, Vestweber 2008, Dejana, Orsenigo and Lampugnani 2008). Its expression is polarized, localizing to specific ends of the cells. When VE-cadherin is bound to another VE-cadherin molecule on an adjacent cell, endothelial cells tend to be quiescent and anchored in place. This information is transmitted intracellularly by a well-established molecular complex, the cadherin/catenin complex (Dejana 2004, Bazzoni and Dejana 2004, Dejana, Tournier-Lasserve and Weinstein 2009, Vestweber 2008, Dejana, Orsenigo and Lampugnani 2008). When homophilic binding occurs between VE-cadherin proteins on neighboring cells, it stabilizes the interaction between VE-cadherin and

beta-catenin. Beta-catenin, in turn, is bound to alpha-catenin. Alpha- catenin is tethered to actin filaments, thus giving the endothelial cells a physical link to one another and the cytoskeleton. During tumor angiogenesis, tumor cells secrete large amounts of VEGF. VEGF binds to its receptor, VEGFR-2, causing VE-cadherin to associate with VEGFR-2. This leads to a phosphorylation cascade, whereby VE-cadherin and beta-catenin become phosphorylated, resulting in the dissociation of the complex. At the physiological level, this leads to an increase in vascular permeability and angiogenesis (Dejana 2004, Bazzoni and Dejana 2004, Dejana, Tournier-Lasserve and Weinstein 2009, Vestweber 2008, Dejana, Orsenigo and Lampugnani 2008). A summary of this pathway can be seen in Figure 1.6.

In addition to endothelial-endothelial adhesion, endothelial to pericyte contact is critical to maintain vessel stability and permeability. The cell adhesion molecule neural cadherin (N-cadherin) is responsible for this kind of contact (Dejana 2004, Bazzoni and Dejana 2004). N-cadherin is expressed in neuronal cells, pericytes, cancer cells, and endothelial cells (Quadri 2012, Cavallaro and Dejana 2011). N-cadherin is no different than other cadherins in its ability to associate with beta-catenin, and when it is phosphorylated or cleaved, leads to dissociation of the complex. N-cadherin does not localize to the adherens junctions, as VE-cadherin does, but it is expressed throughout the membrane (Dejana, Orsenigo and Lampugnani 2008, Cavallaro and Dejana 2011). Therefore, pericytes can bind to accessible areas on the membrane of endothelial cells to support vessels and regulate permeability (Quadri 2012, Cavallaro and Dejana 2011).

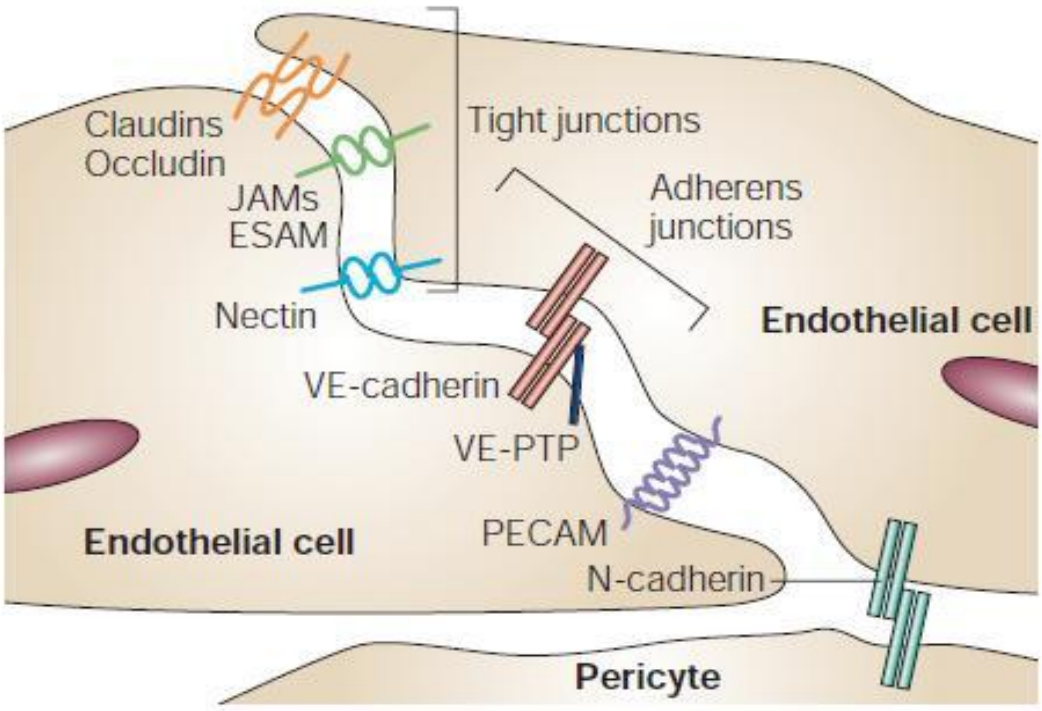

Figure 1.5 Endothelial Junction Organization.

Endothelial cells are held together by tight and adherens junctions, mediated by VE-cadherin among other proteins. Pericytes interact with and bind to endothelial cells through N-cadherin. [Reproduced with permission from (Dejana 2004)]

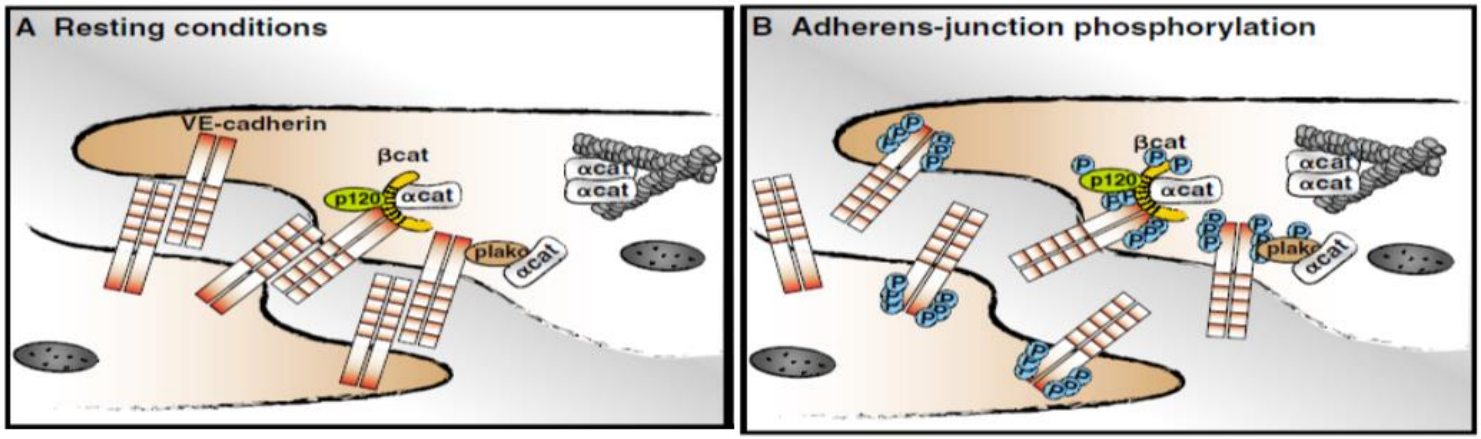

Figure 1.6 VE-cadherin and Beta-Catenin Complex.

A.) Under stable vessel conditions, endothelial cells are held together by VE-cadherin. VE-cadherin is bound to beta-catenin intracellularly, which is linked to the actin cytoskeleton through alpha-catenin. **B.)** In the presence of high amounts of VEGF, VE-cadherin and Beta-catenin are phosphorylated, leading to a disruption of the complex and decreased vessel stability. [Reproduced with permission from (Dejana, Orsenigo and Lampugnani 2008).]

1.9 Statement of Thesis

The overall goal of the dissertation work outlined here was to provide new insights on the development of vasculature in GBM, with a heavy emphasis on YKL-40 mediated mechanisms. Glioblastoma is an extremely complicated disease, with the worst prognosis of all the primary cancers. It is therefore critical that we search for novel avenues to treat this horrible affliction. YKL-40 is an intriguing target, due to the fact that it is overexpressed in many cancers, yet nothing is known about its function in relation to cancer progression. Thus, I wanted to explore its role in GBM development and provide evidence that YKL-40 is a novel target.

In chapter 2, I uncovered some key roles that YKL-40 plays in GBM. Because GBM is characterized by extreme vasculature and radioresistance, that was an excellent place to begin unveiling YKL-40 mediated mechanisms in GBM. YKL-40 was shown to stimulate angiogenesis *in vitro* and *in vivo*. Additionally, blockade of YKL-40 with a newly developed monoclonal anti-YKL-40 antibody dramatically inhibited angiogenesis and prolonged the life of mice in our models. Mechanistically, YKL-40 induced angiogenesis through the membrane proteins Syndecan-1 and integrin $\alpha V\beta 5$, which activated intracellular signaling through focal adhesion kinase and extracellular related kinase 1 and 2. This, in turn, up-regulated the angiogenic factor vascular endothelial growth factor (VEGF), increasing tumor angiogenesis. Moreover, YKL-40 conferred radioresistance to GBM cells through the AKT survival pathway and inhibition of YKL-40 sensitized these cells to radiation induced cell death. This was the first study that provided evidence of the feasibility and efficacy of YKL-40 as a therapeutic target (with the antibody) and displayed some of the mechanisms in which YKL-40 promotes GBM progression.

In chapter 3, the phenomenon known as vasculogenic mimicry (VM), an alternative form of tumor vascularization, was validated and characterized in glioblastoma. We demonstrated that VM was created by mural-like tumor cells that could form functional vessels independent of

endothelial cells. Additionally, we provided a phenotypic marker panel that defines these cells unambiguously as mural-like VM forming cells. Lastly, we established that this mechanism of VM formation is independent of VEGF. This is significant because current targeted therapies against GBM inhibit VEGF-mediated vasculature, but ultimately fail in the clinic. Thus, VM could be an attractive target to block blood flow and stunt tumor growth.

In chapter 4, using the information gathered from chapters 2 and 3, we further explored the idea of YKL-40 as a vasculature promoting factor, illustrating that YKL-40 can contribute to the development of mural-like cells lining angiogenic vessels. Not only do GBM tumors contain both angiogenesis and VM, they also contain "mosaic" vessels comprising host endothelial cells and tumor cells. Here, we describe a role for YKL-40 driving the mural-like phenotype of GBM cells. Functionally, these cells act similarly to host pericytes, supporting cells that line the outside of endothelial derived vessels. YKL-40 promotes cell to cell contacts in these mosaic vessels by controlling the well-established catenin/cadherin pathway. Tumors lacking YKL-40 were hyperpermeable, and developed much slower than tumors with high YKL-40 levels. Overall, YKL-40 plays a major role in vessel integrity and permeability, and tumors with high YKL-40 exhibit a better blood supply network and progress much faster. Ultimately, blocking YKL-40 could be an effective countermeasure against the primary forms of vasculature in GBM and prolong human life considerably. It is my hope the knowledge gained by the research outlined herein on the mechanism of action of YKL-40 will deepen our understanding of glioblastoma as well as provide a suitable target for therapeutics against this deadly disease.

CHAPTER 2

YKL-40 STIMULATES ANGIOGENESIS AND CONFERS RESISTANCE TO RADIATION IN GLIOBLASTOMA

The work presented in this chapter was done in collaboration with Steve Scully, Michael Faibish, Sherry L Taylor, Dennis Oh, Luis Moral, Wei Yan, and Brooke Bentley. Parts of this chapter are taken from the original research article: Francescone RA, Scully S, Faibish M, Taylor SL, Oh D, Moral L, Yan W, Bentley B, Shao R. Role of YKL-40 in the angiogenesis, radioresistance, and progression of glioblastoma. *J Biol Chem.* 2011. Apr 29;286(17):15332-15343.

2.1 Introduction

Tumor angiogenesis, a process of new vasculature formation, is of paramount importance in solid tumor development (Folkman and Klagsbrun 1987). The supply of new blood vessels in tumors not only supports autonomous tumor proliferation but also aids in removing accumulated waste from extensive metabolism that would normally induce necrosis. A number of angiogenic factors such as VEGF, bFGF, and a recently identified secreted glycoprotein YKL-40 (also known as human cartilage glycoprotein-39) have been known to play critical roles in the development of the tumor vasculature (Shao, et al. 2009, Yan, Bentley and Shao 2008, Dreyfuss, Johnson and Park 2009). Thus, they presumably function through synergistic action to give rise to a robust angiogenic phenotype.

YKL-40, a member of the chitinase-like glycoprotein family, was first identified from the medium of a human osteosarcoma cell line MG-63 (Johansen, Williamson, et al. 1992). Structural analysis has demonstrated that YKL-40 contains highly conserved chitin-binding domains; however it functionally lacks the ability to act as a chitinase because of a mutation of an essential glutamic acid residue to leucine in the chitinase-3-like catalytic domain (Renkema, et al. 1998, Fusetti, et al. 2003). While the physiological role of YKL-40 is not completely understood, it is conceivable that YKL-40 is linked with proliferation of connective tissues and activation of vascular endothelial cells (Recklies, White and Ling 2002, De Ceuninck, et al. 2001,

Malinda, et al. 1999). Growing clinical evidence has indicated that aberrant expression of YKL-40 is largely associated with the pathogenesis of a variety of human diseases. For example, YKL-40 levels are elevated in the blood serum of patients with chronic inflammatory diseases such as rheumatoid- and osteo-arthritis, hepatic fibrosis, and Asthma (Sharif, et al. 2006, Johansen, Christoffersen, et al. 2000, Volck, et al. 2001, Kirkpatrick, et al. 1997, Létuvé, et al. 2008), which is suggestive of its pathological function associated with extracellular matrix remodeling. Over the past decade, mounting clinical studies have demonstrated a correlation of elevated serum levels of YKL-40 with aggressive cancers and poorer survival in carcinomas of the breast, colon, ovary, and brain (Pelloski, Mahajan, et al. 2005, Cintin, Johansen, et al. 1999, Cintin, Johansen, et al. 2002, Hogdall, et al. 2003, Johansen, Christensen, et al. 2003, Jensen, Johansen and Price 2003, Bergmann, et al. 2005), suggesting that serum levels of YKL-40 serve as a diagnostic and prognostic biomarker. Recently, we found that YKL-40 is capable of stimulating angiogenesis of microvascular endothelial cells in breast cancer (Shao, et al. 2009). In addition, YKL-40-induced angiogenesis is dependent on the interaction between membrane receptors syndecan-1 (Syn-1) and integrin $\alpha v\beta 3$. These findings have shed light onto the mechanisms through which YKL-40 prompts breast cancer development.

Vascular endothelial growth factor (VEGF) is believed to be a primary promoter of angiogenesis (Yancopoulos, et al. 2000). VEGF binds to two tyrosine kinase membrane receptors, VEGFR-1 (known as Flt-1) and VEGFR-2 (also named as Flk-1). Flk-1 acts as a primary receptor mediating VEGF-induced angiogenesis (Millauer, et al. 1996, Neufeld, et al. 1999, Prewett, et al. 1999). Upon the binding of VEGF, Flk-1 is activated by autophosphorylation of specific tyrosine residues, followed by the binding and activation of Src or proteins containing a Src homology domain 2 (Guo, et al. 1995). Consequently, these mediators activate multiple downstream effectors, including FAK and MAPK (Abedi and Zachary 1997, Wheeler-Jones, et al.

1997). Clinic evidence shows that elevated serum levels of VEGF are related to decreased survival in patients with breast cancers and brain tumors (Ilhan, et al. 2009, Zhao, et al. 2004).

Glioblastoma is the most deadly and aggressive type of brain tumor with a median survival time of 12-15 months. It is characterized by highly vascularized tumors and resistance to radio/chemotherapy (Wen and Kesari 2008). YKL-40 is one of the most over-expressed proteins in glioblastoma (Nigro, et al. 2005, Tanwar, Gilbert and Holland 2002, Lal, et al. 1999)and its level correlates with tumor radioresistance and short survival (Pelloski, et al. 2005). Interestingly, elevated VEGF in glioblastoma is also associated with tumor angiogenesis (Bao, et al. 2006, Pàez-Ribes, et al. 2009, Ido, et al. 2008). However, clinical trials testing an anti-VEGF antibody Bevacizumab (Avastin) in recurrent glioblastoma show minimal overall benefit to survival (Verhoeff, et al. 2009, Kreisl, et al. 2009). Consistent with these results, there is strong evidence in murine models indicating that anti-VEGF therapy alone resulted in opposite outcomes in which angiogenic and malignant tumors unexpectedly developed (Pàez-Ribes, et al. 2009, Ebos, et al. 2009), suggesting that other angiogenic factors may contribute to this evasive mechanism. This hypothesis was partially supported by the evidence that blockade of VEGF via siRNA gene knockdown up-regulates YKL-40 transcript (Saidi, et al. 2008). However, it remains to be determined for the regulatory relationship between YKL-40 and VEGF, and substantial molecular mechanisms underlying tumor radioresistance and angiogenesis, the hallmark of aggressive glioblastomas. In this study, we found that YKL-40 up-regulated VEGF, and both acted as potent angiogenic factors to exert synergistic effects on angiogenesis in the establishment of tumor malignancy. Moreover, YKL-40 protected tumor cell death induced by γ-irradiation. Elucidation of YKL-40's molecular mechanisms may give rise to considerable promise to devising novel therapeutic strategies designed to target YKL-40 in concert with traditional anti-VEGF therapy.

2.2 Experimental Strategy

In this study, we found that YKL-40 up-regulated VEGF, and both acted as potent angiogenic factors to exert synergistic effects on angiogenesis in the establishment of tumor malignancy. Moreover, YKL-40 protected tumor cell death induced by γ-irradiation. Elucidation of YKL-40's molecular mechanisms may give rise to considerable promise to devising novel therapeutic strategies designed to target YKL-40 in concert with traditional anti-VEGF therapy.

2.3 Results

2.3.1 YKL-40 regulates VEGF and both synergistically promote angiogenesis

Two brain tumor cell lines U87 and SNB-75 were utilized to investigate a functional role of secreted angiogenic factors YKL-40 and VEGF in glioblastoma development. YKL-40 was highly detectable in both cell lines at the protein and mRNA levels, while other cell lines did not express YKL-40 or a low level of YKL-40. VEGF was expressed in those two brain tumor lines as well as osteoblastoma cells MG-63 and colon cancer cells HCT-116 (Figure 2.1A). To validate that these angiogenic factors are associated with tumor angiogenesis, each brain tumor cell line was injected subcutaneously into SCID/Beige mice and tumors were monitored weekly for 8 weeks. Immunohistochemical (IHC) analysis showed strong expression of YKL-40 and VEGF, and extensive positive staining of CD31, a marker of vascular endothelial cells, in xenografted tumors (Figure 2.1B), suggesting that both YKL-40 and VEGF may contribute to tumor development through a synergistic mechanism on the development of angiogenesis.

To dissect the relationship between YKL-40 and VEGF in tumor angiogenesis, we employed a YKL-40 gene knockdown approach in U87 cells by a stable retroviral siRNA infection. A noticeable gene blockade was obtained in the cells expressing YKL-40 siRNA1 (S1) (Figure 2.2A). Conversely, engineering YKL-40 siRNA2 (S2) into the cells did not result in a decrease of

YKL-40 as compared to the control cells containing an empty vector (Figure 2.2A). S1 cells displayed a corresponding reduction of VEGF, whereas S2 and control cell lines did not show altered VEGF (Figure 2.2A), suggestive of a regulatory role of YKL-40 in VEGF expression. In order to test the possibility that VEGF may also in turn regulate YKL-40 expression constituting a positive feedback loop for vigorous angiogenesis, parental U87 cells were treated with a neutralizing anti-VEGF antibody. Interestingly, the neutralization of VEGF activity with a short time (24 hr) failed to decrease expression of YKL-40 or VEGF itself relative to IgG-treated cells (Figure 2.2B); however, blockade of VEGF for a week noticeably induced YKL-40 expression (Figure 2.2C). The results indicate that VEGF does not have the ability to regulate YKL-40 directly, but blocking VEGF for a long term up-regulates YKL-40. To assess angiogenic activities of YKL-40 in vascular endothelial cells, human microvascular endothelial cells (HMVECs) were engaged to measure tube formation on Matrigel, the assay that recapitulates vascular angiogenic signature in vivo. U87 conditioned medium treated with an anti-VEGF antibody for one week moderately suppressed tube formation by approximately 35% of IgG-treated tubes (Figure 2.2C, compared with a strong inhibition below), suggestive of a compensatory role played by YKL-40 in angiogenesis after the inhibition of VEGF. We next sought to determine the effects of both YKL-40 and VEGF on angiogenesis. S1 medium drastically inhibited tubules by 58-68% relative to the medium from S2 or control cells (Figure 2.2D). In order to firmly establish the role of YKL-40 and VEGF in angiogenesis in vitro, neutralizing monoclonal antibodies against VEGF and YKL-40 (mAY) were added to the conditioned medium of the U87 control cells for 16 hr. In line with YKL-40 gene knockdown, anti-VEGF antibody suppressed tubules by 57% and mAY reduced tubules by 65% compared to IgG control (Figure 2.2D). Combined treatments with the anti-VEGF antibody and YKL-40 siRNA or mAY strikingly suppressed tube formation by 88% and 93% relative to controls, respectively. Collectively, these data suggest that YKL-40 may have

a role in the regulation of VEGF expression, both of which collaborate to enhance angiogenesis, and that blockade of VEGF induces YKL-40 expression.

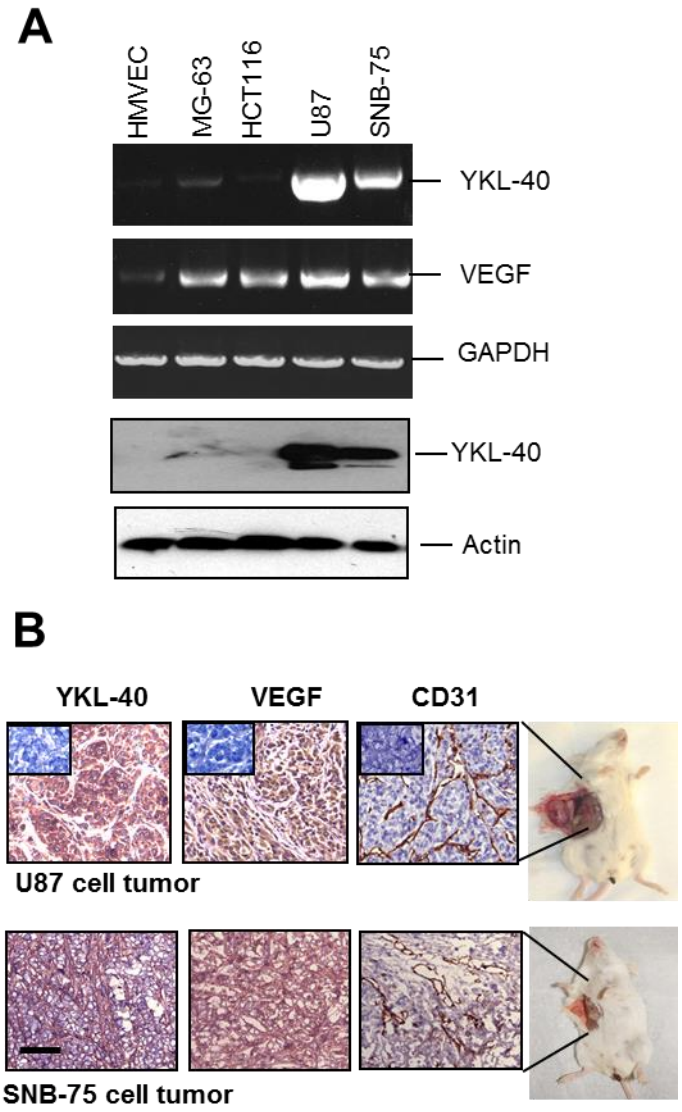

Figure 2.1 YKL-40 and VEGF are highly expressed in two glioblastoma cell lines and in both cell line-induced vascular tumors

A. YKL-40 mRNA and protein levels, and VEGF mRNA levels were analyzed using RT-PCR and Western blot in HMVEC, MG-63, HCT-116, U87 and SNB-75 cells. Actin and GAPDH were used as loading controls for the Western blot and RT-PCR, respectively. **B.** U87 and SNB-75 cells were injected subcutaneously into SCID/Beige mice. CD31 staining of mouse endothelial cells in both a U87 tumor and SNB-75 tumor demonstrated extensive vasculature throughout the tumors. YKL-40 and VEGF were also highly expressed in these tumor samples. Inserts indicate negative controls. Bar: 200 μm.

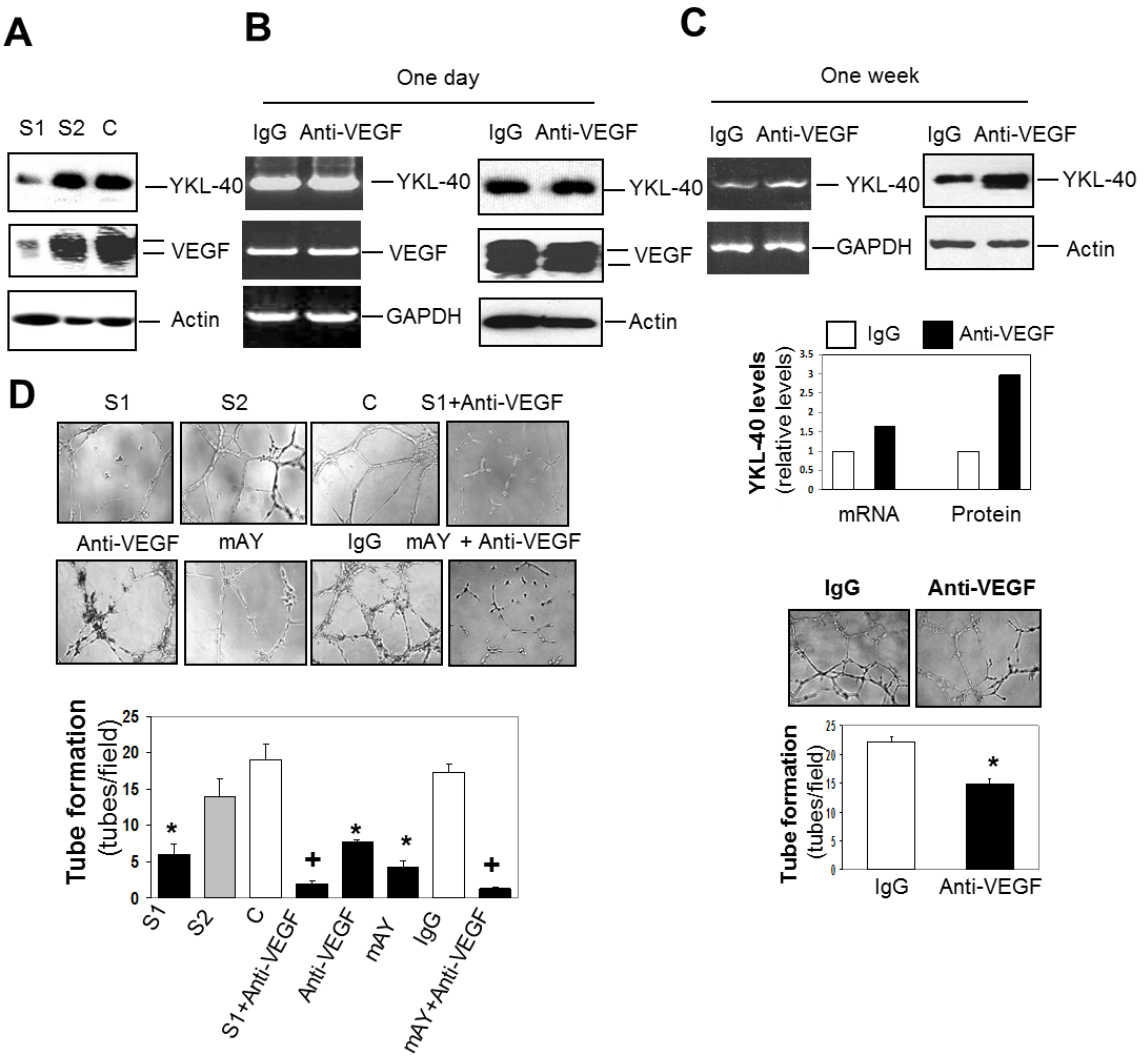

Figure 2.2 YKL-40 regulates VEGF expression and both enhance angiogenesis in vitro.

A. *YKL-40 regulates VEGF expression. YKL-40* gene was knocked down in U87 cells using two different siRNA constructs and YKL-40 and VEGF levels were detected using Western Blotting. Actin was used as loading controls. C, S1, and S2 represent vector control, *YKL-40* siRNA1, and *YKL-40* siRNA2, respectively. **B.** *VEGF does not regulate YKL-40 directly.* U87 cells were treated with an anti-VEGF neutralizing antibody for 24 hrs, and VEGF and YKL-40 levels were tested using RT-PCR and immunoblotting. **C.** *Chronic blockade VEGF induces YKL-40.* One week following treatment with an anti-VEGF antibody, conditioned medium was tested for YKL-40 expression and also for tube formation of HMVECs. Cell lysates were tested for mRNA levels of *YKL-40* using RT-PCR. *P<0.05 compared with IgG control. n=3. **D.** *YKL-40 and VEGF synergistically increase tube formation.* HMVECs were placed on Matrigel in the presence of conditioned media collected from the U87 cells lines (top row) and allowed to grow for 16 hrs. Additionally, HMVECs were also grown on Matrigel with media collected from control U87 cells pre-treated with anti-VEGF antibody, mAY, IgG (10 μg/ml) or combination (bottom row). Tubes were counted for each condition. *P< 0.05 compared with control or IgG group, and $^{+}$P<0.05 compared with single treatment. n= 3.

2.3.2 YKL-40 induces VEGF expression and angiogenesis through signaling activation of integrin αvβ5, Syn-1, FAK, and Erk

In an attempt to define the molecular mechanisms by which YKL-40 regulates VEGF, we focused on signaling activation in U87 cells. Although membrane receptors specific for YKL-40 binding are still unknown, we have demonstrated that YKL-40 triggers coupling of membrane receptor syndecan-1 (Syn-1) and integrin αvβ3 through binding to heparan sulfate of the ectodomains of Syn-1 in HMVECs (Shao, et al. 2009). U87 cells expressed both Syn-1 and integrin αvβ3 and αvβ5 (Figure 2.3). However, YKL-40 gene knockdown did not have an impact on the expression of either receptor. To determine if YKL-40 induces the coordination of these receptors, we utilized a co-immunoprecipitation approach followed by immunoblotting. We surprisingly found that both control and S2 cells demonstrated a strong association of Syn-1 with integrin αvβ5, whereas S1 cells were defective in their interaction (Figure 2.4A). In contrast, neither control nor YKL-40 siRNA cells exhibited the interaction between Syn-1 and integrin αvβ3 (Figure 2.4A). These data provide strong evidence revealing the specificity of this signaling pathway that is dependent on individual cell types. To further identify intracellular signaling pathways, we then measured FAK, Erk-1 and Erk-2. An active level of $pFAK^{397}$ was significantly reduced in S1 cells relative to control cells (Figure 2.4B). Accordingly, pErk-1 and pErk-2 were decreased in S1 cells.

To validate this signaling pathway regulated by YKL-40, we neutralized YKL-40 activity using mAY in the control cells. mAY disrupted the coupling between integrin αvβ5 and Syn-1 from as early as 10 min to 60 min and this inhibition slightly diminished at 6 hr (Figure 2.4C). Consistent with this inhibition, $pFAK^{397}$, pErk-1, and pErk-2 were decreased by mAY, in which $pFAK^{397}$ displayed a trend to recovery from 30 min to 6 hr, whereas pErk-1 and pErk-2 recovered at 6 hr. In order to determine if YKL-40 is able to rescue the signaling impaired in S1 cells, we exposed these cells to recombinant YKL-40 and found that $pFAK^{397}$ was notably increased from

30 to 60 min; then slightly reduced (Figure 2.4D). Like mAY blockade, a delayed response of pErk 1 and pErk 2 to YKL-40 stimulation was observed at 6 hr (Figure 2.4D), suggesting a downstream signaling pathway from FAK to Erk. To ensure that prolonged treatment of S1 cells with YKL-40 can restore VEGF production, these cells were exposed to recombinant YKL-40 for 24 hr. YKL-40 induced expression of pErk-1, pErk-2, and VEGF in a dose-dependent manner (Figure 2.4D).

Next, to determine if the "outside-in" signaling pathway initiated by YKL-40 mediates VEGF expression, we engaged a series of different inhibitors specific for individual signaling mediators which include a small molecule PD98059 targeting MEK, and neutralizing antibodies against YKL-40 (mAY), integrin $\alpha v\beta 3$ (LM609) and $\alpha v\beta 5$ (P1F6). Neutralization of integrin $\alpha v\beta 5$, MEK or YKL-40 resulted in a reduction of $pFAK^{397}$, pErk-1, pErk-2, and VEGF expression compared to either IgG or DMSO-treated controls (Figure 2.4E). Interestingly, LM609 also moderately inhibited VEGF expression, implicating that other factors may also utilize integrin $\alpha v\beta 3$ in the induction of VEGF. Taken together, these results have established an action model for YKL-40 in the regulation of VEGF, in which YKL-40 promotes the coordination of Syn-1 and integrin $\alpha v\beta 5$, and induces intracellular signaling FAK, Erk-1, and Erk-2, leading to VEGF expression.

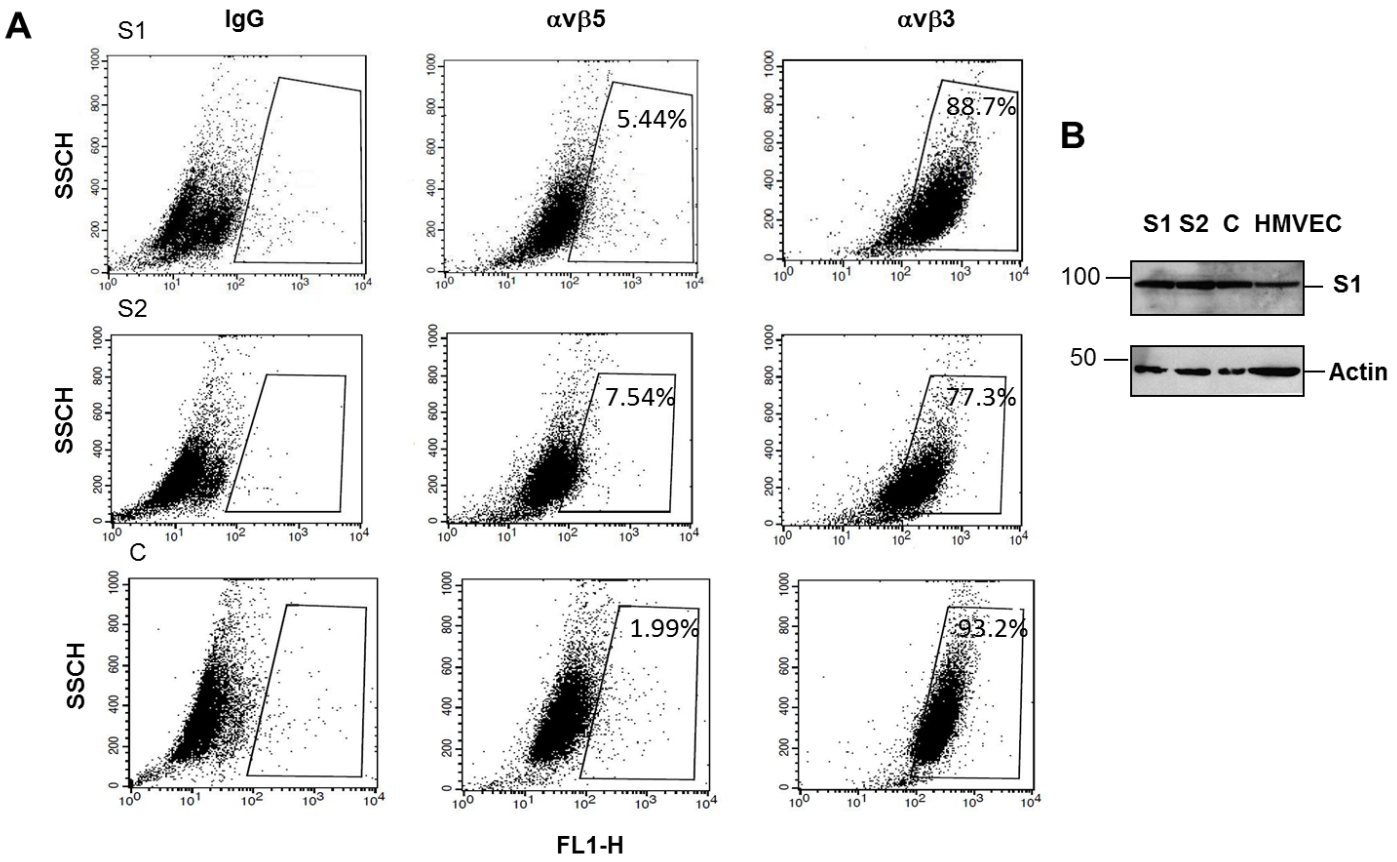

Figure 2.3 Integrin αvβ5, αvβ3, and Syn-1 are expressed in U87 cell lines.

A. U87 cells were blocked with BSA for 45 minutes and then incubated with either anti-integrin αvβ5 (P1F6) or αvβ3 (LM609) monoclonal antibodies for 45 minutes. Then the cells were incubated with anti-mouse FITC conjugated secondary antibodies and subjected to FACS analysis. **B.** Expression of Syn-1 was determined by immunoblotting in the U87 YKL-40 knockdown and control cells. HMVECs were used as a positive control.

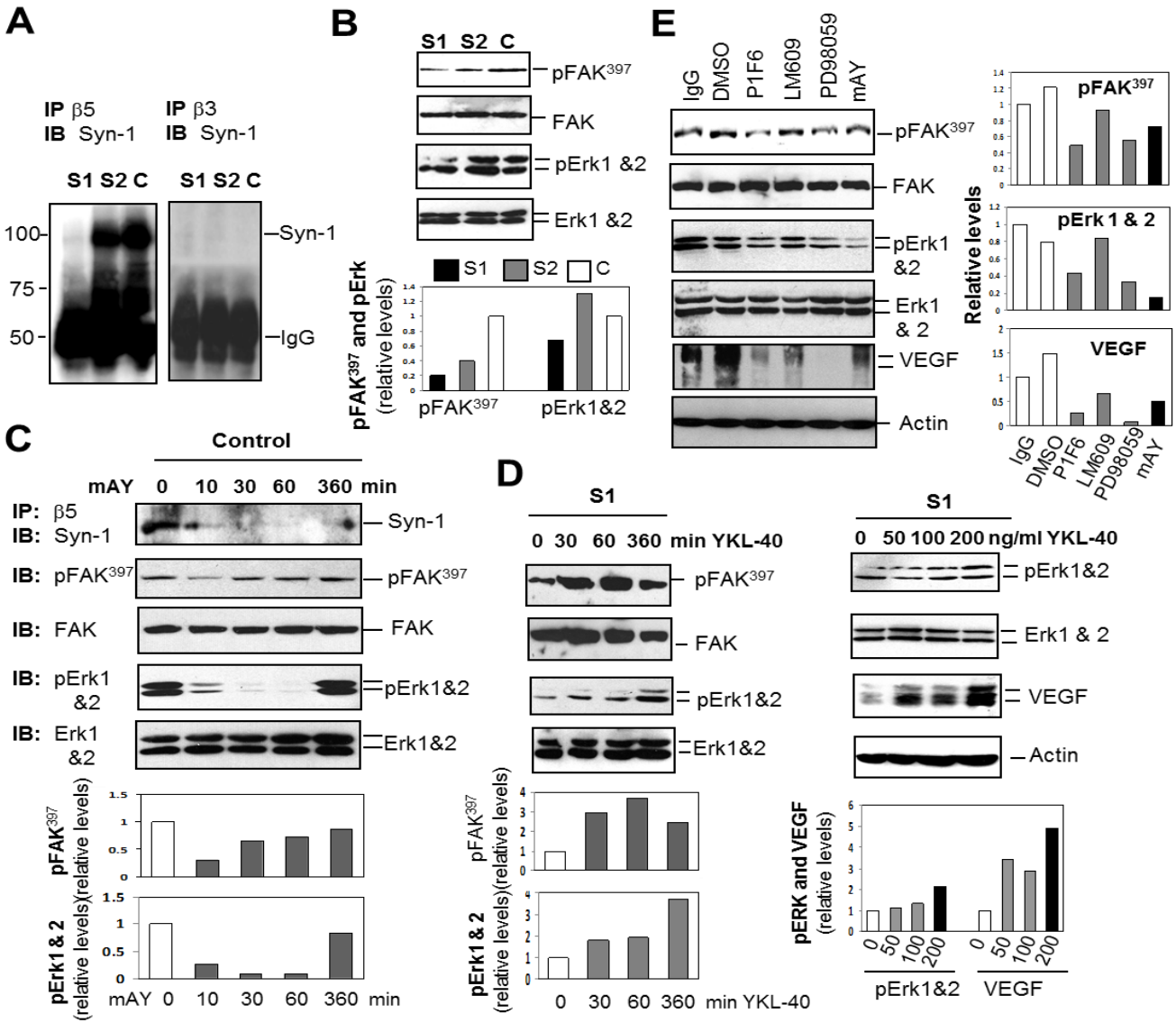
A
IP β5
IB Syn-1
IP β3
IB Syn-1
S1 S2 C
S1 S2 C
100
75
50
Syn-1
IgG
B
S1 S2 C
pFAK397
FAK
pErk1 &2
Erk1 &2
S1 S2 C
pFAK397 and pErk
(relative levels)
pFAK397
pErk1&2
C
Control
mAY 0 10 30 60 360 min
IP: β5
IB: Syn-1
IB: pFAK397
IB: FAK
IB: pErk1 &2
IB: Erk1 &2
Syn-1
pFAK397
FAK
pErk1&2
Erk1&2
pFAK397 (relative levels)
pErk1 & 2 (relative levels)
mAY 0 10 30 60 360 min
D
S1
0 30 60 360 min YKL-40
pFAK397
FAK
pErk1&2
Erk1&2
pFAK397 (relative levels)
pErk1 & 2 (relative levels)
0 30 60 360 min YKL-40
S1
0 50 100 200 ng/ml YKL-40
pErk1&2
Erk1 & 2
VEGF
Actin
pERK and VEGF
(relative levels)
0 50 100 200
0 50 100 200
pErk1&2
VEGF
E
IgG
DMSO
P1F6
LM609
PD98059
mAY
pFAK397
FAK
pErk1 &2
Erk1 & 2
VEGF
Actin
Relative levels
pFAK397
pErk 1 & 2
VEGF
IgG
DMSO
P1F6
LM609
PD98059
mAY

Figure 2.4 YKL-40 increases VEGF expression by signaling through integrin αvβ5, Syn-1, FAK, and Erk

A. *YKL-40 signals through Syn-1 and integrin αvβ5 but not integrin αvβ3.* Baseline Immunoprecipitation of integrin β5 and β3 was performed on the U87 cell lysates, followed by Western blotting against Syn-1. The bands of IgG were used as loading controls. **B.** *YKL-40 knockdown decreases expression of pFAK and pErk.* pFAK, total FAK, pErk-1, pErk-2, total Erk-1, and Erk-2 protein levels were tested in the cells. pFAK, pErk 1 and 2 were quantified by normalizing with total FAK, Erk 1 and 2, respectively. Control pFAK and pErk were set up as one unit. **C.** *Neutralization of YKL-40 by mAY inhibits YKL-40 signaling.* U87 control cells were treated with mAY (10 μg/ml) from 10-360 min and then some of cell lysates were immunoprecipated with an anti-integrin β5 antibody followed by immunoblotting against Syn-1. The rest of lysates were subjected to immunoblotting using anti-pFAK, total FAK, pErk, and total Erk antibodies. pFAK and pErk were quantified as described in B. **D.** *Addition of recombinant YKL-40 protein to S1 cells increases pFAK, pErk-1, pErk-2, and VEGF protein levels.* S1 cells were treated with YKL-40 (200 ng/ml) from 30-360 min. Cell lysates were analyzed for expression of pFAK, total FAK, pErk, and total Erk followed by quantification of pFAK and pErk as described in B. In addition, S1 cells were treated with 0, 50, 100, or 200 ng/mL of recombinant YKL-40 for 24 hrs. pErk, total Erk, and VEGF protein levels were tested by western blotting. pErk 1, pErk 2, and VEGF were normalized with total Erk 1, Erk 2, and actin, respectively. Each expression level without YKL-40 treatment was set up as one unit. **E.** *Inhibition of integrin αvβ5, Erk, or YKL-40 results in reduced pFAK, pErk-1, pEkr-2, and VEGF protein levels.* Control U87 cells were treated with PD98059 (MEK inhibitor, 10 μM) or a

2.3.3 YKL-40 protects γ-irradiation-induced cell death in an AKT-dependent manner

It was established that serum levels of YKL-40 were elevated in glioblastoma patients treated with radiation therapy (Tanwar, Gilbert and Holland 2002). Furthermore, these elevated concentrations positively correlated with cancer recurrence and poor survival, suggesting that serum levels of YKL-40 serve as a prognostic biomarker (Hormigo, et al. 2006). To test the hypothesis that γ-irradiation-induced YKL-40 protects tumor cell death, we monitored the levels of YKL-40 in U87 cells exposed to γ-irradiation. Treatment of control cells with γ-irradiation resulted in an increase of YKL-40 with the strongest induction at 10 Gy γ-irradiation (Figure 2.5A) but not 20 Gy γ-irradiation (data not shown). In contrast, γ-irradiation was unable to markedly induce YKL-40 expression in S1 cells. Although the control cells constantly expressed high levels of VEGF, regardless of the treatment with different doses of γ-irradiation, S1 cells did show a notable reduction in VEGF and exposure of the S1 cells with γ-irradiation failed to induce VEGF dramatically, underscoring an important role of YKL-40 in the regulation of VEGF during radiotherapy. Next, to test if YKL-40 acts as a survival factor in the radiation treatment, both control and S1 cells were challenged with 10 Gy γ-irradiation for 48 hrs. Control cells experienced minimal cell death at 0 Gy and 10 Gy γ-irradiation (Figure 2.5B+C). However, the S1 cells suffered 25% and 35% cell death at 0 and 10 Gy γ-irradiation, respectively (Figure 2.5B+C), both of which increased cell death approximately 2.5-3 fold greater than corresponding control cells; demonstrating a survival function played by YKL-40. Given that YKL-40 controls VEGF expression, we tested if VEGF mediates YKL-40-induced cell survival. A neutralizing anti-VEGF antibody was engaged, but it did not influence cell death in the control cells treated with γ-irradiation (Figure 2.5D and Figure 2.6A). These data indicate that YKL-40 protects γ-irradiation-induced cell death in a VEGF-independent manner.

To explore a molecular mechanism underlying the cell survival, we focused on expression of PI3K and AKT, the common signaling pathways mediating cell survival. Strikingly, 10 Gy γ-irradiation up-regulated pAKT by 50% in the control U87 cells, while the treatment dramatically reduced expression of pAKT in the S1 cells compared to the levels after treatment with or without γ-irradiation in the control cells (Figure 2.5E). Interestingly, while PI3K protein levels were not altered in the cells exposed to γ-irradiation, PI3K kinase activity was decreased by 30% compared with controls when treatment of both γ-irradiation and YKL-40 siRNA (Figure 2.5E), suggesting that YKL-40 protects cell death induced by γ-irradiation at least partially through regulation of the PI3K-AKT pathway. Consistent with the evidence that VEGF did not mediate YKL-40-induced cell survival, neither AKT nor PI3K was altered in the inhibition of VEGF (Figure 2.6B). To further assess if γ-irradiation-induced YKL-40 consequently influences endothelial cell angiogenesis, which recapitulates YKL-40-induced angiogenesis *via* a paracrine fashion *in vivo*, we examined effects of conditioned media from the irradiated U87 cells on tubules formed by HMVECs on Matrigel. Consistent with the earlier findings (Figure 2.2D), conditioned medium of S1 cells decreased 50% of control tubules (Figure 2.5F). Markedly, conditioned medium of U87 cells treated with γ-irradiation induced tubules by 60% relative to non-γ-irradiation-treated medium. But S1 cell medium treated with γ-irradiation suppressed these tubules to the non-treated basal levels. In sum, all the data demonstrate that YKL-40 induced by γ-irradiation prompts tumor cell survival through a PI3K-AKT pathway, and concomitantly stimulates endothelial cell angiogenesis.

To further confirm the survival activity played by YKL-40 in radioresistance, we treated U87 parental cells with mAY in exposure of 10 Gy irradiation for 96 hr. In line with the S1 and control U87 data above, neutralization of YKL-40 activity led to 60% cell death compared with 40% cell death in the absence or presence of IgG after 10 Gy γ-irradiation (2.7), strengthening

the findings that YKL-40 protects γ-irradiation-induced cell death and that mAY may serve as a powerful therapeutic tool to treat radioresistant cancer patients.

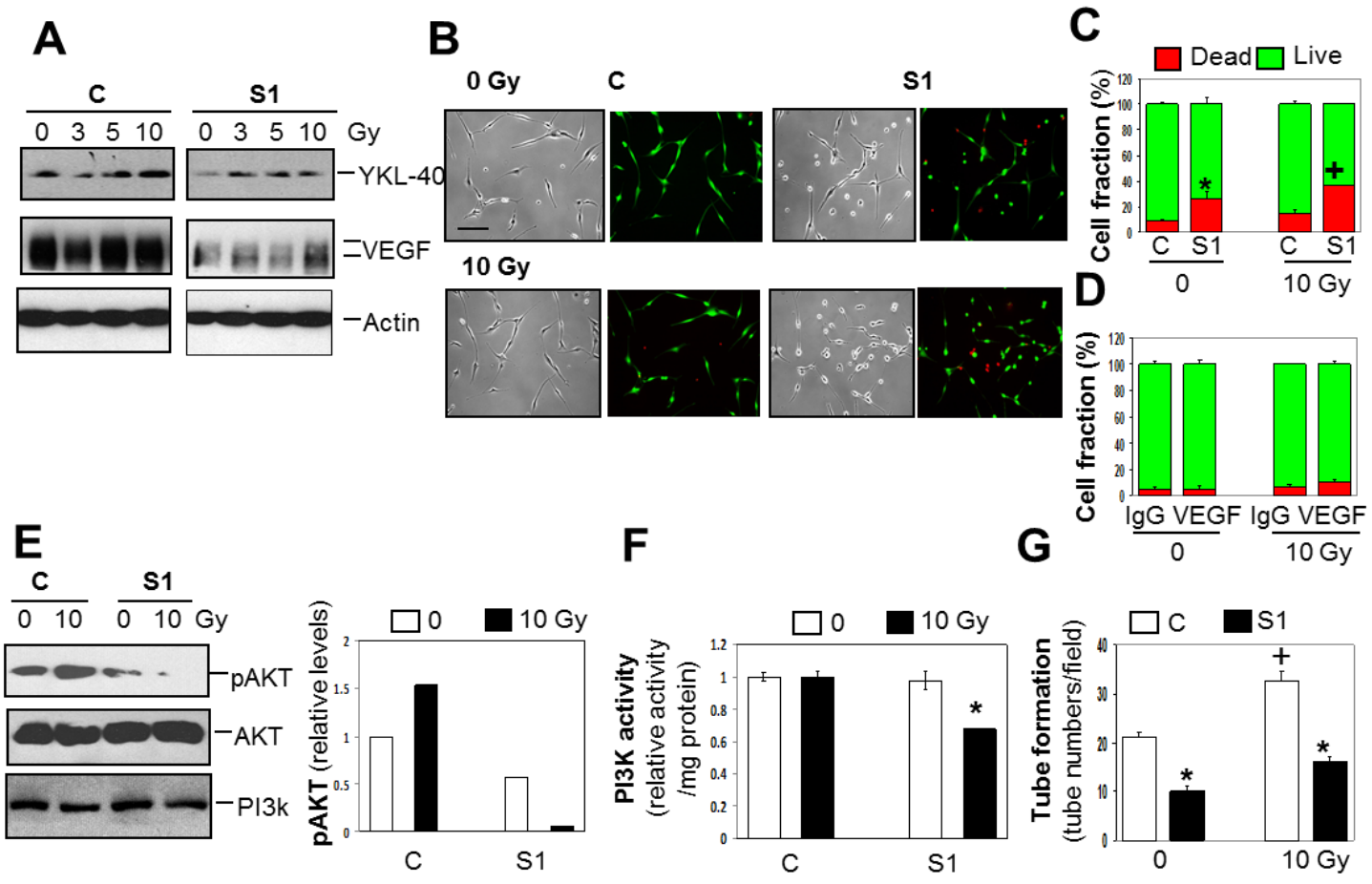
A
C
S1
0 3 5 10
0 3 5 10 Gy
YKL-40
VEGF
Actin
B
0 Gy
C
S1
10 Gy
C
Dead
Live
Cell fraction (%)
C S1 C S1
0
10 Gy
D
Cell fraction (%)
IgG VEGF IgG VEGF
0
10 Gy
E
C
S1
0 10 0 10 Gy
pAKT
AKT
PI3k
pAKT (relative levels)
0
10 Gy
C
S1
F
PI3K activity
(relative activity
/mg protein)
0
10 Gy
C
S1
G
Tube formation
(tube numbers/field)
C
S1
0
10 Gy

Figure 2.5 YKL-40 protects U87 control cells from irradiation-induced death. A. YKL-40, but not VEGF, is up-regulated with irradiation.

U87 control and S1 cells were exposed to 0, 3, 5, or 10 Gy irradiation and media samples were collected 48 hrs after irradiation. **A**. YKL-40 and VEGF protein levels were tested by western blotting. Actin was used as a loading control. **B & C.** *U87 S1 cells are more susceptible to irradiation.* Both U87 control and S1 cells were plated and exposed to 0 or 10 Gy irradiation. Forty-eight hrs later, the live/dead assay was employed to determine cell viability. The results were then quantified. $^{*,+}P<0.05$ compared to controls without irradiation and S1 without irradiation, respectively. n = 3. **D.** *VEGF does not mediate YKL-40-induced cell survival.* U87 control cells were plated and exposed to 0 or 10 Gy irradiation in the absence or presence of an anti-VEGF antibody. Forty-eight hrs later, the live/dead assay was employed to determine cell viability. The results were then quantified. n = 3. **E.** *YKL-40 regulates pAKT levels and PI3K activity in cells exposed to γ-irradiation.* Cell lysates were collected 48 hrs after 0 or 10 Gy irradiation. pAKT, total AKT, and PI3K were tested by western blotting. The levels of pAKT were normalized with total AKT and the control level of pAKT without irradiation treatment was set up as one unit. **F.** *Treatment of both irradiation and YKL-40 knockdown leads to suppression of PI3K activity.* U87 cells were exposed to irradiation for 48 hr and then lysed for analysis of PI3K activity. The activity was normalized with a control level without irradiation as one unit. $P<0.05$ compared with any group. n=3. **G.** *Endothelial cell tube formation is increased by irradiation of U87 cells, but decreased by YKL-40 siRNA.* HMVECs were plated onto Matrigel in the presence of conditioned media collected from U87 control and S1 cells exposed to 0 or 10 Gy irradiation. Tubes were allowed to form for 16 hrs. The number of tubes was counted for each condition. $^{*}P<0.05$ compared to controls and $^{+}P<0.05$ compared to 0 Gy control, n=3.

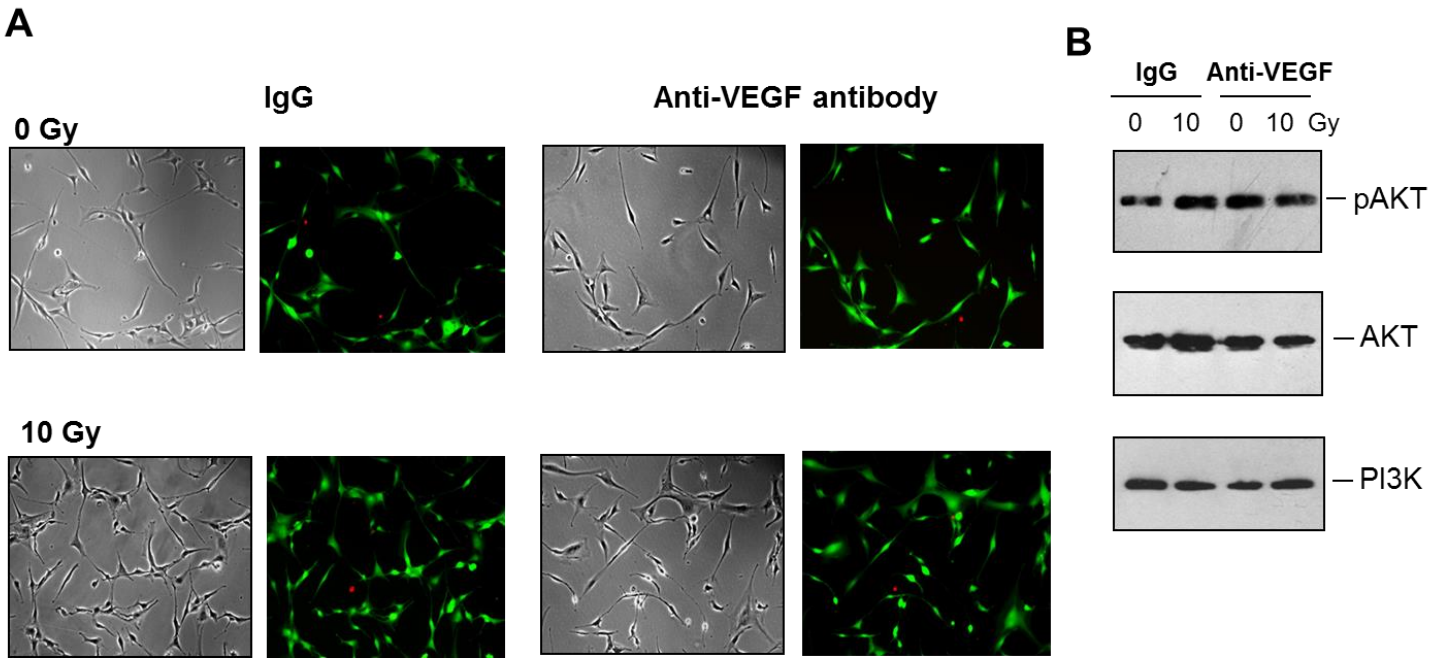

Figure 2.6 VEGF neutralization does not sensitize U87 parental cells to irradiation.

A. U87 cells were treated with either IgG or VEGF monoclonal antibody and subjected to 0 or 10 Gy of γ-irradiation. 48 hours later, the live dead assay was performed and these representative pictures were taken. **B**. Cell lysates were collected 48 hrs after 0 or 10 Gy irradiation in the absence or presence of an anti-VEGF antibody. pAKT, total AKT, and PI3K were tested by western blotting.

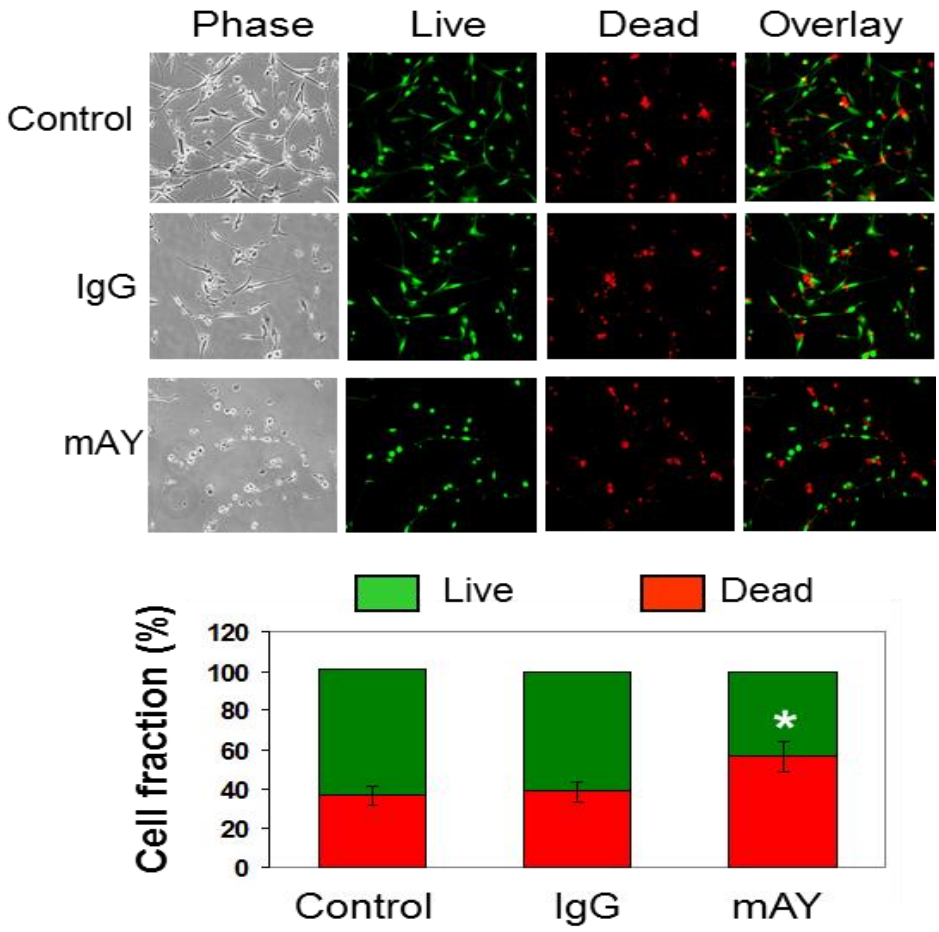

Figure **2.7 A monoclonal neutralizing antibody against YKL-40 increases sensitivity of U87 cells to irradiation.**

U87 Cells were treated with IgG, mAY, or neither of them (control) and then were exposed to 10 Gy irradiation. Ninety-six hrs later, the cells were subjected to the live/dead assay. Representative images were exhibited for each condition (top) and then the number of live and dead cells was quantified (bottom). *P<0.05 compared to control or IgG, n=3.

2.3.4 YKL-40 promotes tumor growth, angiogenesis and metastasis in vivo

While the *in vitro* evidence established thus far has demonstrated that YKL-40 mainly controls angiogenesis, we then sought to ascertain the vital role played by YKL-40 with respect to tumor angiogenesis and progression *in vivo*. We performed two distinct mouse models for the study. In the first model, we attempted to mimic a clinical trial for the treatment of GBM by administering mAY into U87 xenografted mice from week 3 when these mice developed palpable tumors. Mice were given either 5 mg/kg mAY or a monoclonal IgG as controls twice a week for two more weeks prior to sacrifice. mAY treatment significantly inhibited tumor formation as 50% of tumor volume was decreased compared with tumors developed from mice treated with IgG (Figure 2.8A). In order to corroborate the *in vitro* data, we stained CD31 expression for angiogenesis in tumor samples and IHC analysis revealed that mAY markedly reduced CD31 levels compared to IgG counterpart; as the staining intensity was 25% of the control group (2.7B+C). Furthermore, in the analysis of ectopic tumor development, the mAY reduced liver metastasis by 40%, whereas all IgG-treated control animals grew massive tumor cells in the liver (Figure 2.8B+C). Neither IgG nor mAY-treated mice were found to contain disseminating tumor cells in the lung (Figure 2.8B). These data strongly support the notion that mAY can be used as a therapeutic agent targeting angiogenesis and metastasis in advanced tumors.

In the second xenografted model, we injected U87 control and S1 cells into mice in order to determine how YKL-40 gene knockdown would affect tumor development *in vivo.* As demonstrated in Figure 2.8D, all the animals receiving U87 control cells began to form tumors from week 4 and continued to develop exponentially large tumors until the mice were sacrificed by week 7. Conversely, only one of the six mice injected with U87 S1 cells exhibited a two-week

delayed tumor (Figure 2.8D, grey diamonds). Surprisingly, the remainder of these animals failed to form tumors even in the observation period extended to 11 weeks. Subsequently, IHC analysis of angiogenesis in all control tumors indicated strong staining of CD31 and VEGF (Figure 2.8E); whereas one S1 tumor sample showed weak expression of CD31 and VEGF (igure 2.9). Furthermore, liver metastasis was identified in three of six control mice contrary to S1 mice in which one of six individual liver samples harbored tumor cells (Figure 2.8E). Taken together, these mouse models suggest that YKL-40 is associated with tumorigenesis, angiogenesis, and metastasis.

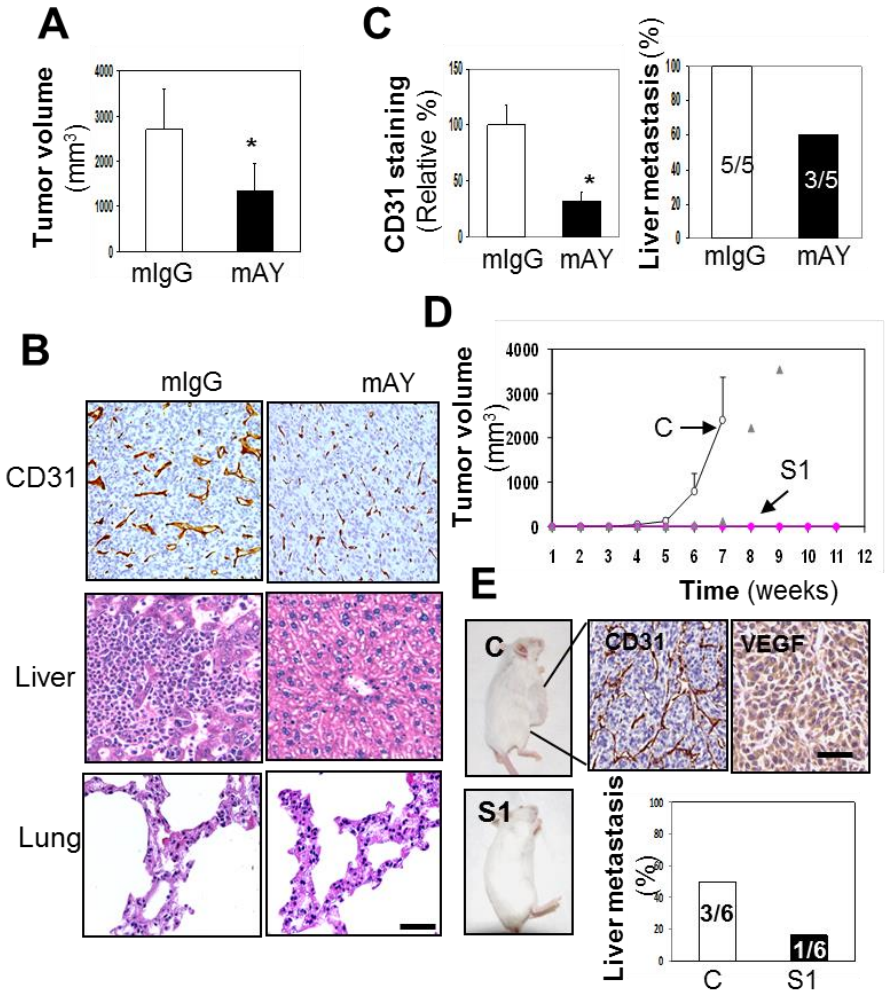

Figure 2.8 YKL-40 is associated with increased tumor development and angiogenesis in two xenografted mouse models.

A. *mAY reduces tumor volume.* U87 parental cells were subcutaneously injected into SCID/Beige mice and once tumors developed by week 3, the animals were treated with 5 mg/kg mAY or IgG by subcutaneous injection twice a week for 2 weeks. Mouse volume was shown at the end of the treatment. **B.** *Tumor angiogenesis and liver metastasis are reduced with mAY treatment.* IHC analysis of CD31 was performed on mouse tumor samples from the IgG and mAY groups. H & E staining was performed on liver tissues from each group as well. Bar: 200 μm. **C.** Quantification of Part B was shown. *P<0.05 compared to controls, n=5. **D.** *YKL-40 S1 knockdown inhibits tumor formation*. U87 control and S1 cells were subcutaneously injected in SCID/Beige mice and observed for tumor development over 11 weeks. All control mice formed tumors within 7 weeks; whereas only 1 of 6 S1 mice formed a tumor between week 7 and 9, and remainder of the mice did not form palpable tumors over 11 weeks. Open circles represent control mice, triangles represent the only one S1 mouse that formed a tumor, and pink diamonds indicate the other five S1 mice. **E.** *U87 control tumors express high levels of CD31 and VEGF.* IHC of CD31 and VEGF was performed on the tumor tissue of the U87 control mice. Liver metastasis was quantified as well for the U87 control and S1 cells (staining images of tumor cells were not shown). Bar: 100 μm.

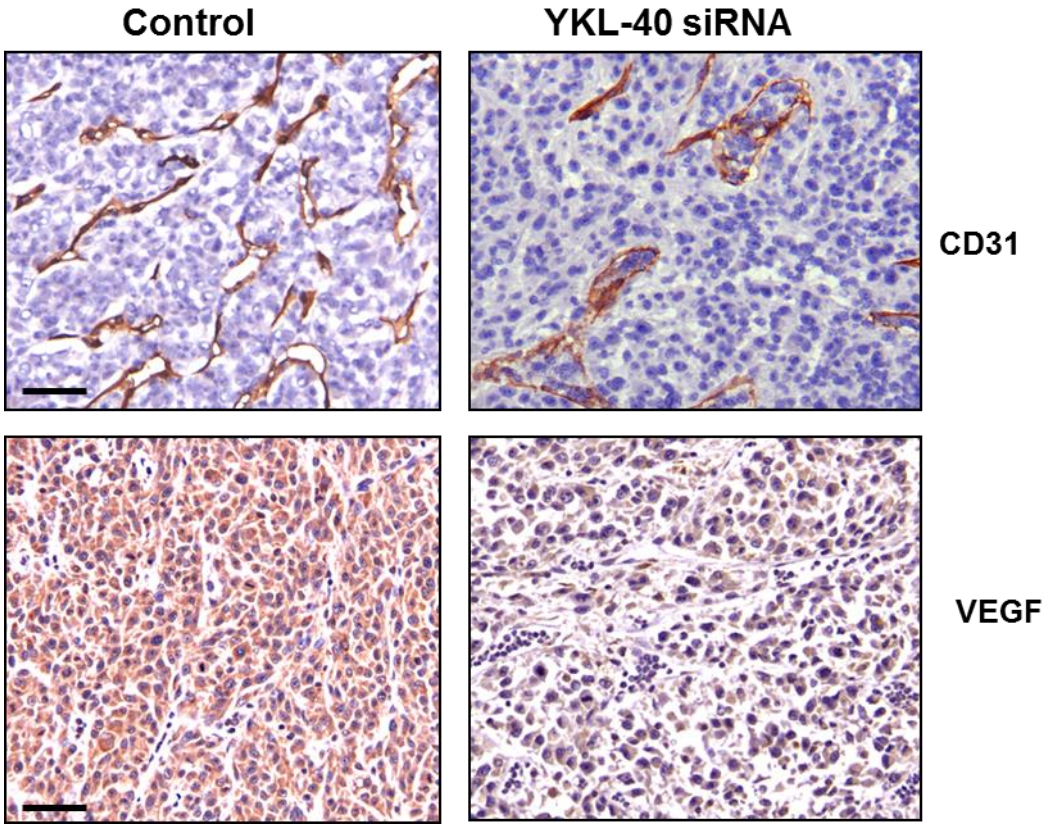

Figure **2.9 U87 YKL-40 siRNA xenograft tumor has reduced CD31 and VEGF expression.**

Immunohistochemical analysis of U87 control and S1 xenograft tumors was performed. CD31 and VEGF were stained in the tumor sections. Bars: 200 mm.

2.3.5 Elevated expression of YKL-40 is associated with increased VEGF and poorer survival of glioblastoma patients

We finally aimed to explore the relationship of YKL-40 with VEGF production, tumor angiogenesis, and tumor malignancy in patients with glioblastomas. Tumor samples from 12 patients diagnosed with glioblastomas were utilized for expression of YKL-40 and VEGF by immunoblotting. Given that variable levels of YKL-40 were observed in these specimens, we classified each patient into two categories: low YKL-40 expression (L) and high YKL-40 expression (H) (Figure 2.10A). An analysis of patient survival showed a median survival of 14.6 vs 5.9 months in these two groups, demonstrating that elevated YKL-40 positively correlated with poor patient survival (Figure 2.10B). YKL-40 levels also appeared to correlate with VEGF expression (Figure 2.10B). To validate the association of these angiogenic factor levels with tumor angiogenesis, we stained these tumor samples for YKL-40, VEGF, and CD34 levels by IHC. Agreed with the immunoblotting data, the higher the YKL-40 expression was, the higher the VEGF expression and the more extensive the vessels appeared to be (Figure 2.11A). YKL-40 levels in the immunoblotting analysis were in parallel with YKL-40 expression analyzed by IHC (Figure 2.11B), confirming the specificity of a polyclonal anti-YKL-40 antibody in recognizing YKL-40 in tumors and also establishing these two sensitive assays for a diagnostic purpose. Statistical analyses of YKL-40, VEGF, and CD34 expression displayed a trend toward positive correlations based on these available samples (Figure 2.11B). Collectively, these human data supported our hypothesis that YKL-40 plays a principal role in the regulation of VEGF, the strong vasculature phenotype, and the tumor malignancy.

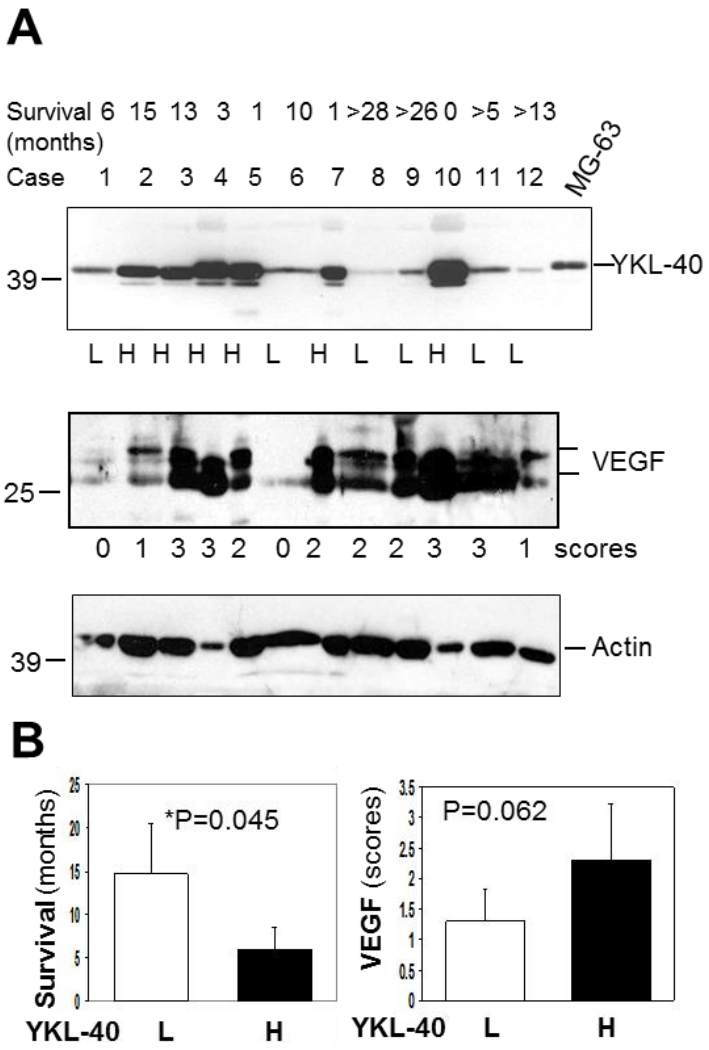

Figure 2.10 YKL-40 and VEGF are over-expressed in glioblastoma patients with poorer survival. A. YKL-40 and VEGF are expressed in glioblastoma patients.
Protein samples were isolated from 12 glioblastoma tumor specimens and subjected to Western blotting. Actin was used as a loading control. MG63 osteosarcoma conditioned medium was used as a positive control. Tumor samples were classified into two groups based on YKL-40 intensity: L = low expression and H= high expression. Additionally, VEGF was scored for band intensity as well: 0 = minimal level, 1 = low level, 2 = medium level, and 3 = high level of VEGF. Top row shows patient survival data. ">" indicates patients currently live longer than these months. **B.** *Elevated levels of YKL-40 are associated with decreased patient survival and possibly increased VEGF expression.* Left: comparison of YKL-40 expression groups (low and high levels, n=6/group) to average patient survival. Right: comparison of YKL-40 expression to VEGF levels.

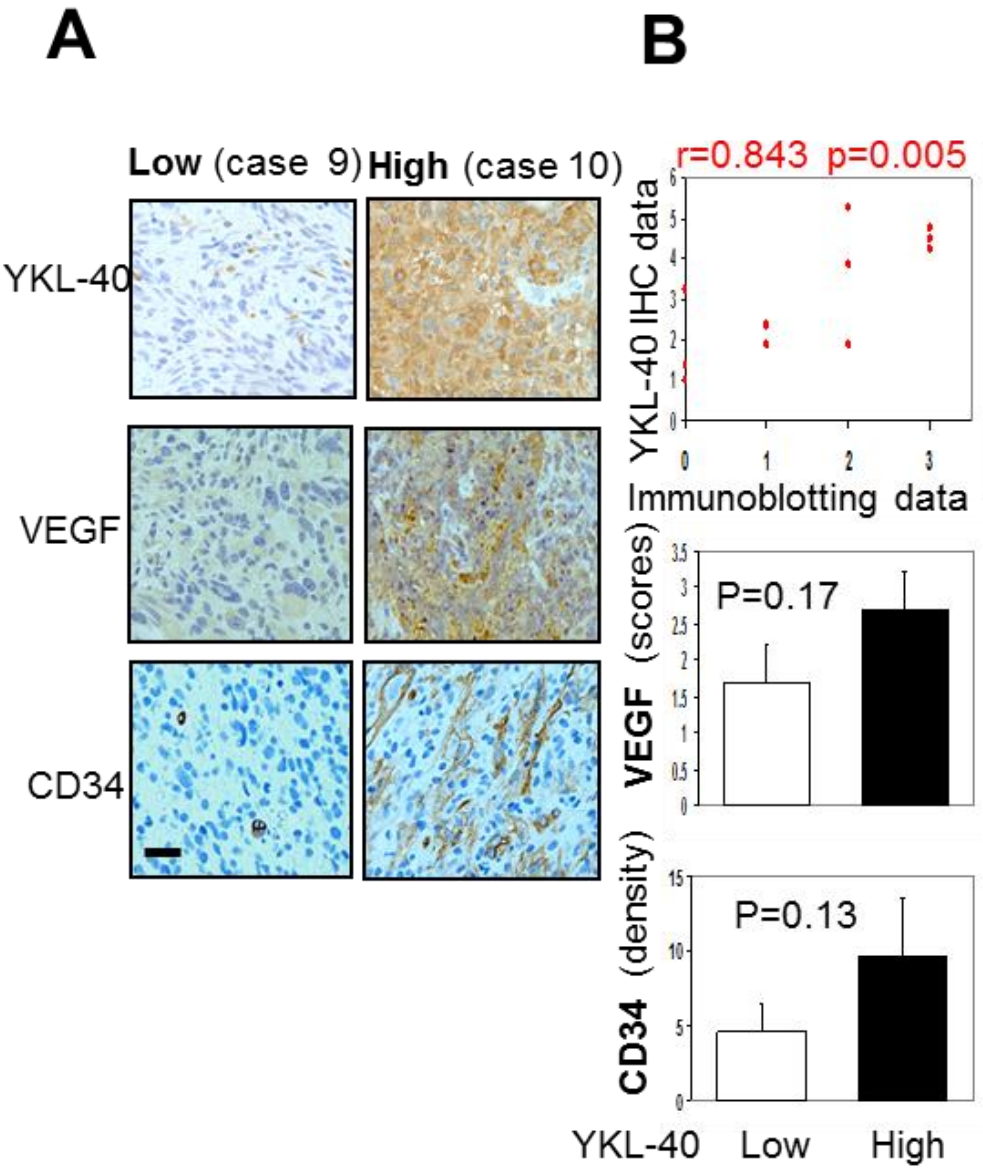

Figure 2.11 YKL-40 levels appear to correlate with VEGF and CD34 levels.

A. *Immunohistochemical analysis of low and high YKL-40 patient cases.* Representative tumor samples from low (L) or high (H) YKL-40 groups (Fig. 7) were stained for YKL-40, VEGF, and CD34. Bar: 100 μm. **B.** Top: YKL-40 staining of IHC was semi-quantified with density (0-3 points) and intensity (0-3 points) scores as described in the Methods, and YKL-40 bands of immunoblots (Fig. 7A) were analyzed based on intensity (0-3 points). The scores were then subjected to a linear regression analysis followed by significance analysis. Bottom: VEGF was semi-quantified based on staining density and intensity (0-6 points) and CD34 was scored by overall staining density.

2.4 Discussion

YKL-40 was recently identified as a potent angiogenic factor capable of inducing endothelial cell angiogenesis in breast cancer, independent of VEGF (Shao, et al. 2009). Our current study demonstrates for the first time the regulatory mechanisms of these two important angiogenic factors in the malignancy of glioblastoma that is characterized by strong vascular proliferation. We have identified that YKL-40 up-regulates VEGF and YKL-40-induced tumor angiogenesis is at least partially dependent on VEGF by means of a multidisciplinary approach including pharmacological and genetic methods, xenograft models *in vivo,* and human tumor samples. In addition, YKL-40 induced by γ-irradiation is the key component responsible for tumor radioresistance, independent of VEGF. mAY can block YKL-40-induced angiogenesis and metastasis. These findings have provided substantial evidence to elucidate the phenomena reported previously that serum and tissue levels of YKL-40 in glioblastomas are markedly elevated and these increased levels positively correlate with radioresistance and shorter survival (Nigro, et al. 2005, Hormigo, et al. 2006). Therefore, the current study not only provides mechanistic insights into the angiogenic properties of glioblastoma; but also establishes YKL-40 as a tumor diagnostic and prognostic biomarker in tumor radioresistance as well as a novel target for anti-angiogenic therapy.

With respect to the regulation of VEGF and angiogenesis, YKL-40 was found to induce the collaboration of Syn-1 with integrin $\alpha v\beta 5$ and then elicit intracellular signaling cascades through $pFAK^{391}$ to MAP kinase. This action model is highly consistent with our previous findings that the coupling of Syn-1 with integrin $\alpha v\beta 3$, in addition to $pFAK^{861}$ to MAPK, mediates YKL-40-induced angiogenic responses in vascular endothelial cells (Shao, et al. 2009). Interestingly, LM609, the anti-integrin $\alpha v\beta 3$ antibody, was also found to partially reduce VEGF expression in U87 cells, implying that other factors may also induce signal through integrin $\alpha v\beta 3$ to regulate

VEGF. This hypothesis was supported by multiple lines of *in vitro* and *in vivo* evidence previously (Hood, et al. 2003, Lorger, et al. 2009). For example, integrin $\alpha v\beta 3$ signaling was demonstrated to constitutively up-regulate VEGF expression in MDA-MB-435 breast cancer cells implanted into SCID mice (Lorger, et al. 2009). Indeed, we found that treatment of U87 cells with mAY alone failed to fully block VEGF expression (Figure 2.4C) or tube formation induced by both YKL-40 and VEGF (Figure 2.2D). Nevertheless, we demonstrate that YKL-40 plays a predominant role in the regulation of VEGF and angiogenesis. In addition, our data highlight the notion that the receptor cross-talk model is essential for the transduction of YKL-40 "outside-in" signaling into the cells, in which divergent signaling mediators participate in distinct functions (Figure 2.12).

We found that γ-irradiation induced YKL-40 expression which not only protected tumor cell death, but also elicited endothelial cell angiogenesis in a paracrine fashion. This YKL-40-induced tumor cell survival was independent of VEGF, a factor that mediates endothelial cell survival (Zhang, et al. 2010). However, this survival activity was through PI3K-AKT activation, a common pathway which mediates survival of multiple types of cells (Chetty, et al. 2010, Inoue and Meyer 2008). Consistent with our results, MAPK and AKT were reported to mediate YKL-40-induced survival in tumor cells and mitogenic signaling in connective tissue cells (Recklies, White and Ling 2002, Li, Kim and Waldman 2009). In addition, IHC analysis of glioblastomas indicated that elevated expression of YKL-40 correlated with expression levels of pAKT and pMAPK in poorer response of those patients to radiotherapy (Pelloski, Mahajan, et al. 2005, Pelloski, Lin, et al. 2006). Therefore, our new data in context with others offered substantial insight into radioresistance of glioblastomas that express increased levels of YKL-40 and demonstrate poor prognosis (Figure 2.12).

mAY has been characterized in neutralizing YKL-40's activities (Faibish et al. manuscript submitted). Here, mAY displays the capability of blocking tumor angiogenesis and growth *in vivo*

but failed to resemble the inhibitory extent of *YKL-40* gene knockdown that completely abolished the tumor development. The discrepancy may be attributed to different settings on YKL-40 inhibition, in which mAY targets palpable tumors contrary to the siRNA approach that genetically decreases *YKL-40* levels in the tumor cells. We also interestingly found that subcutaneous injection with U87 cells gave rise to liver metastasis but not lung metastasis, which is different from metastases of other tumor cells that disseminated to the lung and other organs (Minn, et al. 2005, Richert, et al. 2005, Yan and Shao 2006). The inconsistency may be due to the differences in administration methods of xenotransplants, invasiveness of tumor cells, and tumor microenvironment that predisposes them to residing in specific sites. Nonetheless, our data demonstrate that blockade of YKL-40 expression or activity suppresses tumor growth, angiogenesis, and metastasis. Moreover, the results also implicate the therapeutic utility of mAY in the future clinical treatment.

Both immunoblotting and IHC analyses on twelve cases of glioblastomas revealed that half of these samples express strong YKL-40, the high population of which is consistent with the data documented in literature (Pelloski, Mahajan, et al. 2005, Tanwar, Gilbert and Holland 2002). In addition, these elevated expression levels of YKL-40 positively correlate with poorer survival. The results demonstrate that these two tests can serve as diagnostic and/or prognostic tools for predicting the outcomes of the disease. A more detailed epidemiological analysis of YKL-40, VEGF, and CD34 with a large population will be essential for establishing that YKL-40 has utility as a target for anti-angiogenic intervention in patients.

Insufficient anti-angiogenic therapy in glioblastoma patients has recently received considerable attention because the benefits of these agents such as the anti-VEGF antibody bevacizumab appear to be transitory (Verhoeff, et al. 2009, Wick, et al. 2010). These effects may be due to drug resistance, tumor re-growth, and rapid vasculature recovery once the

therapy is terminated. In agreement with these clinical trials, xenografted tumor models provided convincing evidence demonstrating conflicting outcomes of anti-VEGF treatment, including extensive revascularization, increased invasiveness, and ectopic dissemination (Pàez-Ribes, et al. 2009, Casanovas, et al. 2005). In line with this evidence, a short-term therapy with sunitnib (VEGF receptor kinase inhibitor) and SU11248 (VEGF and PDGF receptor kinase inhibitor) accelerated local tumor invasion and multiple distant metastases after intravenous injection of tumor cells or removal of primary tumors (Ebos, et al. 2009). Immediate adaptation to the anti-angiogenic therapies is believed to be associated with the angiogenic switch by which tumors undergo robust revascularization and malignant transformation. Our data showing the up-regulation of YKL-40 following a long course of anti-VEGF treatment strongly suggests that YKL-40 may play an angiogenic role in the resistance of enduring anti-VEGF therapy. This assumption was also supported by a study of *VEGF* gene knockdown in U87 cells that expressed elevated YKL-40 compared to control cells (Saidi, et al. 2008). Therefore, an alternative neutralization of YKL-40 should be taken into account in the clinical setting for the possible elimination of this angiogenic rebound. A putative model has been illustrated demonstrating the enhanced tumor angiogenesis associated with YKL-40 (Figure 2.12). YKL-40 acts as an independent angiogenic factor and simultaneously up-regulates VEGF expression; thereby giving rise to a synergistic impact on vascularization. In addition, tumors can rebound upon anti-VEGF treatment alone because of up-regulation of YKL-40 by decreased VEGF. Although molecular mechanisms underlying the induction of YKL-40 are still elusive, the levels of VEGF may be rate-limiting for YKL-40 regulation, possibly constituting a negative feedback loop. Thus, targeting both YKL-40 and VEGF could be an efficacious regimen in concert with radiotherapy to eventually eradicate this deadly disease.

In summary, our findings demonstrate the angiogenic signature for YKL-40 in a vascular phenotype of glioblastoma, the hallmark of tumor invasiveness. YKL-40 can not only induce angiogenesis as an independent angiogenic factor, but also has the ability to stimulate VEGF expression, resulting in synergistic effects on angiogenesis. In addition, YKL-40 acts an important component to mediate angiogenic rebound induced by anti-VEGF treatment as well as tumor radioresistance. Therefore, combined therapies including anti-YKL-40 and other traditional anti-angiogenic agents together with chemo/radiation therapy warrant further clinical investigation.

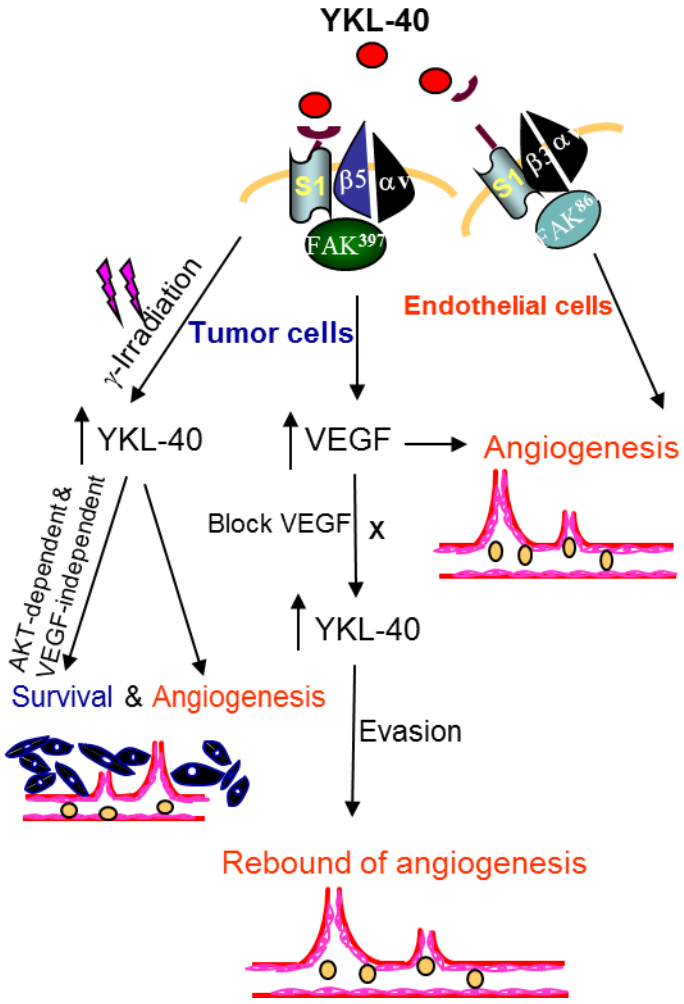

Figure 2.12 A hypothetical scheme elucidating YKL-40-induced angiogenesis of glioblastoma, partially dependent on VEGF.

YKL-40 up-regulates VEGF, both of which synergistically induce endothelial cell angiogenesis, and YKL-40 also has the ability to directly promote angiogenesis as described previously (Shao, et al. 2009). Constant inhibition of VEGF leads to up-regulation of YKL-40 that may stimulate rapid vascular recovery and tumor re-growth, which contributes to anti-VEGF resistance and evasive mechanisms for the tumor malignancy. In addition, γ-irradiation induces YKL-40 expression that increases tumor cell survival and also promotes endothelial cell angiogenesis, leading to resistance to radiation therapy.

2.5 Materials and Methods

2.5.1 Cell Culture

U87 cells (ATCC, Manassas, VA) and SNB-75 cells (NCI, Frederick, MD) were grown in DMEM supplemented with 10% FBS and penicillin/streptomycin. HMVECs were grown in EBM-2 (Lonza, Allendale, NJ) supplemented with 5 μg/ml hydrocortisone, 5 μg/ml insulin, 10 ng/ml hEGF, 10% FBS, and penicillin/streptomycin.

2.5.2 RT-PCR

Total RNA from cells was extracted with Tri-reagent (Molecular Research Inc, Cincinnati, OH). RNA concentration and purity were determined spectrophotometrically (A260/280). cDNAs with poly A tails were subsequently synthesized through a reverse transcriptional reaction in the presence of 15-oligo (dT) (Promega, Madison, WI). A fragment of VEGF and GAPDH DNA was synthesized by a polymerase chain reaction with sense primer 5'-CTTTCTGCTGTCTTGGGTGC-3' and antisense primer 5'- GTGCTGTAGGAAGCTCATCTCTCC-3', and sense primer 5'-

2.5.3 Immunoprecipitation and immunoblotting

Cell lysate samples were processed as described previously (Shao, et al. 2009). Briefly, cell lysates were then incubated with either an anti-integrin β5 or integrin β3 antibody (Chemicon International, Temecula, CA) at 4^0C overnight followed by incubation with protein A sepharose beads at 4^0C for 4 hr. The immunocomplex was extensively washed and the samples were subjected to running SDS-PAGE. PVDF membranes were incubated with one of a series of primary antibodies against YKL-40, VEGF (Sigma St. Louis, MO), Syn-1 (Santa Cruz Biotechnology,

Santa Cruz, CA), pFAK^{397} (Biosource, Camarillo, CA), FAK, pErk, Erk (Santa Cruz), pAKT and AKT (Cell Signaling, Beverly, MA), PI3K (Upstate Biotech, Lake Placid, NY), or actin (Sigma). Membranes were then incubated with goat anti-mouse or anti-rabbit secondary antibodies (Jackson Lab, Bar Harbor, Maine). Specific signals were detected by enhanced chemiluminescence (VWR, Rockford, IL).

2.5.4 YKL-40 Gene knockdown

DNA oligos (19 bp) specifically targeting N-terminal (siRNA 1) or C-terminal (siRNA 2) region of YKL-40, were selected and then templates (64 oligo nucleotides) containing these oligos were subcloned into a retroviral pSUPER-puro-vector (OligoEngine, Seattle, WA). 293T retroviral packaging cells were transfected with pSUPER siRNA constructs in the presence of pCL 10A1 vector using Fugene 6 (Roche, Indianapolis, IN). Forty-eight hours after transfection, the supernatant was harvested and filtered through 0.45-μm pore size filter and then the viral medium was used to infect U87 cells. Selection with 1 μg/ml of puromycin was started 48 hr after infection and the puromycin-resistant cell populations were used for subsequent studies.

2.5.5 Tube formation assays

Human microvascular endothelial cells (HMVECs) (1 x 10^4cells) were transferred onto 96-well Matrigel (BD Bioscience, San Jose, CA) in the presence of conditioned medium of tumor cells with or without neutralizing antibody treatments. After 16 hours of incubation, tube-forming structures were analyzed. Images were analyzed with an inverted microscope. Averages of tubules were calculated from three fields in each sample.

2.5.6 Irradiation of Cells and Live/Dead Assay

U87 cell lines were exposed to 0-10 Gy γ-irradiation from a radioactive Cesium source. To assay cell viability, the Live/Dead Assay (Invitrogen, Carlsbad, CA) was employed. Briefly, 48 or 96 hours after γ-irradiation, cells were incubated with the Live/Dead mixture (calcein AM and ethidium homodimer) to assess the number of live and dead cells. Fluorescent images of live (green) and dead (red) cells were analyzed. The percentages of live and dead cells were quantified.

2.5.7 PI3K kinase activity

Freshly isolated cell lysates were subjected to measuring kinase activity according to the manufacture's instruction of a kit (Millipore Inc. Bedford, MA).

2.5.8 Tumor xenografts in mice

All animal experiments were performed under the approval of Institutional Animal Care and Use Committee of the University of Massachusetts. SCID/Beige mice were subcutaneously injected with U87 (5-7.5 x 10^6) or SNB-75 (5 x 10^6) cells in 0.2 ml of PBS. At week 3 when mice developed palpable tumors, mice received either a mouse monoclonal anti-YKL-40 antibody (mAY, 5 mg/kg body weight) or mouse IgG (5 mg/kg) by subcutaneous injection twice a week for 2 weeks. Tumor growth from these injected cells was monitored weekly for 5 weeks before the animals were humanely sacrificed. Tumors were measured and tumor volume was calculated as follows: volume = length x width^2 x 0.52.

2.5.9 Immunohistochemistry

Paraffin-embedded or frozen tumor tissues were cut to 6 μm thickness and processed for immunohistochemical analysis. In brief, samples were incubated with 3% H_2O_2 for 30 min to block endogenous peroxidase activity, followed by incubation with blocking buffer containing 10% goat serum for 1 hr. The samples then were incubated at room temperature for 2 hr with monoclonal rat anti-CD31 (1: 50, BD Pharmingen, San Diego, CA) and mouse anti-CD34 (1:200) antibodies (Dako Inc, Carpentaria, CA), or rabbit polyclonal anti-VEGF (1:100, Santa Cruz) and anti-YKL-40 (1:400). Goat anti-rat, mouse or rabbit secondary antibodies (1: 100, Dako Inc) conjugated to HRP were added for one hr. Finally, DAB substrate (Dako Inc) was introduced for several minutes and after washing, methyl green was used for counterstaining.

2.5.10 Human glioblastoma samples and IHC data analysis

The study of brain tumor samples was approved by Baystate Medical Center Institutional Review Board. YKL-40 and VEGF staining was evaluated as combined scores of percent and intensity of positive staining cells as following 1) percent: no staining is 0 points; <10% of cells stained is 1 point; 11-50% of cells stained is 2 points; and >50% of cells stained is 3 points; 2) intensity: no staining is 0 points, weak staining is 1 point, moderate staining is 2 points and strong staining is 3 points. Thus, the valid range of scores was 0 to 6. CD34 density was quantified by an NIH image analysis program.

CHAPTER 3

MECHANISMS OF VASCULOGENIC MIMICRY IN GBM

The work presented in this chapter is part of an original research article: Francescone R, Scully S, Bentley B, Yan W, Taylor SL, Oh D, Moral L, Shao R. Glioblastoma-derived tumor cells induce vasculogenic mimicry through Flk-1 protein activation. *J Biol Chem*. 2012 Jul 13;287(29):24821-24831.

3.1 Introduction

Glioblastoma (GBM) is an extremely aggressive brain tumor with a median survival of approximately 12 months, irrespective of surgical resection and post-operative adjuvant radio/chemotherapy (Wen and Kesari 2008). More than 70% of patients with GBM succumb to the disease in 2 years and fewer than 10% are alive 5 years following initial diagnosis (Norden, Drappatz and Wen 2009). Aggressiveness of this disease is characterized by strong vascular proliferation which is highly correlated with the malignancy of GBM. Thus, most of the current chemotherapies against GBM aim at vascular endothelial cells that orchestrate a significant component of blood vessels (Nghiemphu, et al. 2009). However, it has been increasingly documented that an anti-angiogenic monotherapy did not give rise to a promise for improvement of patient overall survival, as drug resistance or angiogenic rebound occurs once the treatment is terminated (Bergers and Hanahan 2008, Ellis and Hicklin 2008). For example, clinical trials using a neutralizing anti-VEGF antibody (Bevacizumab, also named Avastin) in recurrent GBMs revealed minimal benefit to patient survival (Bergers and Hanahan 2008, Verhoeff, et al. 2009, Kreisl, et al. 2009). Consistent with clinical evidence, the anti-angiogenic preclinical studies using animal models reported conflicting outcomes in which malignant tumors unexpectedly developed (Ebos, et al. 2009, Pàez-Ribes, et al. 2009), implicating that escape mechanisms may account for the malignancy.

Recently, a number of research groups have demonstrated that vasculogenic mimicry (VM), an alternative vascular mechanism, contributes a central role to the vascularization of GBM in which tumor cells participate (Yue and Chen 2005, El Hallani, et al. 2010, Liu, et al. 2011). Growing evidence suggests that this matrix-embedded, blood-perfused microvasculature renders tumor progression independent of endothelial cell angiogenesis (Maniotis, et al. 1999, Folberg and Maniotis 2004). In addition, this VM is believed to be at least partially ascribed to the multipotency of glioblastoma stem cells (GSCs) capable of transdifferentiation into vascular non-endothelial cells (Ping and Bian 2011, Chen, et al. 2012). Furthermore, these studies suggest that transdifferentiation of GSCs into mural-like tumor cells enable these vascular cells to constitute blood-perfused channels, whereas endothelial cells induce angiogenesis in GBM.

An angiogenic factor VEGF is appreciated to evoke vascular endothelial cell angiogenesis mainly through binding its membrane-bound receptors such as VEGF receptor 1/Flt-1 and VEGF receptor 2/Fms-like tyrosine kinase-1 or kinase domain receptor (Flk-1/KDR) (Neufeld, et al. 1999, Yancopoulos, Klagsbrun and Folkman 1998). Flk-1 is the earliest differentiation marker for endothelial cells and blood cells (Eichmann, et al. 1997, Shalaby, et al. 1995). Expression of Flk-1 in the adult is restricted to endothelial cells and transiently up-regulated during angiogenesis (Neufeld, et al. 1999). Deletion of Flk-1 gene in mice results in embryonic lethality owing to the lack of hematopoietic and endothelial lineage development (Shalaby, et al. 1995, Fong, et al. 1995). Once binding with VEGF, Flk-1 undergoes autophosphorylation of tyrosine residues located in an intracellular kinase domain and subsequently activates multiple intracellular signaling cascades such as focal adhesion kinase (FAK) and MAP kinase activation, leading to endothelial cell angiogenesis (*e.g.* cell proliferation, migration and tube formation) (Yan, Bentley and Shao 2008, Sun, et al. 2005). Interestingly, previous studies showed that transdifferentiation of embryonic stem cells into vascular endothelial cells and mural cells

required expression of Flk-1 (Yamashita J, et al. 2000, Yang L 2008, Taura, et al. 2009). However, it is largely unknown whether Flk-1 plays an essential role in the development of VM.

3.2 Experimental Strategy

Here we take advantage of GBM-derived tumor cell lines capable of developing VM to investigate a role of Flk-1 in the vasculogenesis of GBM. Deciphering the molecular mechanisms will offer considerable value for devising novel therapeutic regimen targeting non-endothelial vascular proliferation in concert with current anti-angiogenic therapy.

3.3 Results

3.3.1 Identification of Vasculogenic Mimicry in Human Glioblastoma Cases

To determine if VM is present in GBM, we examined tumor samples from 11 patients with GBM. Hematoxylin and eosin (H & E) showed a vascular pattern spread throughout the majority of the tumor sections of 7 of 11 tumors and periodic acid-Schiff (PAS) staining of vascular basement membrane revealed extensive blood-perfused channels, most of which harbored vascular cells that displayed a torturous phenotype dissimilar to endothelial cells (Figure 3.1A+B). Two of the other tumors contained a minimal level of vascular channels, while the final two were avascular. To determine if these vascular channels are comprised of mural cells, we utilized an immunohistochemical (IHC) approach by staining the samples with smooth muscle alpha actin (SMa) and platelet-derived growth factor receptor (PDGFR), both of which are vascular pericyte markers. A number of these vessels exhibited strong staining of both SMa and PDGFR (Figure 3.1C+D). In a dual staining analysis of SMa and CD31, a vascular endothelial cell marker, we found that some vessels contained endothelial cells and others consisted of SMa-positive cells (Figure 3.1E). In addition, IHC analysis indicated that these mural cell-

associated vessels were positive for Flk-1 (Figure 3.1F). To validate that these mural-like tumor cells express Flk-1, we performed a dual immunofluorescent assay and found that a significant component of the vascular channels co-expressed SMa with Flk-1 (Figure 3.1G), but not with CD31 (Figure 3.1H). These data demonstrate that VM present in GBM is principally comprised of mural cells that express Flk-1.

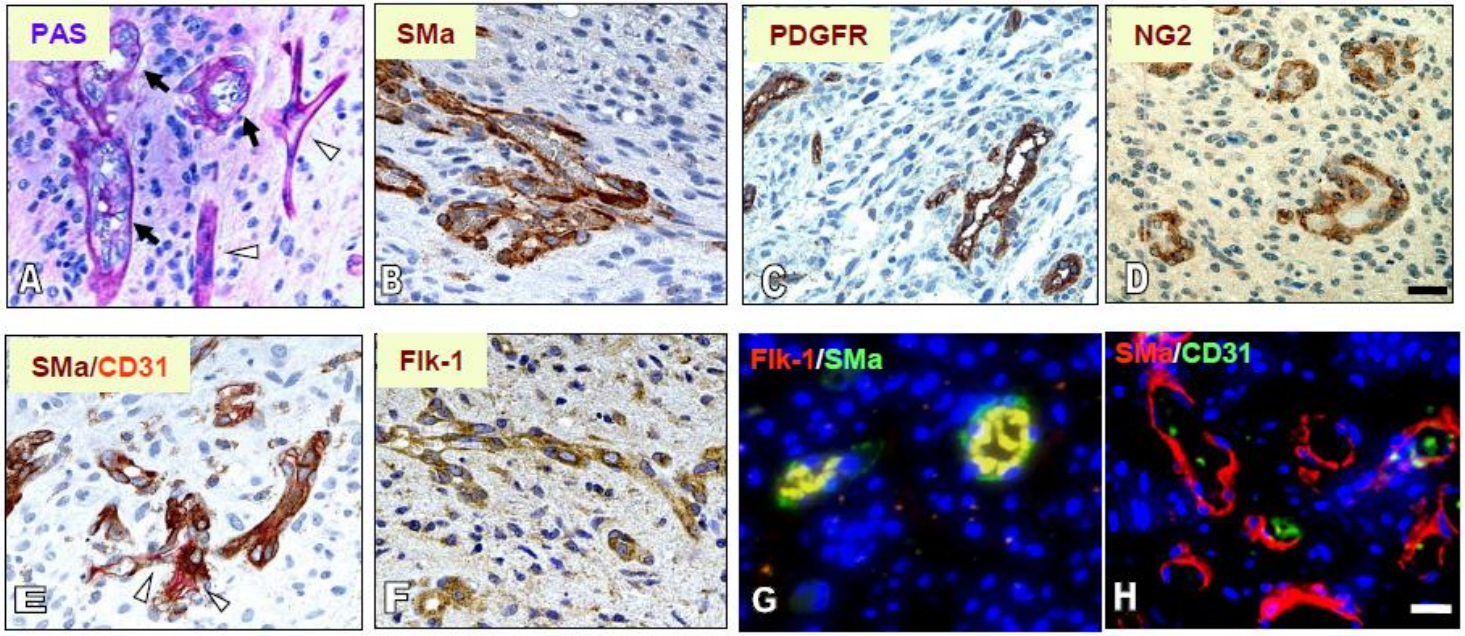

Figure 3.1 Extensive tumor cell-associated, blood-perfused channels co-express SMa, PDGFR, and Flk-1 in GBMs.

Tumor specimens were subjected to staining of PAS **(A)**, IHC of SMa **(B)**, PDGFR **(C)**, NG2 **(D)**, SMa and CD31 **(E)**, Flk-1 **(F)**, and immunofluorescent co-staining of SMa with Flk-1 **(G)**, and SMa with CD31 **(H)**. In **A**, arrows represent tumor cell-associated vascular channels in which blood cells are located (thick vessel walls); whereas arrow heads indicate endothelial cell-associated vessels (thin vessel walls). In **E**, an arrow head indicates CD31-positive vessels. In **G**, vessels were strongly positive for Flk-1 and SMa, whereas in **H**, a few vessels expressed CD31. Bars: 100 μm.

3.3.2 GBM Cells Possess a Mural-like Phenotype

To test our hypothesis that tumor cells act as vascular mural-like cells to participate in VM, we investigated two glioblastoma tumor cell lines: U87 cells and GSDCs that were established from patients with GBM. We performed immunoblotting to assess expression of mural and endothelial cell markers. Both tumor lines U87 and GSDCs expressed stronger Flk-1 than that observed in HMVECs (Figure 3.2A). Contrary to HMVECs that express a barely detectable level of SMa, U87 cells and GSDCs expressed a higher level of SMa. Immunocytochemistry analysis unveiled the same expression pattern of Flk-1 and SMa as the immunoblotting results (Figure 3.2A+B). However, it was notable that both U87 cells and GSDCs, in contrast to HMVECs, did not express endothelial cell-specific markers VE-cad, CD31, Tie1 or Tie2, demonstrating that GSDCs are distinct from endothelial cells. U87 cells and GSDCs expressed higher N-cad than did HMVECs, consistent with previous reports that vascular endothelial cells also express N-cad in addition to VE-cad (Paik, et al. 2004, Luo, et al. 2006). In order to confirm that this mural cell expression pattern was not just an artifact of one particular patient-derived cell line, a second patient-derived cell line, GSDC-2, was created. GSDC-2 also showed a nearly identical expression pattern as GSDCs (Figure 3.3A+B), suggesting that this mural marker expression is a common characteristic of GBM cells.

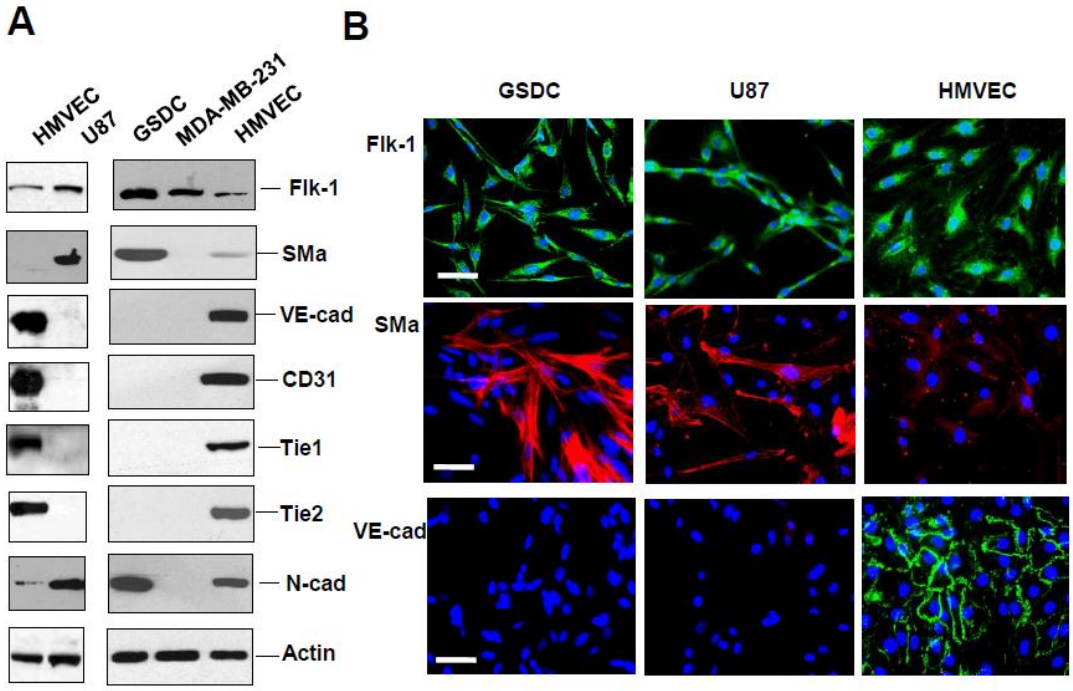

Figure 3.2 U87 cells and GSDCs express SMa and Flk-1, but not endothelial cell markers.

A. Cell lysates of U87 cells, GSDCs, MDA-MB-231 cells and HMVECs were analyzed by immunoblotting against Flk-1, SMa, VE-cad, CD31, Tie1, Tie2, N-cad, and actin. MDA-MB-231 cells were used as a negative control. **B.** These cells were also used for immunocytochemistry staining of SMa, Flk-1, and VE-cad. DAPI is nuclear staining. Bars: 50 μm.

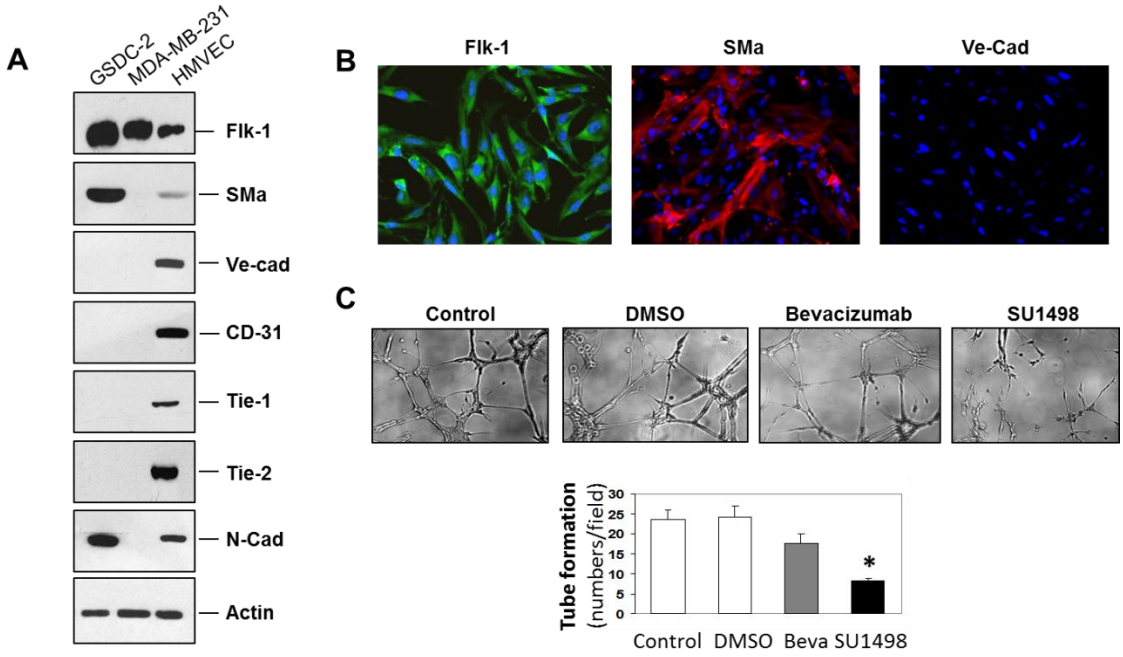

Figure 3.3 A second GBM patient derived cell line, GSDC-2, has a similar molecular and functional profile as GSDC.

A. Western blot analysis of mural and endothelial markers. MDA-MB-231 cellswere used as a negative control and HMVEC was a positive control for endothelial markers. Actin is a loading control. **B.** Immunocytochemical analysis of GSDC-2 for the expression of Flk-1, SMa, and VE-cadherin. **C.** Functional analysis of tube formation of GSDC-2. GSDC-2 were treated with an anti-VEGF antibody (Bevacizumab, Beva.) (10 µg/ml) or SU1498, a Flk-1 inhibitor, (12.5 µM). Tubules were quantified. n=4.*P<0.05 compared with controls or DMSO treatment.

3.3.3 GBM Cells Have *in vitro* Vasculogenic Activity Dependent on Flk-1

Should U87 cells and GSDCs truly represent cells capable of developing vascular channels, they might possess the vasculogenic activity as do endothelial cells (Shao and Guo 2004, Francescone, Faibish and Shao 2011). To test this hypothesis, we performed a tube formation assay that commonly recapitulates the ability of endothelial cells to develop vasculature *in vitro*. U87 cells and GSDCs formed a capillary phenotype on Matrigel in a cell number-dependent manner (Figure 3.4A+B). To evaluate if this vascular event is dependent on Flk-1 as expressed by mural cells (Figure 3.1) in GBM, we employed a Flk-1 kinase inhibitor SU1498. Treatment with SU1498 inhibited the ability of both cells to induce capillary-like structure by approximately 72-80% relative to controls (Figure 3.4C+D). To provide additional genetic evidence that Flk-1 is important for vasculogenic function, we used an *Flk-1* shRNA gene knockdown approach. Suppression of *Flk-1* was associated with a corresponding reduction in SMa expression and tube formation as tubules were decreased by 80% of control tubules (Figure 3.4E). These findings were also validated with the GSDC-2 cell line derived from another patient (Figure 3.3C). In all the tube formation assays, treatment of either SU1498 or Flk-1 gene knockdown did not result in cell growth arrest or cell death (Figure 3.5).

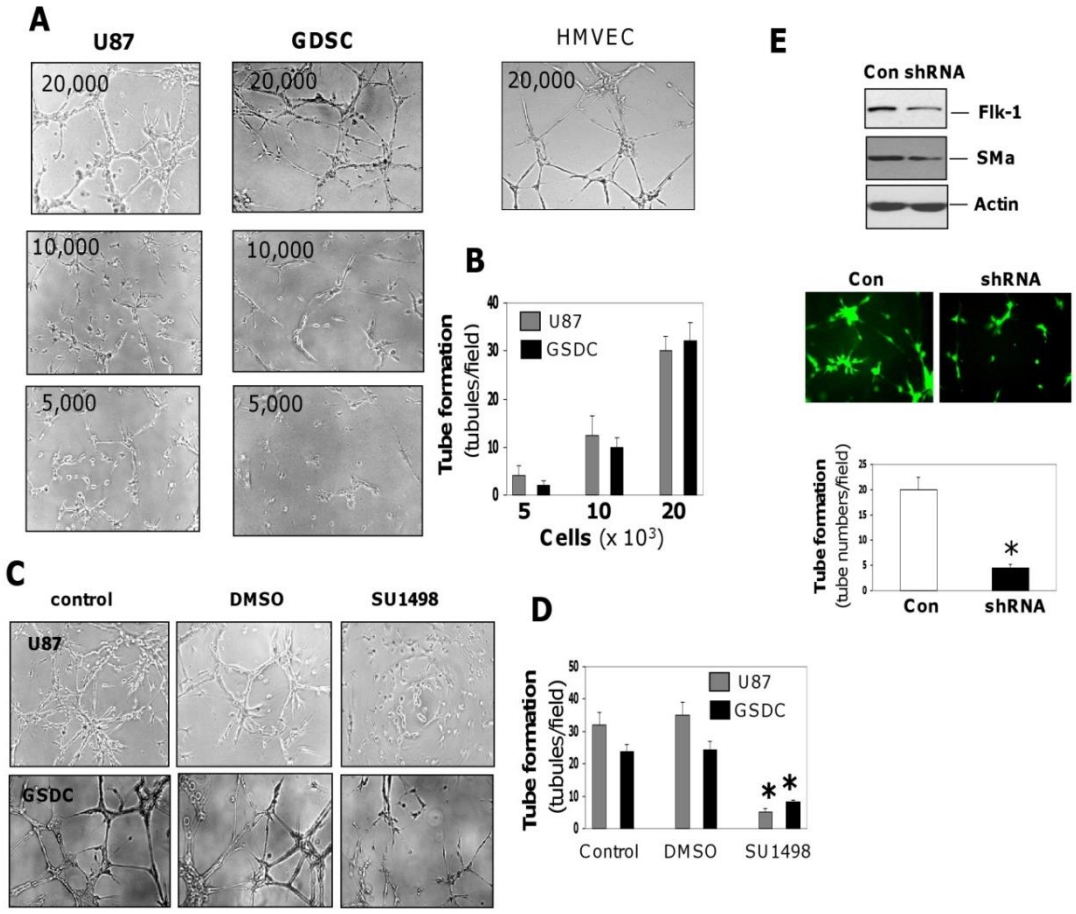

Figure 3.4 U87 cells and GSDCs are able to induce vascular tube formation, the process dependent on Flk-1.

A. Different cell numbers of U87 cells and GSDCs were cultured on Matrigel for tube formation. HMVECs served as a positive control. n=3. **B.** The tubules formed by these cells were quantified, demonstrating a cell number-dependent relationship. **C.** Tube formation was performed overnight with U87 cells and GSDCs (2 x 10^4) in the presence of SU1498 (12.5 μM). **D.** Tubules were quantified. n=4. *P<0.05 compared with controls or DMSO treatment. **E.** U87 cells were used to knock down Flk-1 gene. Cell lysates were collected for detection of Flk-1, SMa and actin by immunoblotting. Cells carrying scrambled RNA GFP-vector or shFlk-1 RNA GFP-vector were analyzed for tube formation under a florescence microscope followed by quantification. n=3. *P<0.05 compared with a control.

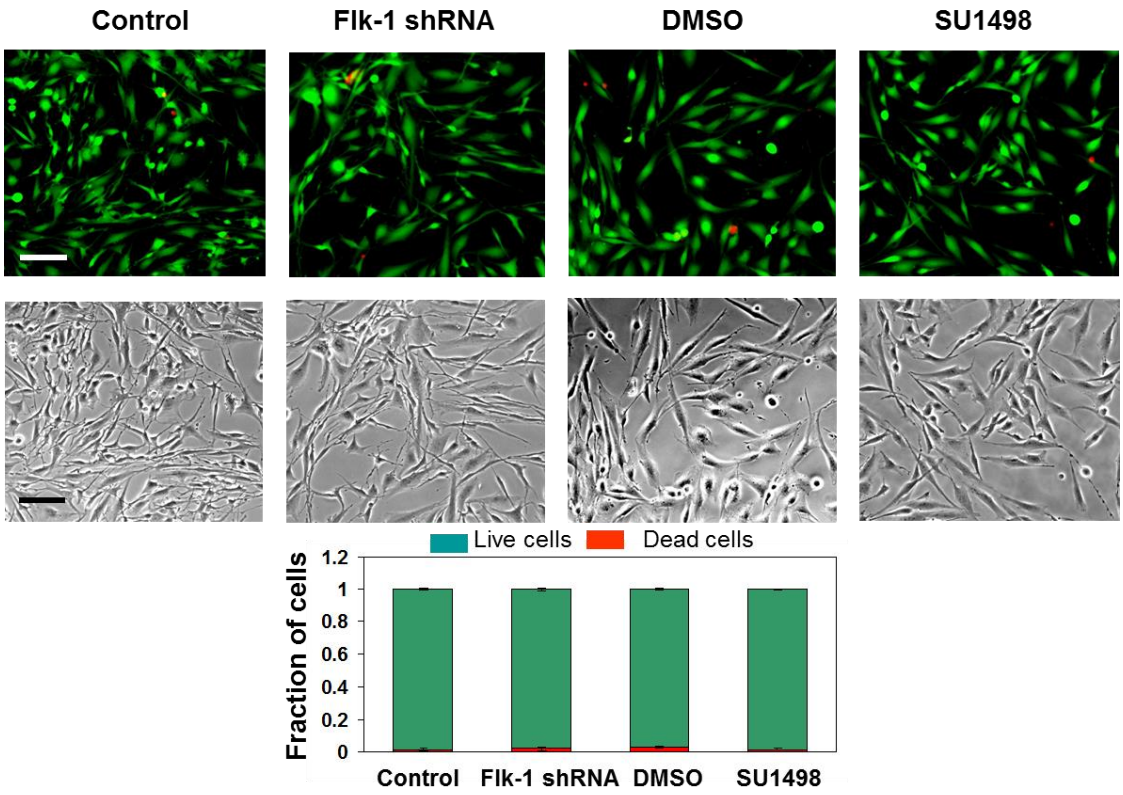

Figure 3.5 Flk-1 Inhibition does not cause cell death or impair growth of GBM cells.

GSDCs were either treated with control shRNA, Flk-1 shRNA, DMSO, or SU1498 (12.5 µM). 2 days later, cells were subjected to the Live/Dead Assay (Invitrogen) to measure cell death. Green indicates live cells, as stained by Calcein AM, while red indicates dead cells, as stained by ethidium homodimer (the top panel). Corresponding phase contrast pictures were shown (the middle panel). Quantification of the fraction of living and dead cells for each treatment group. N= 3, *P >0.05 (the bottom panel).

3.3.4 Flk-1 Mediated VM is Independent of Vascular Endothelial Growth Factor

Next, we determined if this Flk-1-mediated vascular activity requires VEGF. We treated these tumor cells with an anti-VEGF neutralizing antibody Bevacizumab in the tube formation. As tested earlier, both U87 cells and GSDCs decreased the ability to develop tubules in the presence of SU1498. In contrast, they did not display dysfunction of the vascular formation once Bevacizumab was added (Figure 3.6A + Figure 3.3C). Accordingly, expression of SMa in these cells was reduced by SU1498 but not by Bevacizumab, indicative of a VEGF-independent event (Figure 3.6B). Regardless of higher expression of VEGF by U87 cells and GSDCs than that by HMVECs, this vasculogenic capability of these tumor cells was distinct from the angiogenic signature of vascular endothelial cells that highly responded to Bevacizumab in the development of tubules (Figure 3.6C).

To further validate that Flk-1-mediated vasculogenesis does not require VEGF, we stimulated U87 cells with VEGF in the tube formation assay. Exposure of both U87 control cells and the cells expressing Flk-1 shRNA to VEGF did not alter vascular development, as VEGF did not either enhance vascularization in the control cells or rescue the impaired capability of tube formation in Flk-1 shRNA cells (Figure 3.6D). These data support the notion that Flk-1-mediated VM is independent of VEGF.

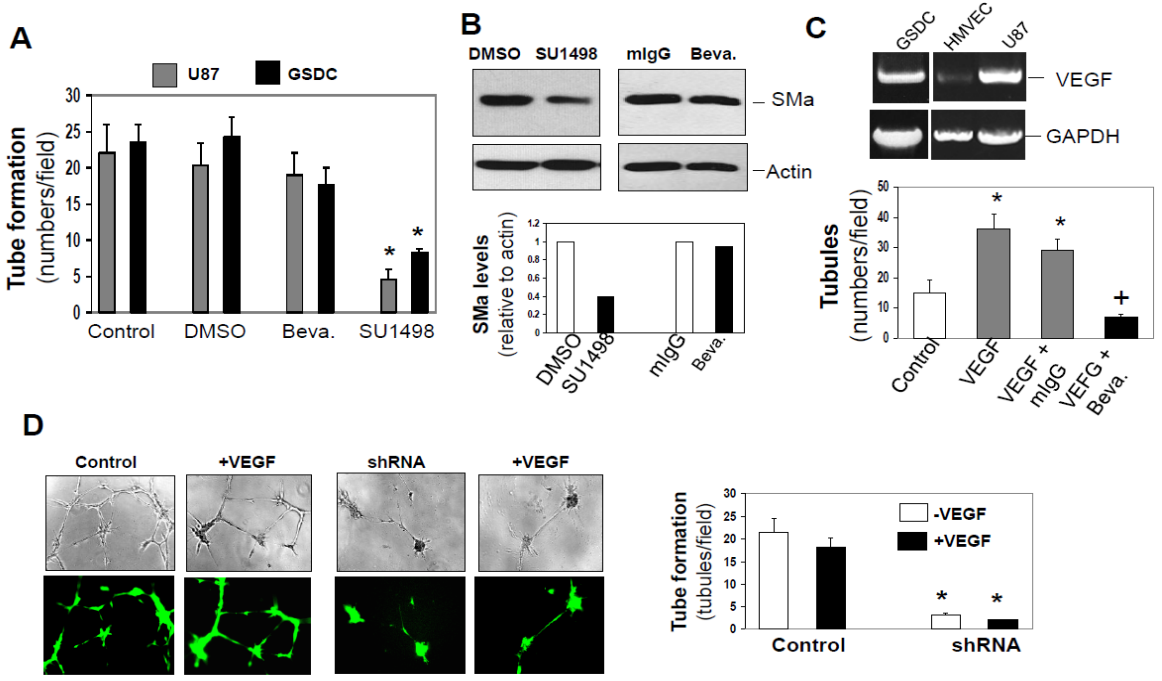

Figure 3.6 Flk-1-mediated vasculogenesis is independent of VEGF.

A. U87 cells and GSDCs were used for tube formation in the presence of an anti-VEGF antibody (Bevacizumab, Beva.) (10 μg/ml) or SU1498 (12.5 μM). Tubules were quantified. n=4. *P<0.05 compared with controls or DMSO treatment. **B.** U87 cells were treated with Beva (10 μg/ml) or SU1498 (12.5 μM) for 24 hr and cell lysates were subjected to immunoblotting against SMa and actin followed by quantification. **C.** HMVECs were stimulated with VEGF (10 ng/ml) on Matrigel in the presence of Beva (10 μg/ml). Data were quantified. n=4. *,+P<0.05 compared with control and VEGF + mIgG, respectively. **D.** U87 cells expressing non-sense RNA or Flk-1 shRNA GFP-vector were subjected to tube formation in the presence of VEGF (10 ng/ml). Tubules were imaged with a phase contrast and fluorescent microscope. n=3. Data were quantified. *P<0.05 compared with corresponding control cells bearing scrambled RNA.

3.3.5 Inhibition of VEGF does not alter Flk-1 activated signaling

We then sought to determine if Flk-1 kinase activity plays a core role in signaling activation independent of VEGF. Both U87 cells and GSDCs were treated with either SU1498 or Bevacizumab overnight (Figure 3.7A). Consistent with earlier functional analyses, treatment of these cells with SU1498 resulted in 80-86% reduction of tyrosine phosphorylated Flk-1 compared with control levels (Figure 3.7A+B). In contrast, Bevacizumab failed to alter pFlk-1 levels. To further identify intracellular signaling pathways in response to Flk-1 activation, we focused on FAK and downstream effector MAP kinase Erk1/2, as these intracellular factors mediate Flk-1 signaling in vascular endothelial cells (Yamashita J, et al. 2000, Shao, Hamel, et al. 2009). We measured tyrosine phosphorylated FAK and Erk1/2 after treatment of U87 cells and GSDCs with Bevacizumab and SU1498, and we found that activated levels of pFAK in SU1498-treated cells were reduced by approximately 50-75% relative to control or Bevacizumab-treated cells (Figure 3.7A+B). Accordingly, pErk1/2 were significantly decreased in SU1498 but not Bevacizumab-treated cells. As a result, SU1498 treatment led to suppression of SMa expression by 67-75% compared with the level in control or Bevacizumab-treated cells. All the data demonstrate that Flk-1 activation in tumor cells leads to intracellular signaling cascades FAK and Erk1/2, and SMa expression; but this event does not require VEGF stimulation.

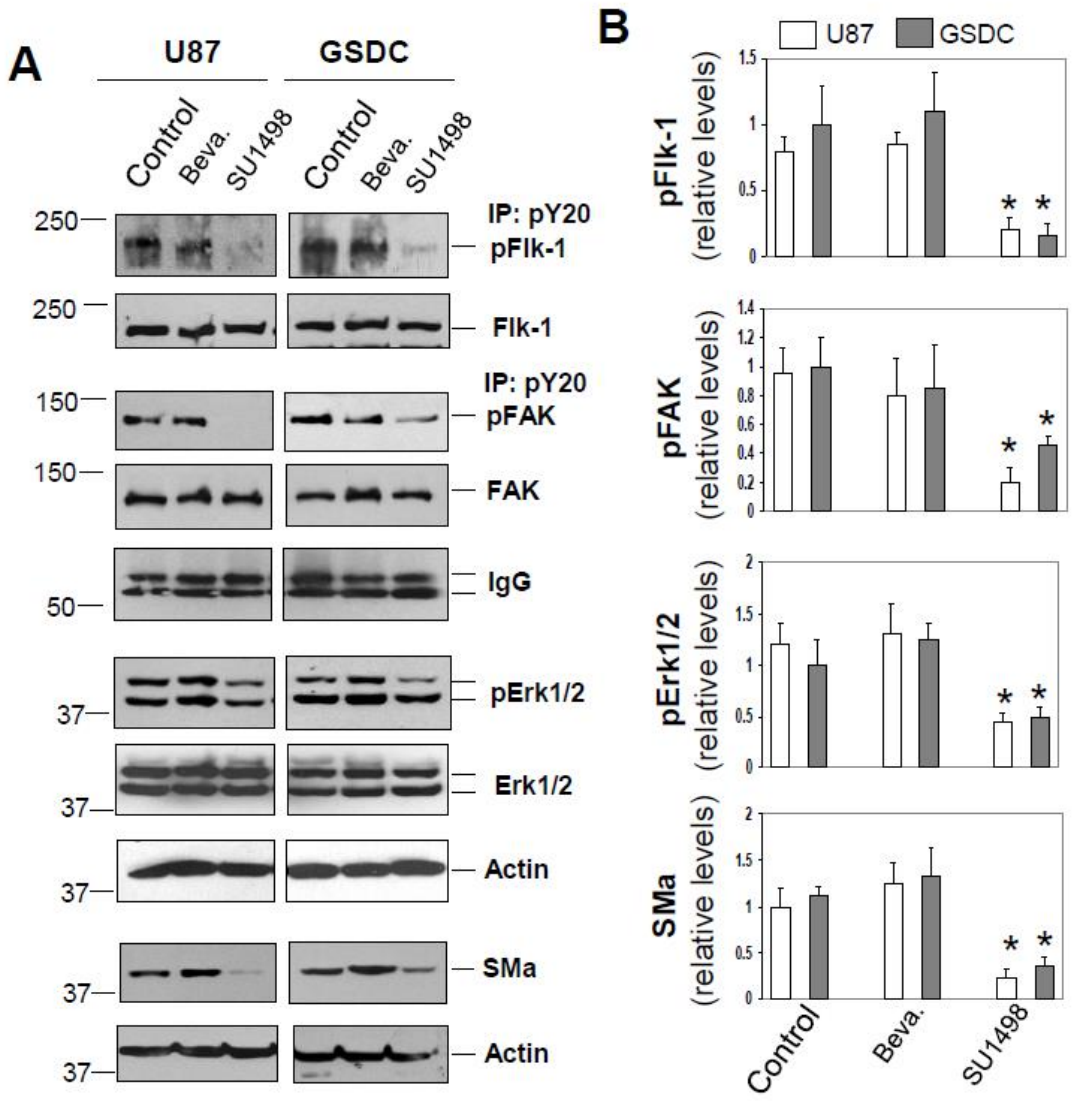

Figure 3.7 Flk-1-mediated intracellular signaling activation is independent of VEGF.

A. U87 cells and GSDCs were treated with either Bevacizumab (Beva, 10 μg/ml) or SU1498 (12.5 μM) overnight and then collected for co-immunoprecipitation with an anti-pY20 antibody followed by immunoblotting with an anti-Flk-1 or FAK antibody. IgG of the anti-pY20 antibody was tested as loading controls. Some of these cell lysates were used for immunoblotting against Flk-1, FAK, pErk1/2, Erk1/2, and actin. In addition, some cells were treated with Beva 10 μg/ml) or SU1498 (12.5 μM) for three days, and then lysates were measured for SMa expression. **B.** Active forms of pFlk-1, pFAK, pErk1/2, and SMa were quantified by normalization with their corresponding total non-phosphorylated forms or actin. n=3. *P<0.05 compared with corresponding control or Beva-treated groups.

3.3.6 MAPK Participates in VM Signaling

In order to further confirm the intracellular signaling pathway mediating Flk-1 activation, we used a MAPK inhibitor, PD98059 (10 μM). Protein expression levels of both pErk1/2 and SMa were reduced by the inhibitor by 35% and 60% for U87 cells and 33% and 50% for GSDCs relative to the DMSO control (Figure 3.8A+B). Like Flk-1 inhibition, PD98059 reduced tube formation in both U87 and GSDC cells by 68% and 79% respectively (Figure 3.8C). All the data support the notion that Erk1/2 participate in vascular signaling pathway.

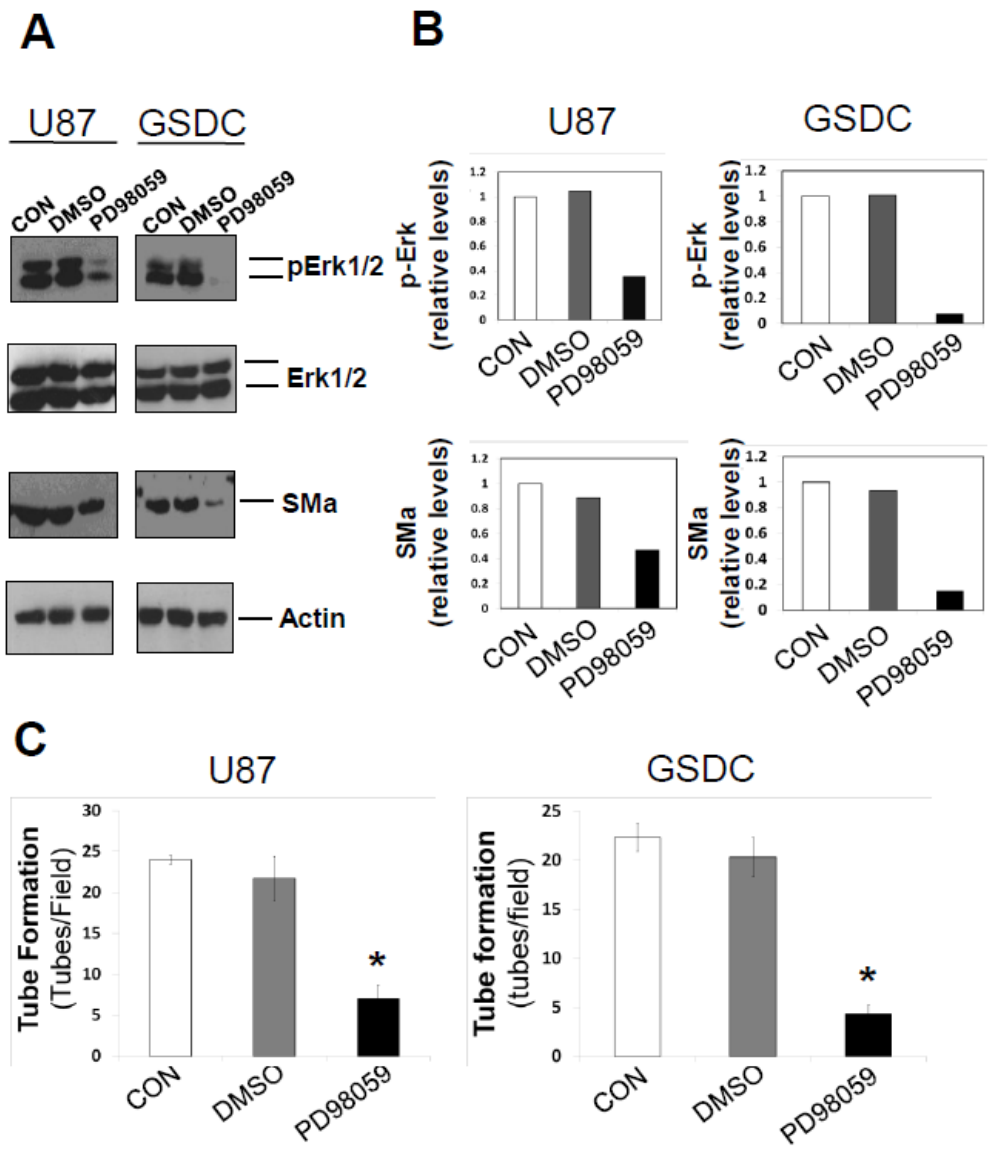

Figure 3.8 Inhibition of downstream ERK signaling yields similar results to Flk-1 inhibition.

A. U87 or GSDC cells were either untreated (CON) or treated with DMSO, or a MAPK inhibitor (PD98059, 10 μM) overnight and lysates were collected. Immunoblotting of the lysates for Erk1/2, pErk1/2, SMa, and actin expression was performed. **B.** Quantification of amounts of SMa and pErk1/2 shown in part A. **C.** Quantification of the functional analysis of the MAPK inhibitor on tube formation of either U87 or GSDC cells on Matrigel. n=3, *P<0.05 compared with corresponding control groups.

3.3.7 GSDCs Form VM in Animal Models *in vivo*

In an attempt to determine if these GBM-derived tumor cell lines can develop VM *in vivo*, we utilized a tumor xenograft model by transplantation of GSDCs into SCID/Beige mice. Six of mice receiving GSDCs rapidly developed tumors in the eight-week period and removed tumors were analyzed for tumor vasculogenesis. PAS staining revealed vigorous formation of vasculature in the tumors (Figure 3.9A) reminiscent to its original vascular phenotype in GBM (Figure 3.1B). These extensive vascular channels expressed strong SMa (Figure 3.9B), GFAP (Figure 3.9C), and Flk-1 (Figure 3.9D), in which blood cells were located. In addition, these tumor cell-derived vessels did not express mouse CD31 (Figure 3.9E+F), confirming that VM is divergent from endothelial cell angiogenesis. To test the possibility that GSDCs may undergo differentiation *in vivo* into endothelial cells that participate in angiogenesis, we employed different antibodies specific for recognizing human endothelial cells. Neither using an anti-human CD31 antibody nor an anti-CD34 antibody showed positive staining in the tissue (Figure 3.9G+H), which indicates incapability of tumor cell transdifferentiation into endothelial cells. To validate that these Flk-1-positive vessels are derived from tumor cells, not from host endothelial cells, we employed a co-immunofluorescent assay in which GFAP and Flk-1 were stained with red and green fluorescence, respectively. Indeed, Flk-1-positive vascular channels co-expressed GFAP that is specific for glioblastoma cells (Figure 3.9I+L). Finally, in order to demonstrate that these GBM-lined VM channels were functional *in vivo*, we utilized primary GBM cells expressing GFP, together with an intravenous injected fluorescent dye known as Evan's blue 30 minutes prior to sacrificing (Figure 3.10). Evan's blue was detected in the lumen of GFP^+ vessels, highlighting that these vascular channels are functional *in vivo*. These *in vivo* data suggest that transplanted glioblastoma cells participate in VM, rather than endothelial cell angiogenesis.

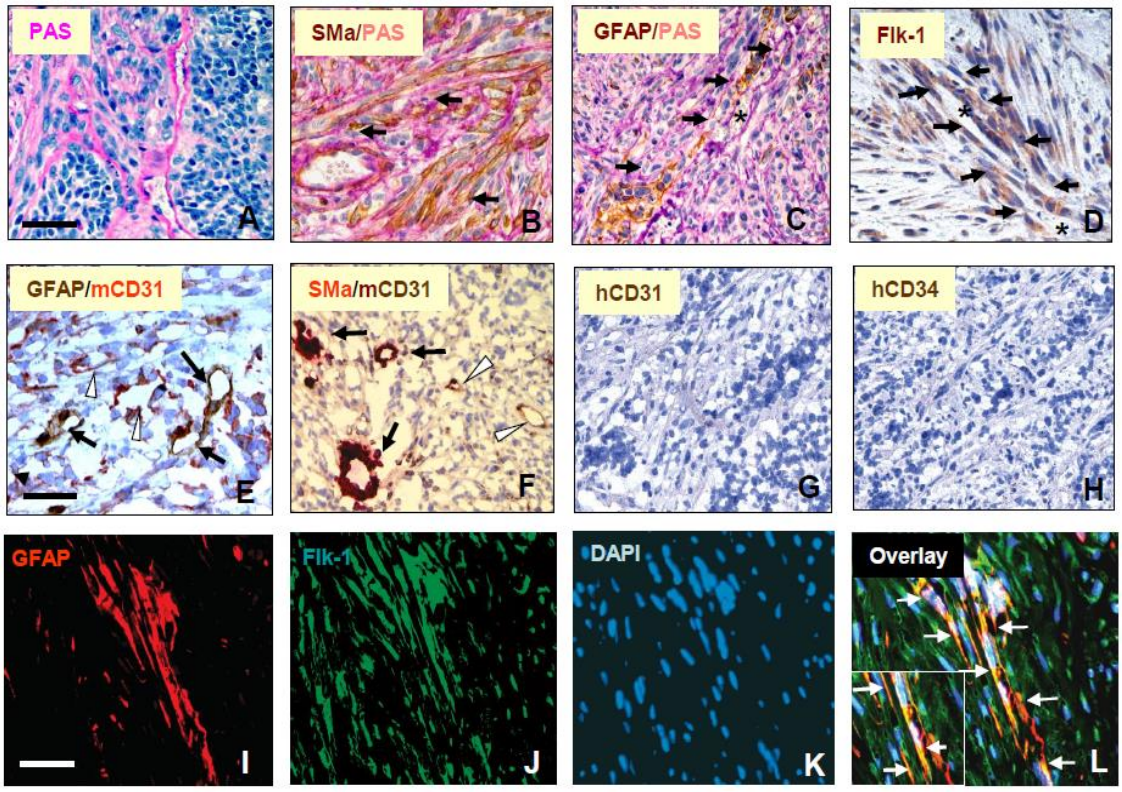

Figure 3.9 GSDCs develop tumors that consist of tumor cell-associated vasculature co-expressing SMa, GFAP, and Flk-1.

Eight weeks following subcutaneous transplantation of GDSCs, tumors were removed and processed for IHC analysis of PAS **(A)**, co-staining of SMa and PAS **(B)**, GFAP and PAS **(C)**, Flk-1 **(D)**, GFAP and mCD31 **(E)**, SMa and mCD31 **(F)**, hCD31 **(G)**, hCD34 **(H)**, and co-immunofluorescent staining of GFAP **(I)**, Flk-1 **(J)** and DAPI **(K)** in which an overlay image was displayed in **(L)**. Black arrows **(B, C, D, E, F)** indicate positive staining of VM vessel markers. Asterisks **(C, D)** specify the lumen of VM channels. White arrowheads **(E, F)** indicate positive staining of endothelial cell vessel markers. White arrows **(L)** indicate VM channels. An insert shows a large image for the channel. Bars: 100 μm.

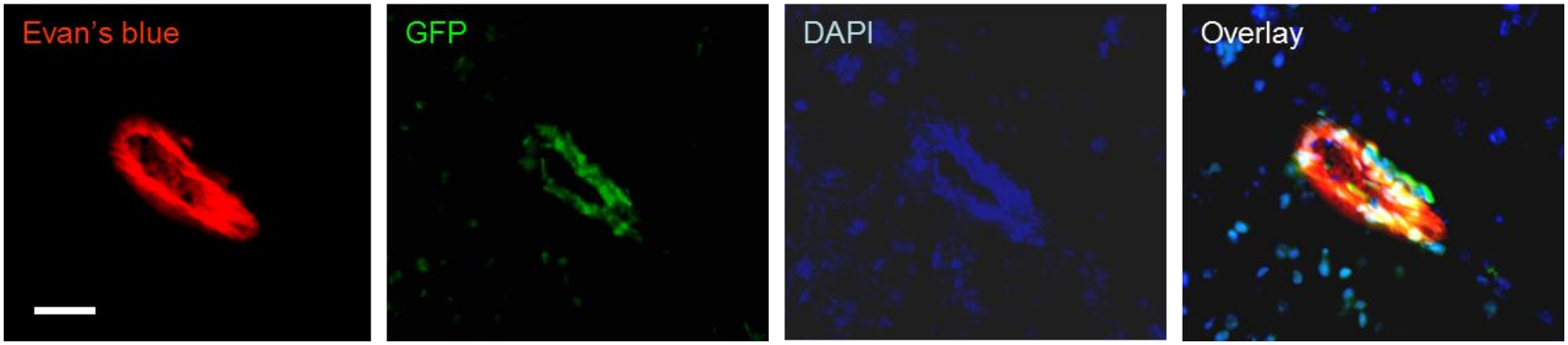

Figure 3.10 Primary GBM cells form functionally active vessels in vivo.

Mice bearing primary GBM cell derived tumors (GFP positive) were intravenously injected with Evan's Blue Dye 30 minutes before sacrificing. Sections of the tumor tissue were analyzed for Evan's blue atuofluorescence (red), GFP autofluorescence (green). Representative pictures were taken of a tumor cell lined vessel, as Evan's blue dye is clearly stained within that vessel surrounded by a few GFP-positive tumor cells, indicating that this vessel is connected to the circulatory system. DAPI (blue) was used to stain nuclei. A bar: 100 mm.

3.3.8 Flk-1 is Vital to VM Development *in vivo*

In order to establish a functional role for Flk-1 in the development of VM and tumor formation, we utilized another tumor xenograft model by transplantation of SCID/Beige mice with U87 cells expressing either control vector or *Flk-1* siRNA. All six animals receiving control U87 cells developed palpable tumors within three weeks and all could be imaged for green fluorescence by week 8 (Figure 3.11A+B). In contrast, tumorigenesis was significantly delayed in mice receiving *Flk-1* shRNA-expressing U87 cells, and they did not develop palpable tumors until week 6. By weeks 6 and 8, these tumors were approximately 70% smaller than those observed in control counterparts, and the fluorescent images were undetectable during this period (Figure 3.11A+B). Post-mortem histological analyses of tumors revealed that the control tumors harbored numerous tumor cell-derived channels, as demonstrated by extensive arbors of GFP-positive ramified channels throughout the entire tumor section (Figure 3.11C), the event that resembled mural-like cell lined channels identified in GBMs and above GSDC tumors (Figure 3.1 + Figure 3.9). In concert with earlier findings, the concomitant expression of PAS, SMa, and CD31 distinguished tumor cell-lined vasculature from endothelial cell vessels. SMa-positive vessels in control tumors were 7-fold greater than those found in shRNA tumors (Figure 3.11C-c, C-d, and D). While SMa-positive channels were minimal in tumors expressing Flk-1 shRNA, a significant fraction of vessels showed positive staining for mCD31, suggesting that endothelial cells orchestrate blood vessels in the absence of VM (Figure 3.11C-e and C-f). In addition, IHC analysis using a single anti-hCD31 antibody revealed no detectable signal in either condition of tumors, consistent with early findings (Figure 3.9G+H). These results indicate lack of endothelial cell transdifferentiation from tumor cells (Figure 3.11Cg and Ch). Collectively, all the *in vivo* data

demonstrate that GBM cells promote VM, dependent on Flk-1; while host endothelial cells contribute to tumor angiogenesis.

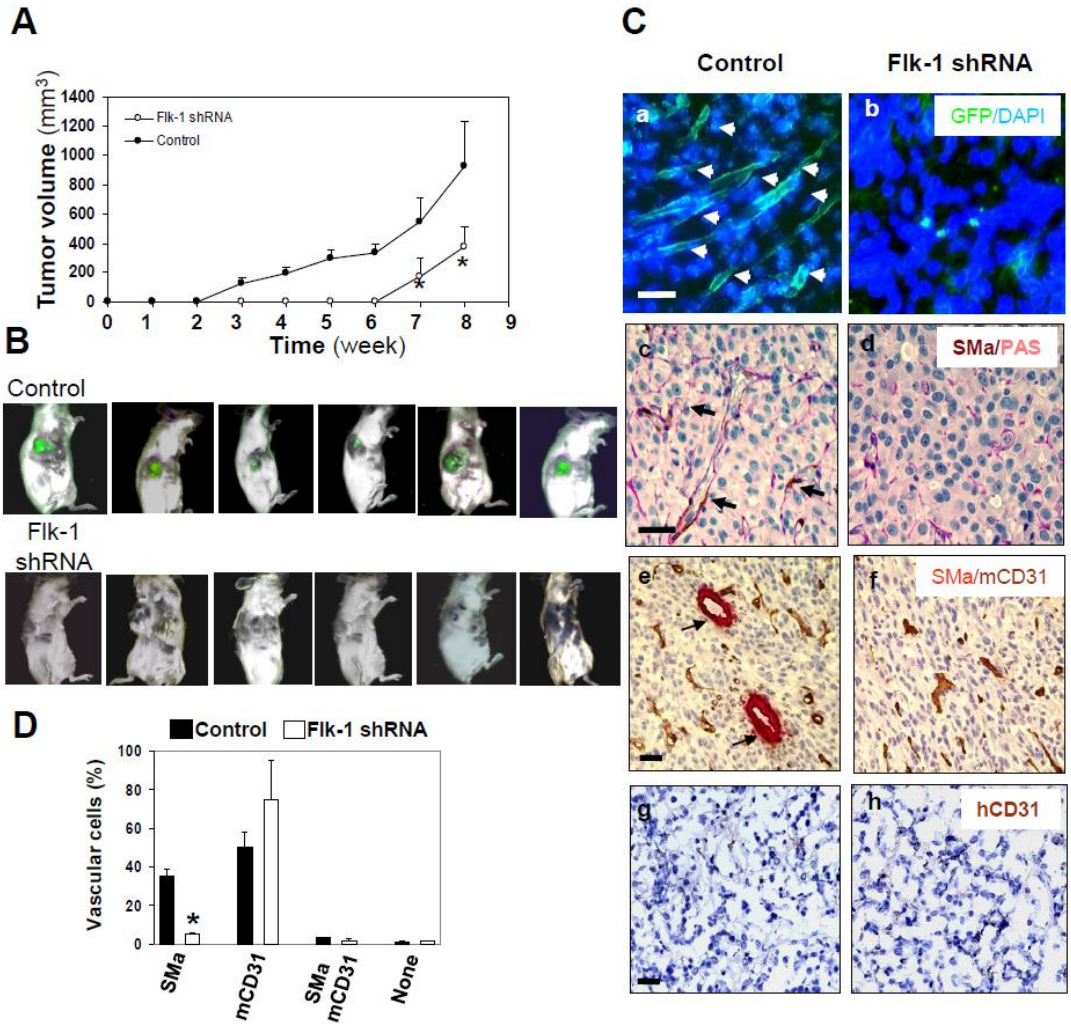
A
Tumor volume (mm3)
1400
1200
1000
800
600
400
200
0
Flk-1 shRNA
Control
0 1 2 3 4 5 6 7 8 9
Time (week)
B
Control
Flk-1 shRNA
C
Control
Flk-1 shRNA
a
b
GFP/DAPI
c
d
SMa/PAS
e
f
SMa/mCD31
g
h
hCD31
D
Control
Flk-1 shRNA
Vascular cells (%)
100
80
60
40
20
0
SMa
mCD31
SMa mCD31
None

Figure 3.11 Flk-1 shRNA in U87 cells inhibits tumor growth and VM.

A. *Flk-1 gene knockdown results in suppression of tumor growth.* U87 cells expressing *Flk-1* shRNA-GFP or GFP vector were injected subcutaneously into SCID/Beige mice and tumor size was measured weekly for 8 weeks. n=6. **P*<0.05 compared with corresponding controls. **B.** *Tumor fluorescence was detectable only in mice injected with U87 cells expressing GFP vector.* Before sacrifice, mice were examined for tumor fluorescence. Each image represented a single animal imaged 8 weeks after injection of the cells. **C.** *Formation of tumor cell-associated vascular channels was inhibited by Flk-1 gene knockdown.* Tumor fragments were examined for GFP fluorescence (a & b) and further analyzed by IHC for expression of co-staining of SMa with PAS (c & d), SMa with mCD31 (e & f), and a single staining of hCD31 (g & h). Arrows indicate GFP-positive (a) or SMa-positive tumor-cell-lined channels (c & e). Bars: 50 μm. **D.** *Quantification of vessels of VM and angiogenesis.* Density of SMa and CD31-positive vessels present in (e & f) was analyzed as described in the Methods. n=6. *P<0.05 compared with corresponding control tumors.

3.4 Discussion

Tumor vasculature is traditionally assumed to arise from an endothelial cell origin (Folkman 1971). However, mounting evidence suggests that VM, the matrix-embedded, blood-perfused microvasculature, is an alternative mechanism for the development of tumor vessels, independent of endothelial cell angiogenesis (Maniotis, et al. 1999, Folberg and Maniotis 2004). For example, highly aggressive melanoma cells generate numerous matrix-rich patterned channels containing blood cells, and the formation of these channels positively correlates with the tumor malignancy (Hendrix, et al. 2003, Folberg, Arbieva, et al. 2006). A mosaic model consisting both of tumor cell and endothelial cell-integrated networks was also described in the development of colon cancer (di Tomaso, et al. 2005, Chang, et al. 2000). Other recent reports suggest that mural-like tumor cells differentiated from GSCs promote VM (Soda, et al. 2011, Wang, et al. 2010, Ricci-Vitiani, et al. 2010). Consistent with these data, we identified that blood vessels of VM in GBM are comprised of mural cell-lined vasculature, while endothelial cells contribute to angiogenesis, highlighting the different targets for clinical therapy. Furthermore, we demonstrate that tumor cell lines developed from GBM possess mural cell properties capable of forming vascular channels and this vasculogenesis is dependent on Flk-1 activity.

VM has recently received considerable attention in the study of tumor development in clinic, because a simplistic vasculature model focusing on endothelial cell angiogenesis merely is deemed insufficient to describe the entity of sophisticated neovascular networks in which tumor cells also participate (Döme, et al. 2007, Folberg, Hendrix and Maniotis 2000). For example, clinical trials of recurrent GBMs with Bevacizumab alone for inhibition of VEGF-induced angiogenesis did not result in significant improvement of disease survival (Bergers and Hanahan 2008, Verhoeff, et al. 2009, Kreisl, et al. 2009). Thus it is conceivable that the evasive responses

may be at least in part attributed to VM. Indeed, our studies using Bevacizumab *in vitro* found that this Flk-1-mediated vascularization is VEGF-independent.

Flk-1 emerges as an essential angiogenic mediator to trigger signaling cascades induced by VEGF because of the expression of Flk-1 by endothelial cells. But this expression is not limited to endothelial cells only; instead, a number of non-endothelial cells including stem cells and some tumor cells also express Flk-1. For example, expression of Flk-1 acquired by embryonic stem cells confers differentiation into cardiac tissue and vascular cells such as endothelial cells and mural cells (Yamashita J, et al. 2000, Yang L 2008, Taura, et al. 2009). Flk-1^{+}-neural stem cells have the potential to give rise to vascular endothelial cells (Wurmser, et al. 2004). In this study, we found that GBM-derived tumor cell lines express Flk-1 that controls VM in a VEGF-independent fashion. Furthermore, activation of Flk-1 triggers intracellular signaling cascades from FAK to MAPK Erk1/2, resembling angiogenic signaling in endothelial cells (Yamashita J, et al. 2000, Shao, Hamel, et al. 2009). Although molecular mechanisms that regulate Flk-1 activation are currently still enigmatic in these cells, it is quite possible that it can be activated indirectly by other factors present in tumor microenvironment such as extracellular matrix proteins. Most of these proteins (*e.g.* fibronectin) can bind to membrane-associated integrins and induce coordination of integrins with Flk-1, leading to Flk-1 activation (Eliceiri 2001, Wijelath, et al. 2002, Borges, Jan and Ruoslahti 2000). It is also possible that Flk-1 could be mutated to lose its binding affinity with VEGF or become constitutively active in the cells. Animal tumor models deficient of VEGF seem to be necessary to establish the notion that Flk-1 is an indispensable receptor tyrosine kinase independent of VEGF, which regulates mural cell-associated VM in GBM.

An anti-VEGF therapy with Bevacizumab was approved for the first-line treatment of a variety of advanced carcinomas including brain tumor (Nghiemphu, et al. 2009), breast cancer

(Miller, et al. 2007), colorectal cancer (Hurwitz, et al. 2004), and non-small-cell lung cancer (Sandler, et al. 2006, Manegold 2008). However, the outcomes of this anti-angiogenic therapy in advanced tumors are still controversy. For instance, a long term of the monotherapy with Bevacizumab in GBMs only receives transitory benefit without significantly prolonged survival (Norden, Drappatz and Wen 2009, Norden, Young, et al. 2008). Once the therapy stops, tumors undergo vascular recovery and rapidly regrow. Analogous to these clinical reports, evidence from animal studies using either anti-VEGF or VEGF receptor therapy shows opposite results including blood revascularization, increased invasiveness, and distant metastasis (Ebos, et al. 2009, Mancuso, et al. 2006, Keunen, et al. 2011). However, some interesting evidence from both clinical and preclinical trials using Flk-1 kinase inhibitors AZD2171, SU5416, or an anti-Flk-1 antibody showed promising responses as these therapies ameliorate vascular normalization and alleviate peritumoral edema in GBMs and other cancers as well (Batchelor, et al. 2011, Kamoun, et al. 2009, Winkler, et al. 2004, Timke, et al. 2008, Kozin, et al. 2001). In line with these data, our current findings have supported the hypothesis that VEGF and Flk-1 may independently regulate diverse vascularizations through divergent vascular cells in GBM. Therefore, the conjunct therapies against both VEGF and Flk-1 could be taken into account for the treatment of patients with GBM.

Our animal models derived from both U87 cells and GSDCs exhibited extensive vascular channels formed by mural cells, recapitulating the vascular phenotype of GBM in which mural-like cell-associated vascular channels constitute a major component of vasculature. Interestingly, using an anti-human CD31 antibody failed to identify vessels positive for hCD31, demonstrating that tumor cells, unlike GSCs, are unable to undergo differentiation into endothelial cells. However, it is noteworthy that there is a significant population of mouse CD31-positive endothelial cells that are associated with tumor angiogenesis. This host-derived

angiogenic response is plausibly ascribed to the accumulation of angiogenic factors secreted from the xenotransplanted tumor cells. Nevertheless, the mural cell-associated, Flk-1-dependent VM, but not endothelial cell angiogenesis, plays an essential role in the tumor development.

It is also important to note that we used DMEM media supplemented with 10% FBS to grow both the U87 cell line and the primary GBM cell line, GSDC. In a separate study by Lee et al, they demonstrated the cancer cell lines grown in serum free media supplemented by growth factors could cause cells to have a phenotye and genotype more indicative of primary tumors (Lee, et al. 2006). Therefore, we cannot rule out a pheno/genotypic change in the U87s or GSDCs in the presence of serum. Nonetheless, the vascular phenotype *in vivo* of our cell lines resembles the observed vasculature in GBM patient tumors, indicating the VM mechanism represents the human condition to a certain extent.

In sum, our current findings provide mechanistic insights into the development of VM by tumor cells, the vascularization that occurs in a wide array of human cancers apart from GBM such as melanoma (Maniotis, et al. 1999), breast cancer (Basu, et al. 2006), prostate cancer (Liu, et al. 2002), colorectal cancer (Chang, et al. 2000), and ovarian cancer (Sood, et al. 2002). Identification of Flk-1 as a key factor regulating VM could offer a novel therapeutic target for the patient treatment. As a result, multiple anti-vascular approaches including targeting VM and angiogenesis together with chemotherapy may represent the best possible regimen in the fight against this devastating disease.

3.5 Materials and Methods

3.5.1 Cell Culture

U87 cells were purchased from ATCC. GSDCs were established from a tumor sample of a patient with GBM after the study was approved by Baystate Medical Center Institutional Review Board. Briefly, a small fragment of a tumor sample was digested with an enzymatic mixture containing 1.3 mg/ml Trypsin (Sigma, St. Louis, MO), 0.67 mg/ml type 1-S hyaluronidase (Sigma), and 0.13 mg/ml kynurenic acid (Sigma). Following extensive wash, cells were re-suspended and cultured in DMEM/F12 supplemented with B27 (Invitrogen, Carlsbad, CA) and 20 ng/ml bFGF and EGF for 2 weeks. Then the cells were transferred to a new plate and grew in DMEM supplemented with 10% FBS as the same medium used for U87 cells. GSDCs at passages between 10 and 20 were used for the study. Human microvascular endothelial cells (HMVECs) established previously were grown in a medium of EBM2 kit supplemented with hydrocortisone, EGF, and 10% FBS (Lonza Inc, Allendale, NJ)(27).

3.5.2 Tube formation

Tube formation was performed as described previously (Francescone, Faibish and Shao 2011). In brief, cells were plated on growth factor-reduced Matrigel (10 mg/ml, BD Lab, Bedford, MA) overnight and tubules were fixed with 10% formalin and imaged followed by quantification. Density of tubules was quantified from random selection of three fields under a microscope.

3.5.3 Flk-1 gene knockdown

A PGPU6-GFP-neo shRNA expression vector containing DNA oligos (21 bp) (GenePharma, Shanghai, China) specifically targeting C-terminal (5'-GCTTGGCCCGGGATATTTATA-3') of *Flk-1* or the vector with non-sense oligos as a control were transfected into U87 cells using Fugene 6.

Cells were selected in 800 μg/ml of G418 starting 48 hr after transfection and GFP expression was monitored to evaluate transfection efficiency.

3.5.4 Immunoprecipitation and Immunoblotting

Cell lysates were processed as described previously (Shao, Hamel, et al. 2009). The lysates were then incubated with an anti-pY20 antibody (ICN Biomedicals, Aurora, OH) at 4^0C overnight followed by incubation with protein A sepharose beads at 4^0C for 4 hr. The immunocomplex was extensively washed and the samples were run on SDS-PAGE. Then proteins were transferred to a PVDF membrane (VWR, Rockford, IL) and incubated with an anti-Flk-1 monoclonal (Santa Cruz Inc., Santa Cruz, CA) or anti-FAK polyclonal antibody (Biosource, Camarillo, CA). Membranes were then incubated with a goat anti-mouse secondary antibody (Jackson Lab, Bar Harbor, Maine). Specific signals were detected by enhanced chemiluminescence (VWR). For immunoblotting only, blot membranes were incubated with one of a series of primary antibodies against Flk-1, CD31, Tie1, Tie2 (Santa Cruz), SMa (Abcam, Cambridge, MA), VE-, N-cad (Invitrogen, Piscataway, NJ), FAK (Biosource), pErk1/2, Erk1/2 (Santa Cruz), or actin (Sigma).

3.5.5 Immunocytochemistry

Cells plated on 24-well plates were fixed with 4% paraformaldehyde and permeabilized with 0.5% Triton-X 100 in PBS. The samples were incubated overnight with antibodies specific for Flk-1 (rabbit), VE-cad (mouse), and SMa (rabbit). Alexa Fluor 488 and 555 goat anti-mouse and rabbit antibodies (Invitrogen) were added for 1 hr followed by nuclear staining with 4',6-diamidino-2-phenylindole (DAPI) (Invitrogen).

3.5.6 Live/Dead Assay

Live/Dead Assay Kit (Invitrogen) was employed to determine living *vs.* dead cells as instructed by the manufacturer. Briefly, living cells were stained with 2 μM Calcein AM (green) and dead cells were stained with 4 μM ethidium homodimer (red) for 30 minutes. Cells were then imaged and live/dead cells were quantified.

3.5.7 Tumor xenografts in mice

All animal experiments were performed with the approval of Institutional Animal Care and Use Committee of the University of Massachusetts and Baystate Medical Center. SCID/Beige mice were injected subcutaneously with U87 cells (8×10^6) or GSDCs (5×10^6) in 0.2 ml of PBS. Tumors arising from injected cells were monitored weekly for 8 weeks, after which the animals were humanely sacrificed. Mice were examined for expression of GFP using the Maestro *in vivo* imaging system (CRI, Woburn, MA). The tumors were measured and volume was calculated as follows: volume = length x width^2 x 0.52.

3.5.8 Immunohistochemistry and immunofluorescence

Paraffin-embedded or frozen tumor tissues were cut to 6 μm thickness and processed for immunohistochemical analysis. In brief, samples were incubated with 3% H_2O_2 for 30 min to block endogenous peroxidase activity, followed by incubation with blocking buffer containing 10% goat serum for 1 hr. The samples then were incubated at room temperature for 2 hr with mouse anti-Flk-1 (1:200) (Santa Cruz), anti-hCD31 (1: 100), anti-hCD34 (1:200), anti-SMa (1: 500) (Dako Inc, Carpentaria, CA), rat anti-mCD31 (1: 50, BD Bioscience, San Jose, CA) monoclonal antibodies, or rabbit anti-PDGFR, (Santa Cruz), anti-GFAP (1:5000, Dako) polyclonal antibodies. Goat anti-mouse or anti-rabbit secondary antibodies (1: 100) conjugated to HRP were added for

one hr. Finally, DAB substrate (Dako Inc) was introduced for several minutes and after washing, methyl green or PAS was used for counterstaining. Dual immunohistochemistry labeling was performed using one primary antibody at $4^{o}C$ overnight followed by application of the secondary antibody conjugated to alkaline phosphatase and incubated with permanent red as a substrate (G2 Kit, Dako). After extensive washing with TBST, the samples were then incubated with another primary antibody at room temperature for 2 hrs followed by application of a secondary antibody conjugated to HRP. Finally, DAB substrate and counterstaining were performed as described above.

Vasculature quantification: Three to five specimens randomly cut from each tumor block were processed for the IHC staining. Following the double staining with SMa and CD31, each sample was subjected to quantification of all the vessels that were positively stained for SMa, CD31, or both SMa and CD31, and that were negative staining but contained blood cells in the lumens. NIH ImageJ software was used to quantify vessel density.

For dual immunofluorescent staining, tumor specimens were incubated with a mouse anti-hCD31 or Flk-1 for 2 hr followed by incubation with a goat anti-mouse Alexa Fluor secondary antibody (1: 250) for 1 hr. Then the samples were similarly incubated with a rabbit anti-SMa or GFAP antibody followed by incubation with a goat anti-rabbit Alexa Fluor antibody. Finally, DAPI was added to stain nuclei.

3.5.9 Statistics

Data are expressed as mean ± SE and n refers to the numbers of individual experiments performed. Differences among groups were determined using one-way ANOVA analysis followed by the Newman-Keuls test. The 0.05 level of probability was used as the criterion of significance.

CHAPTER 4

TUMOR-DERIVED MURAL-LIKE CELLS COORDINATE WITH ENDOTHELIAL CELLS: ROLE OF YKL-40 IN MURAL CELL-MEDIATED ANGIOGENESIS

The work presented in this chapter was done in collaboration with, Nipaporn Ngernyuang, Wei Yan, and Brooke Bentley. Parts of this chapter are taken from the published work: Francescone R, Ngernyuang N, Yan W, Bentley B, Shao R. Tumor-derived mural-like cells coordinate with endothelial cells: role of YKL-40 in mural cell-mediated angiogenesis. *Oncogene.* 2013. May 13. Epub.

4.1 Introduction

Neo-vascular networks function to deliver nutrients, oxygen, and other molecules to developmental tissue or pathologic lesion, the process known to mediate vasculogenesis and angiogenesis (Hanahan 1997, Hanahan and Folkman 1996). The key step of this event involves the formation of the neo-vasculature wall that is primarily composed of both endothelial cells and mesenchyme-derived mural cells including smooth muscle cells and/or pericytes (Jain 2003). In physiological angiogenesis (*e.g.* wound healing), endothelial cells initially sprout to form neo-vessels followed by recruitment of mural cells in a paracrine manner dependent on PDGFB-PDGFRβ and angiopoietin-1-Tie-2 reciprocal activation (Hellström, et al. 2001, Bloch, et al. 2000). It is acknowledged that vasculature in the central nervous system contains the highest amount of mural cell coverage (Armulik, Genové and Betsholtz 2011).

Once mural cells are recruited onto the abluminal surface of endothelial cell-based vessels, intercellular junctions between endothelial cells, mural cells, and/or endothelial-mural cells act as a central factor to render the vascular network mature and stable. A number of intercellular adhesion molecules are appreciated to regulate vessel fenestration, permeability, and stability. For instance, vascular endothelial cadherin (VE-cadherin) plays an important role in controlling endothelial-to-endothelial cell contacts (Carmeliet P 1999, Dejana, Orsenigo and

Lampugnani 2008, Orlova, et al. 2006), while neural cadherin (N-cadherin) mediates endothelial-to-mural cell and mural-to-mural cell communication (Paik, et al. 2004, Gerhardt, Wolburg and Redies 2000, Luo, et al. 2006). A key intracellular mediator of the cadherin-associated cell-to-cell contacts is β-catenin that acts as a physical link to the cytoskeleton assembly including actin (Dejana, Tournier-Lasserve and Weinstein 2009, Vestweber 2008). Disruption of the complex between cadherins and β-catenin results in decreased cell-cell interactions and increased cell permeability. Other gap junction proteins such as claudins, occludin, and connexins also participate in distinct intercellular interactions (Jain 2003, Armulik, Genové and Betsholtz 2011). The spatial cooperation and regulation of these cell-cell tight contacts commit endothelial cells and mural cells to orchestrate the vessel wall, which offers adequate nutrients and oxygen for tissue proliferation.

Although it remains to be clarified if different identities and/or functions of mural cells exist between tumor and normal vessels, chaotic vasculature with either abundant or insufficient coverage of mural cells is frequently observed during tumor angiogenesis (Carmeliet and Jain 2011). Deletion of mural cells in tumor-bearing mice exhibited an impaired vascular phenotype with diminished mature vessel formation and increased vessel permeability, thus retarding tumor progression (Huang, et al. 2010, Abramsson, Lindblom and Betsholtz 2003). As the most potent angiogenic factor, vascular endothelial growth factor (VEGF), also known as a vascular permeability factor, promotes endothelial permeability and destabilizes vascular integrity via interrupting VE-cadherin function in endothelial cells (Weis, et al. 2004, Gavard and Gutkind 2006). In light of VEGF activity in mural cell coverage of tumor vessels, there is strong evidence indicating that ablation of myeloid cell-derived VEGF in mice led to increased mural cell coverage of the vessels and acceleration of tumorigenesis. These findings unveil a new

pathologic signature of VEGF in functional inhibition of mural cell-associated vessels (Greenberg, et al. 2008, Stockmann, et al. 2008).

YKL-40 (human cartilage glycoprotein-39 or chitinase-3-like-1) is a secreted glycoprotein that was originally identified from culture medium of a human osteosarcoma cell line MG-63 (Johansen, Williamson, et al. 1992). Human YKL-40 protein contains an open reading frame of 383 amino acids with a molecular mass of 40 kDa and it is a member of glycoside hydrolase family 18 that contains chitinases. But YKL-40 can only bind chitin-like oligosaccharides and does not have chitinase/hydrolase activity because of the substitution of an essential glutamic acid with leucine in the chitinase-3-like catalytic domain (Renkema, et al. 1998, Fusetti, et al. 2003). YKL-40 is normally expressed by different cell types such as vascular smooth muscle cells (Shackelton, Mann and Millis 1995), macrophages (Rehli, Krause and Andreesen 1997), neutrophils (Kzhyshkowska, Gratchev and Goerdt 2007), chondrocytes (Hu, et al. 1996), and synoviocytes (Nyirkos and Golds 1990). To date, its biophysiological function in those cells including mesenchyme-derived mural cells/vascular smooth muscle cells is incompletely understood.

Multiple independent studies have shown that high serum levels of YKL-40 are correlated with metastasis and poor survival in a broad spectrum of human carcinomas including breast cancer (Jensen, Johansen and Price 2003), colorectal cancer (Cintin, Johansen, et al., Serum YKL-40 and colorectal cancer 1999), ovarian cancer (Hogdall, et al. 2003), leukemia (Bergmann, et al. 2005), lymphoma (Hottinger, et al. 2011), and glioblastoma (Pelloski, Mahajan, et al. 2005), suggesting that serum levels of YKL-40 serve as a diagnostic and prognostic cancer biomarker. We have recently demonstrated that YKL-40 acts as an angiogenic factor to stimulate vascular endothelial cell development in breast cancer and brain tumors (Shao, Hamel, et al. 2009, R. Francescone, S. Scully, et al. 2011). YKL-40 is also known to be associated with

tumor mesenchymal transition, displaying a poor prognosis (Phillips, et al. 2006). However, it is largely unknown how YKL-40-induced neo-vessels are stabilized to be functional and what the role of YKL-40 plays in tumor vasculogenesis characterized by communication between endothelial cells and mural cells.

4.2 Experimental Strategy

Here, we sought to explore the molecular mechanisms through which YKL-40 controls vascular permeability, stability, and angiogenesis mediated by mural cells in addition to vascular endothelial cells. To achieve this purpose, we took advantage of our recently established tumor cells named GSDC that are originally derived from human brain tumors and behave as vascular mural-like cells (R. Francescone, S. Scully, et al. 2012). This model demonstrates 1) tumors with vigorous vasculature when they are transplanted in animals; 2) a mesenchymal phenotype strongly expressing YKL-40, smooth muscle actin alpha (SMa), PDGFRβ, and vimentin; and 3) YKL-40 expressed by mural-like cells acts as a key factor regulating tumor vascularization. The current study has informed a key role of YKL-40 in both mural cell and endothelial cell biology during tumor angiogenesis.

4.3 Results

4.3.1 Tumor vascular coverage, stability, and angiogenesis are dependent on GSDCs expressing YKL-40.

To interrogate if YKL-40, a mesenchymal marker expressed by mural-like cells, GSDCs, acts as a central factor to establish vessel stability and integrity during tumor angiogenesis, we began our study by employing a gene knockdown approach utilizing a retroviral infection of shRNA against the YKL-40 gene in GSDCs. Two shRNA constructs sufficiently suppressed YKL-40 expression by over 90% compared to a shRNA scrambled control, as examined by western

blotting (Figure 4.1A). Accordingly, YKL-40 gene knockdown led to decreased expression of SMa, a mural cell marker, and cell motility (Figure 4.1A-C).

To investigate a potential role of YKL-40 in tumor vascular stability, permeability, and angiogenesis *in vivo*, we engaged an orthotopic xenografted tumor model by injecting GSDCs expressing scramble RNA or one of YKL-40 shRNAs (shRNA 1) into the brains of SCID/Beige mice for a 5-month observation period. After the mice were sacrificed, we examined tumor sections for angiogenesis by staining CD31, an endothelial cell marker. GSDC control tumors revealed a strong vascularized phenotype as an intense CD31-positive vessel density was found throughout the entire tumor region (Figure 4.2A-a). In contrast, YKL-40 shRNA tumors displayed a significant reduction of the vessel density by approximately 60% (Figure 4.2A-b +B). In addition, most of the vessels in the control tumors contained a visible lumen, whereas vessels in the YKL-40 shRNA tumors were collapsed and vessel diameters diminished to 30% relative to the control ones (Figure 4.2A-a, b, + B). An analysis of mural cell coverage by co-staining CD31 and SMa indicated that over 90% of endothelial cell-based vessels in the control tumors were covered with mural cells, in comparison with less than 40% of vessels lined with mural cells in the YKL-40 shRNA tumors (Figure 4.2A-c, d, & C). To distinguish vessels covered by the tumor-derived GSDCs from those by host-derived mural cells, we similarly injected GSDCs carrying green fluorescent protein (GFP) into different mice. The majority of endothelial cell vessels (CD31) were surrounded by GFP-positive GSDCs at the abluminal site where GFP and SMa were co-localized, while a few vessels were stained with CD31 only (Figure 4.3A-F), suggesting that tumor-derived mural-like cells make a significant contribution to tumor vessel coverage. Consistent with this finding, YKL-40 was expressed by SMa-positive mural cells in addition to tumor cells (Figure 4.3H + I). Vessel permeability was measured by diffusion of fibrinogen from the blood circulation. A limited amount of fibrinogen was identified to be diffused out of

capillaries in the control tumors, contrary to that in the YKL-40 shRNA tumors which contained more than 6-fold greater diffusion of fibrinogen, indicative of leakier vessels (Figure 4.2A-e, f, + Fig. D). These *in vivo* data suggest that YKL-40 expressed by GSDCs mediates vascular mural cell coverage, stability, and angiogenesis.

To characterize effects of YKL-40 on tumor development, the tumors were tested for the proliferation marker Ki67. GSDC control tumors displayed positive staining of Ki67 by 3.3-fold greater than did YKL-40 shRNA tumors (Figure 4.2E + F). Monitoring tumor cell growth in cultured condition revealed a decrease of cell proliferation by 10% in YKL-40 shRNA cells relative to counterparts (Figure 4.2G), suggestive of partial contribution of YKL-40 to the cell growth. In concert with tumor growth and angiogenesis, mice receiving control cells showed a trend towards decreased overall survival as compared with YKL-40 shRNA mice over this 5-month trial Figure 4.2H). In sum, the *in vivo* animal models gave rise to evidence supporting our hypothesis that YKL-40 derived from mural-like cells plays a vital role in maintaining vascular permeability, stability, and angiogenesis in tumors through mural cell coverage; thus fueling tumor growth and development.

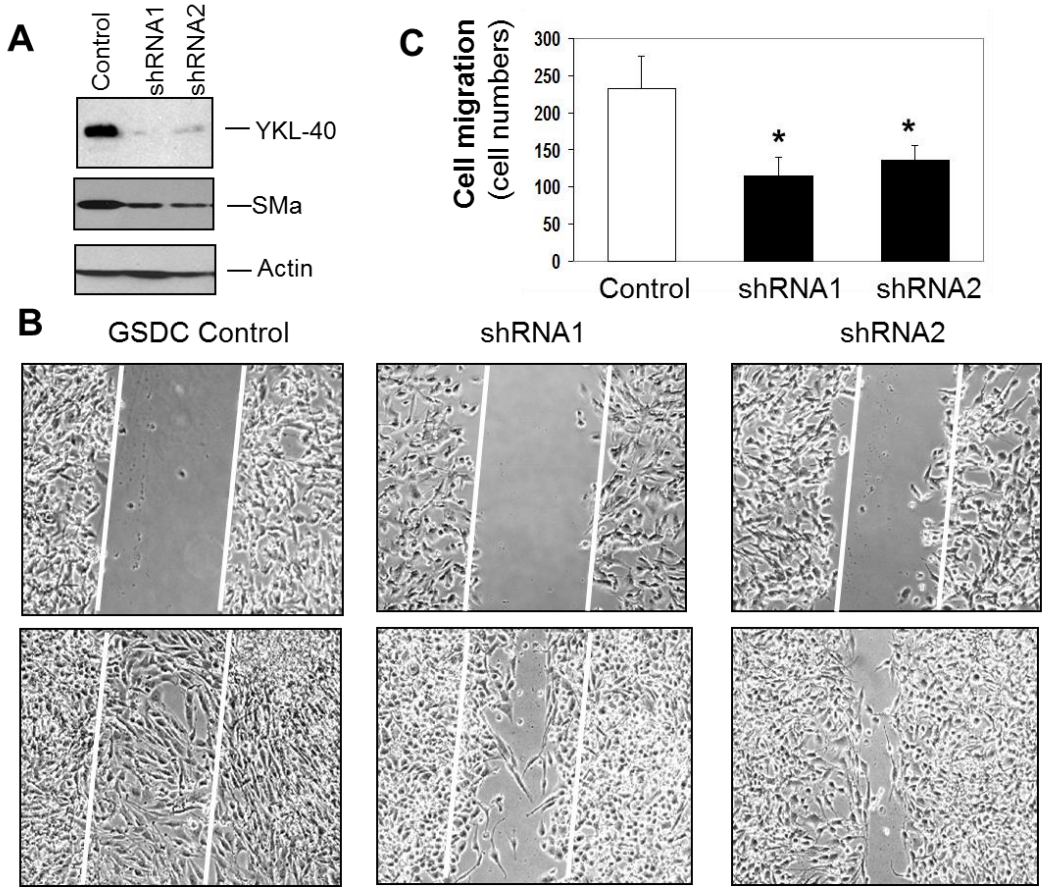

Figure 4.1 YKL-40 gene knockdown reduces SMa expression and the migratory capacity of GSDCs.

A. Western blot of the YKL-40 shRNA and the corresponding decrease in SMa expression. Actin is used as a loading control. **B.** Scratch wound migration assay at time point 0 h (Top panels) and 24 h later (Bottom panels) of the control and shRNA GSDCs. **C.** Quantification of the scratch wound migration assay portrayed in **(B.)**. N=3, * P≤0.05 compared to control.

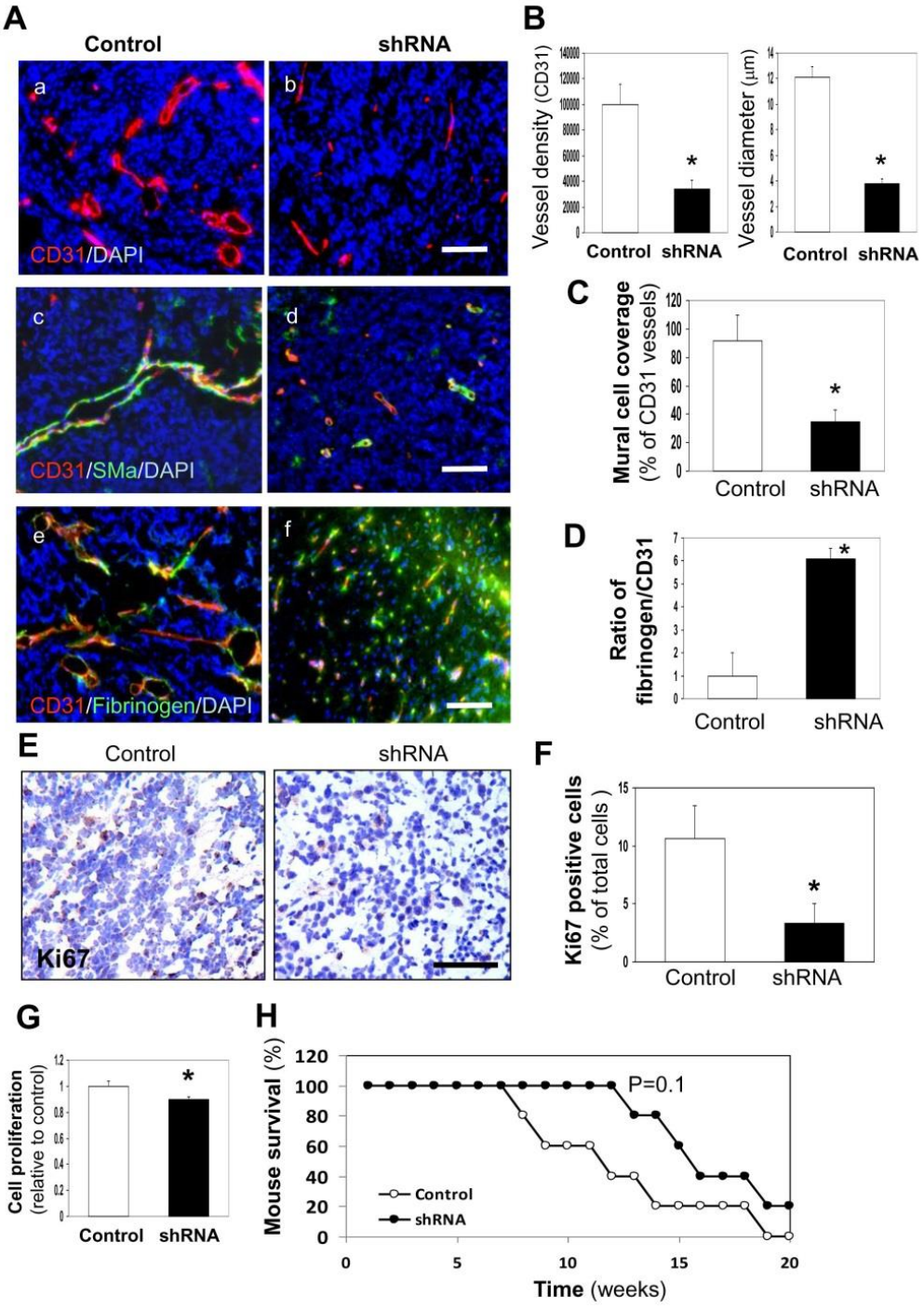
A
Control
shRNA
a
b
CD31/DAPI
c
d
CD31/SMa/DAPI
e
f
CD31/Fibrinogen/DAPI
B
Vessel density (CD31)
Control
shRNA
Vessel diameter (μm)
Control
shRNA
C
Mural cell coverage
(% of CD31 vessels)
Control
shRNA
D
Ratio of
fibrinogen/CD31
Control
shRNA
E
Control
shRNA
Ki67
F
Ki67 positive cells
(% of total cells)
Control
shRNA
G
Cell proliferation
(relative to control)
Control
shRNA
H
Mouse survival (%)
P=0.1
Control
shRNA
Time (weeks)

Figure 4.2 YKL-40 expression in GSDC-transplanted tumors is associated with vascular stability, mural cell coverage, angiogenesis, and tumor growth.

A. Representative immunofluorescent images of control and YKL-40 shRNA GSDC brain tumor sections from SCID/Beige mice depicted single staining of CD31 (red) **(a, b)** and double staining of CD31 (red) with either SMa (green) **(c, d)** or fibrinogen (green) **(e, f)**. DAPI (blue) was used to stain the nuclei. **B.** Quantification of CD31 vessel density and vessel diameter from A (a, b) as described in the Methods. The latter was an average of individual luminal diameters. **C.** Quantification of percent mural cell coverage of CD31 vessels from A (c, d). The data were derived from the ratio of SMa density to CD31 density. **D.** Quantification of the ratio of fibrinogen *vs.* CD31 for vessel leakiness from A (e, f), in which the ratio of fibrinogen density to CD31 density in the control tumors

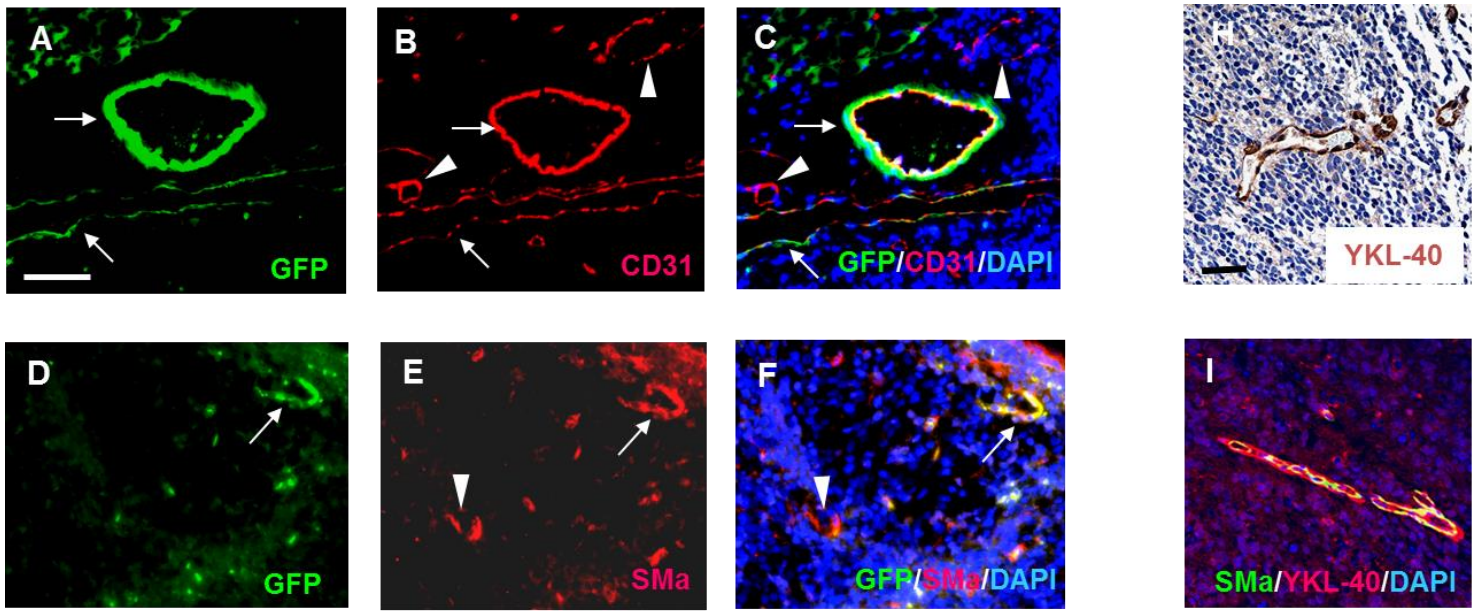

Figure 4.3 GSDCs cover a large portion of tumor vessels.

Brain tumor sections of SCID/Beige mice injected with GSDCs containing GFP were analyzed for GFP **(A. + D.)**, CD31 **(B)**, GFP + CD31 **(C)**, SMa **(E.)**, or GFP + SMa **(F)**. In **A-C**, most of vessels were lined by GSDCs indicated by arrows and a few vessels were devoid of GSDCs indicated by arrowheads. In **D-F**, co-expression of GFP and SMa surrounding vessel structures was shown by arrows. Mural cell-associated vessels expressing SMa but not GFP were indicated by arrowheads. Tumor tissue from GSDCs was stained for YKL-40 with IHC (H) and for SMa (green) and YKL-40 (yellow) with co-immunofluorescent assay (I). Bars: 100 mm.

4.3.2 YKL-40 expression is associated with strong intercellular contacts and adhesion of GSDCs

To explore molecular mechanisms that possibly mediate intercellular contacts and vascular coverage found earlier *in vivo*, we examined expression and interaction of N-cadherin/β-catenin/SMa in control and YKL-40 shRNA GSDCs. While N-cadherin remained unchanged, expression of β-catenin and SMa was decreased when the YKL-40 gene was knocked down (Figure 4.4A and Figure 4.3A). In control cells, VEGF production was barely detectable; but was dramatically up-regulated in YKL-40 shRNA cells. To determine if the interaction of N-cadherin with β-catenin and its downstream effector SMa was diminished due to the decreased levels of β-catenin and SMa by YKL-40 shRNA, we performed a co-immunoprecipitation assay followed by immunoblotting. Both interactions of N-cadherin with β-catenin and β-catenin with SMa in control cells were stronger than those in YKL-40 shRNA cells (Figure 4.4B). Accordingly, immunocytochemical analysis confirmed about two-fold higher association of N-cadherin with β-catenin in the control cells than that in the YKL-40 shRNA cells (Figure 4.4C). Likewise, the similar association patterns of β-catenin with SMa were found in these cells by immunocytochemistry (data not shown). However, the reduced association of N-cadherin and β-catenin in the YKL-40 shRNA cells could not be rescued by VEGF neutralization. These results suggest that YKL-40 expression by GSDCs is associated with the interaction of N-cadherin, β-catenin, and SMa, independent of VEGF activity.

In order to determine if these altered cell-cell contacts lead to changes in intercellular adhesion activity, we measured cell aggregation. YKL-40 shRNA inhibited cell aggregation by 55% compared to a control level (Figure 4.4D). Neutralizing N-cadherin via an anti-N-cadherin antibody in control GSDCs resembled the inhibition of YKL-40 shRNA, and combination of the N-cadherin blockade and YKL-40 shRNA slightly enhanced the inhibition on cell-cell adhesion,

implying that N-cadherin may contribute a primary role to YKL-40-mediated cell to cell adhesion (Figure 4.4D). Overall, these data underscore the importance of YKL-40 in the ability of GSDCs to maintain cell to cell junctions through the N-cadherin/β-catenin/SMa pathway.

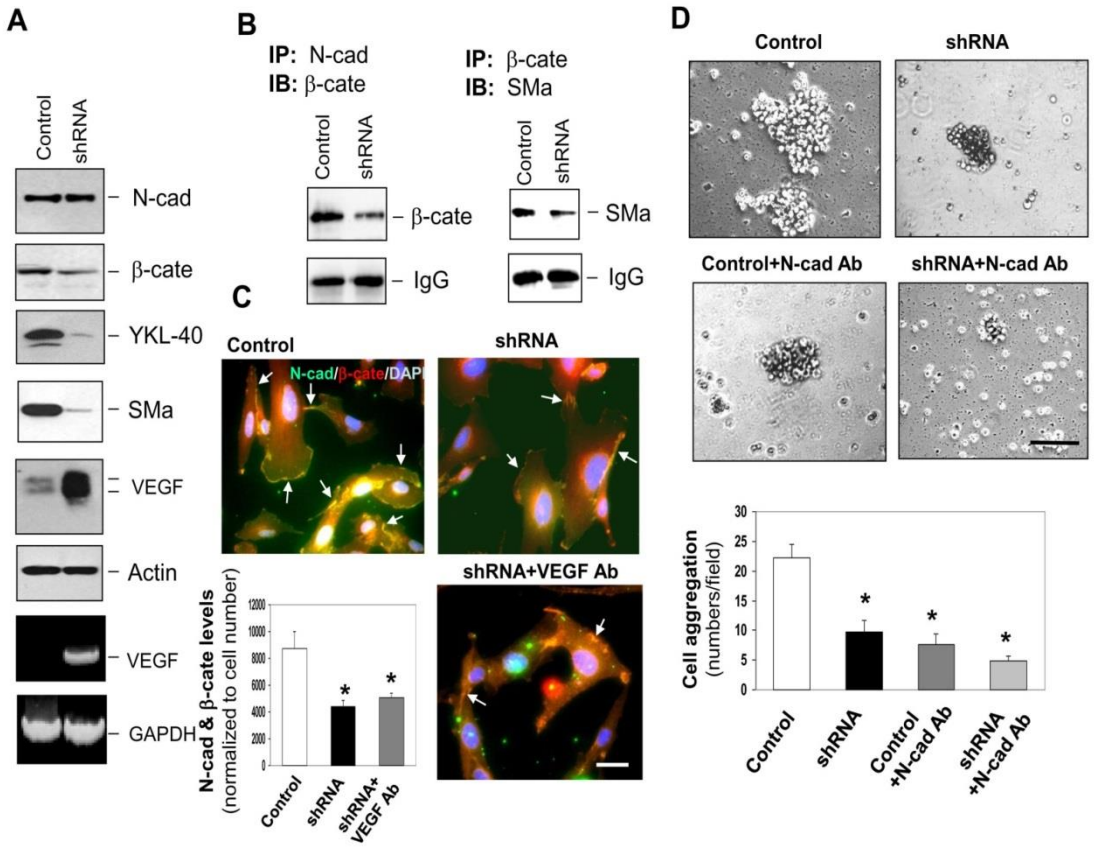

Figure 4.4 YKL-40 expression is associated with interaction of N-cadherin/β-catenin/SMa and cell-cell adhesion in GSDCs.

A. GSDC control and YKL-40 shRNA cell lysates were probed for N-cadherin (N-cad), β-catenin (β-cate), YKL-40, SMa, VEGF, and actin expression through western blotting. VEGF mRNA levels were also tested by RT-PCR with GAPDH as a loading control. **B. (Left)** Immunoprecipitation of N-cad from control and YKL-40 shRNA cell lysates was tested for its association with β-cate by western blotting against β-cate. **(Right)** Immunoprecipitation of β-cate from control and YKL-40 shRNA cell lysates was tested for its association with SMa by western blotting against SMa. IgG protein levels were used to ensure equal levels of antibody pull down. **C.** GSDC control and YKL-40 shRNA cells were treated with or without a neutralizing anti-VEGF antibody (100 ng/ml) overnight. Immunocytochemistry of N-cad (green) and β-cate (red) to determine overlapping staining (yellow) indicated by arrows. Cell nuclei were stained by DAPI (blue). A bar: 10 μm. Quantification of co-staining between N-cad and β-cate by normalization of overlapping images to cell number. N=3, *P≤0.05 compared with control. **D.** Representative pictures of the cell aggregation assay. Cells were subjected to serum-free media with either IgG or an N-cad neutralizing antibody (Ab, 50 μg/ml) for one hour. Cell aggregates of 10 or more cells were counted for each condition and quantified below. A bar: 100 μm. N=3, * P≤0.05 compared with control.

4.3.3 GSDC-conditioned medium containing YKL-40 mediates intercellular contacts and adhesion of endothelial cells

To explore effects of YKL-40 expressed by GSDCs on intercellular junctions of vascular endothelial cells via a paracrine manner, we used conditioned media from control or YKL-40 shRNA GSDCs in the culture of human microvascular endothelial cells (HMVECs) and measured intercellular contacts of VE-cadherin and β-catenin. HMVECs expressed a stronger level of VE-cadherin than N-cadherin, suggestive of a main role of VE-cadherin in cell to cell contacts (Figure 4.5A). The media from control and YKL-40 shRNA cells did not alter expression of VE-cadherin, N-cadherin, or β-catenin Figure 4.5A + Figure 4.6A). However, like GSDCs, co-immunoprecipitation studies showed that media from YKL-40 shRNA cells inhibited the interaction of VE-cadherin with β-catenin, and β-catenin with actin in HMVECs (Figure 4.5 + Figure 4.6B). A minimal level of N-cadherin/β-catenin association was detected in HMVECs treated with conditioned media from either control or YKL-40 shRNA cells (data not shown). Because VEGF secretion was significantly elevated in the conditioned media from YKL-40 shRNA cells (Figure 4.4A), the increased VEGF may contribute mainly to the reduced VE-cadherin/β-catenin interaction. To test this possibility, we used an anti-VEGF neutralizing antibody in the co-immunoprecipitation assay of HMVECs. VEGF blockade restored the association of VE-cadherin with β-catenin (Figure 4.5B). Consistent with the co-immunoprecipitation data, HMVECs treated with conditioned medium of YKL-40 shRNA cells displayed reduced co-localization of VE-cadherin and β-catenin to 13% relative to control cell medium, and treatment with an anti-VEGF neutralizing antibody recovered the co-localization to approximately 63% of the control levels (Figure 4.5C + D). In addition, the cell aggregation analysis unveiled the similar inhibition of cell to cell adhesion (by 46-54%) by conditioned media from YKL-40 shRNA, control cells treated with a VE-cadherin neutralizing antibody, or YKL-40 shRNA cells treated a VE-cadherin antibody (Figure 4.5E). To confirm the key role played by YKL-40 in endothelial cell to

cell interaction, we also treated conditioned medium of the control GSDCs expressing YKL-40 with a neutralizing YKL-40 antibody (mAY) (Faibish, et al. 2011). The conditioned medium containing mAY abolished the interaction between VE-cadherin and β-catenin relative to the control mIgG medium (Figure 4.5F). Accordingly, the control GSDC medium in the presence of mAY suppressed HMVEC aggregation by 60% compared to the aggregation in the presence of mIgG (Figure 4.5G). While neither the neutralizing anti-VEGF antibody nor mAY altered expression of VE-cadherin, N-cadherin and β-catenin in HMVECs (data not shown), treatment of control GSDCs with mAY inhibited YKL-40 expression; in contrast, the anti-VEGF antibody in YKL-40 shRNA GSDCs induced VEGF (Figure 4.6C), suggestive of distinct responses of mural cells to individual inhibitors. Collectively, these data suggest that YKL-40 may induce the VE-cadherin/β-catenin/actin pathway and cell to cell adhesion in endothelial cells, and that YKL-40 blockade inhibits these effects, which is largely dependent on VEGF.

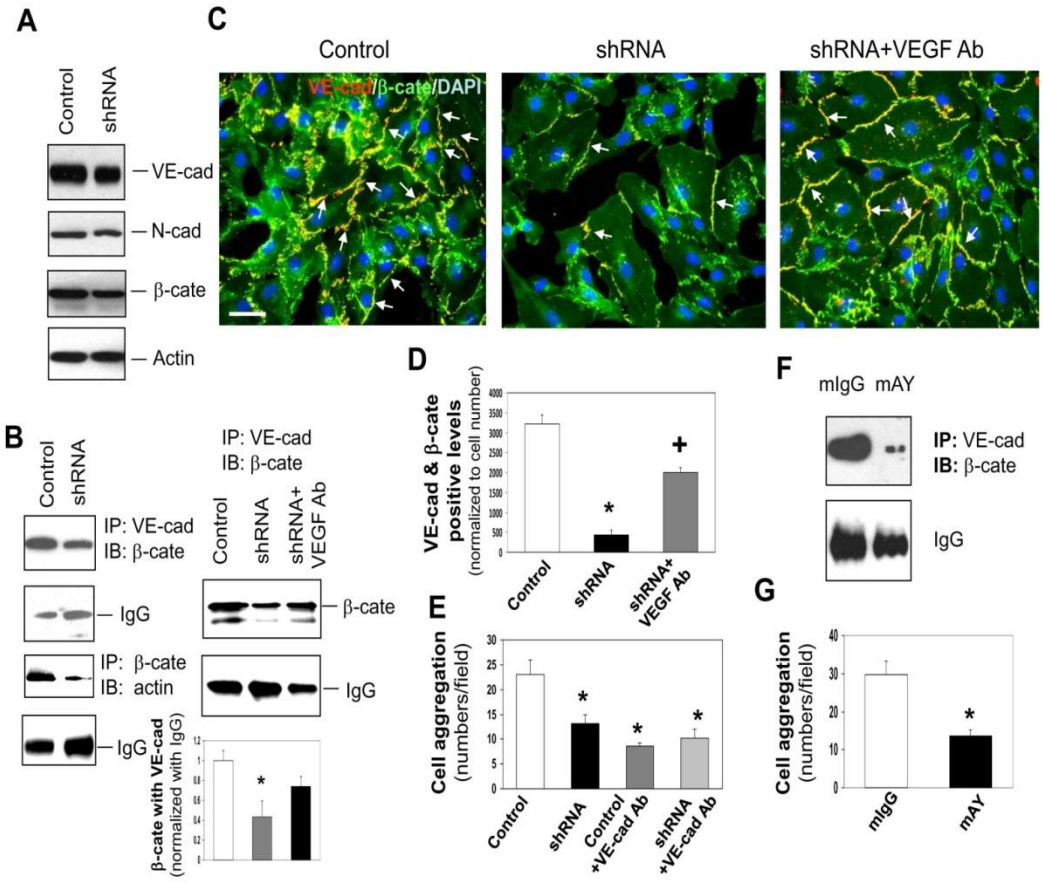
A
Control
shRNA
VE-cad
N-cad
β-cate
Actin
C
Control
shRNA
shRNA+VEGF Ab
VE-cad/β-cate/DAPI
B
Control
shRNA
IP: VE-cad
IB: β-cate
IgG
IP: β-cate
IB: actin
IgG
IP: VE-cad
IB: β-cate
Control
shRNA
shRNA+ VEGF Ab
β-cate
IgG
β-cate with VE-cad
(normalized with IgG)
D
VE-cad & β-cate positive levels
(normalized to cell number)
Control
shRNA
shRNA+ VEGF Ab
E
Cell aggregation
(numbers/field)
Control
shRNA
Control +VE-cad Ab
shRNA +VE-cad Ab
F
mIgG
mAY
IP: VE-cad
IB: β-cate
IgG
G
Cell aggregation
(numbers/field)
mIgG
mAY

Figure 4.5 YKL-40 mediates the interaction of VE-cadherin/β-catenin/actin and cell-cell adhesion in HMVECs.

A. Western blot analysis of VE-cad (VE-cad), N-cad, β-cate, and actin protein expression from the lysates of HMVECs treated with either control or YKL-40 shRNA GSDC-conditioned media for 24 hours. **B.** Immunoprecipitation of VE-cad from the HMVEC lysates treated for 24 hours with conditioned media from control, YKL-40 shRNA, or YKL-40 shRNA cells plus an anti-VEGF Ab (100 ng/ml) followed by immunoblotting of β-cate. IgG levels were used as a control. Immunoprecipitation of β-cate followed by immunoblotting against actin was similarly performed in HMVEC lysates. *P<0.05 compared with control. n=3. **C.** Double staining of VE-cad (red) with β-cate (green) in HMVECs treated with conditioned media from control, YKL-40 shRNA, or YKL-40 shRNA cells plus an anti-VEGF Ab to determine the extent of co-localization (yellow) indicated by arrows. Nuclei (blue) were stained by DAPI. A bar: 20 μm. **D.** Quantification of the immunocytochemistry images in part C, normalized to cell number. N=3, *P≤0.05 compared to control. $^{+}$P≤0.05 compared to control and YKL-40 shRNA. **E.** HMVEC aggregation was measured and quantified in the presence of GSDC control or YKL-40 shRNA media with an anti-VE-cad Ab (50 μg/ml). N=3, *P≤0.05 compared to control. **F.** HMVECs were treated with GSDC control medium in the presence of mAY or mIgG (10 μg/ml) overnight. Cell lystates were subjected to immunoprecipitation with an anti-VE-cadherin antibody followed by immunoblotting against β-cate. **G.** HMVECs treated with GSDC control medium in the presence of mAY or mIgG (10 μg/ml) were measured for cell aggregation. N=3, *P≤0.05 compared to control.

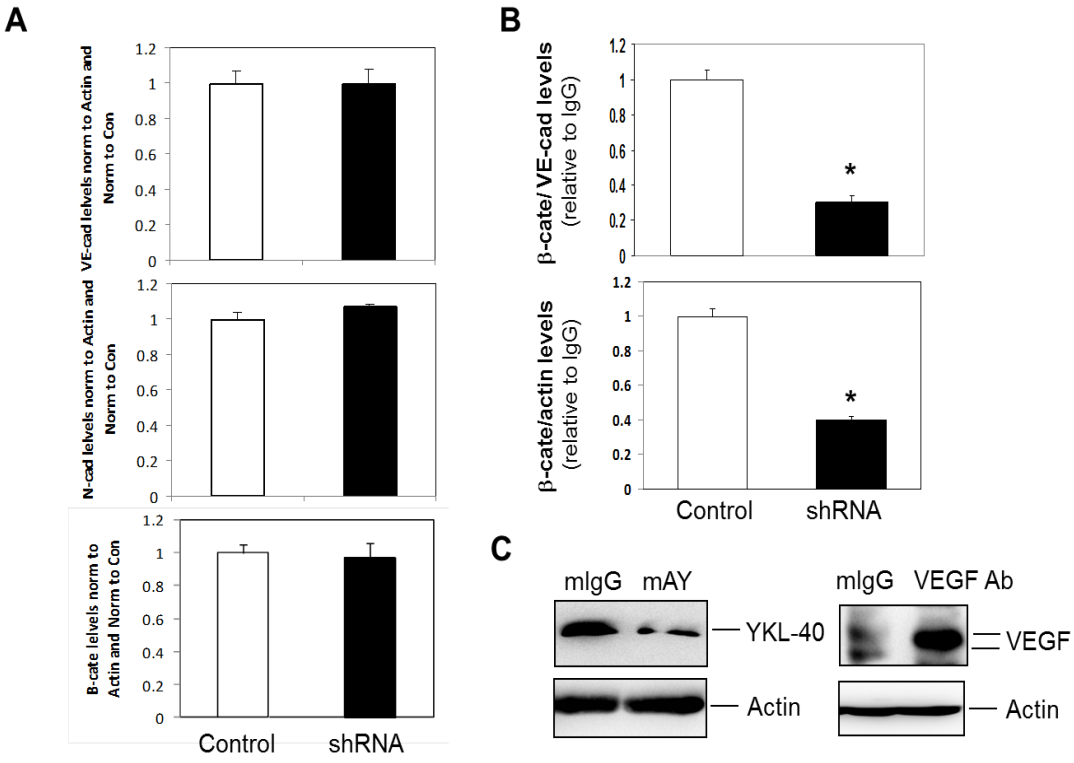

Figure 4.6 Data quantification and immunoblots.

A. Quantified data from immunoblotting of VE-cad, N-cad, and b-cate normalized with actin. **B.** Quantified data from immunoprecipitation and immunoblotting of VE-cad, b-cate, and actin normalized with IgG. N=2-4. *P<0.05 compared with controls. **C.** Control GSDCs and YKL-40 shRNA GSDCs were treated with mAY and a VEGF antibody, respectively, overnight. The conditioned media were used for immunoblotting against YKL-40 and VEGF.

4.3.4 YKL-40, in contrast to VEGF, stimulates interaction of VE-cadherin with β-catenin in HMVECs

In order to investigate the roles that YKL-40 and VEGF play individually in the association between VE-cadherin and β-catenin in HMVECs, we treated the cells with recombinant protein of VEGF or YKL-40. Treatment of HMVECs with YKL-40 or VEGF did not alter protein expression of VE-cadherin, N-cadherin, or β-catenin (data not shown). However, YKL-40 induced the interaction between VE-cadherin and β-catenin; in contrast, VEGF inhibited their association (Figure 4.7A). The immunocytochemical analysis validated this result that YKL-40 significantly increased co-localization of VE-cadherin and β-catenin by 60% relative to the control, while VEGF treatment decreased their co-localization by 43% (Figure 4.7B + C). In a trial using different concentrations of these proteins, VEGF (10 ng/ml) and YKL-40 (200 ng/ml) at the pathologic levels were found to have more effects on these adhesion molecule interactions than other concentrations (data not shown). The results indicate that YKL-40, in contrast to VEGF, induces the interaction of VE-cadherin and β-catenin in HMVECs, further supporting the earlier findings using GSDC-conditioned media expressing YKL-40.

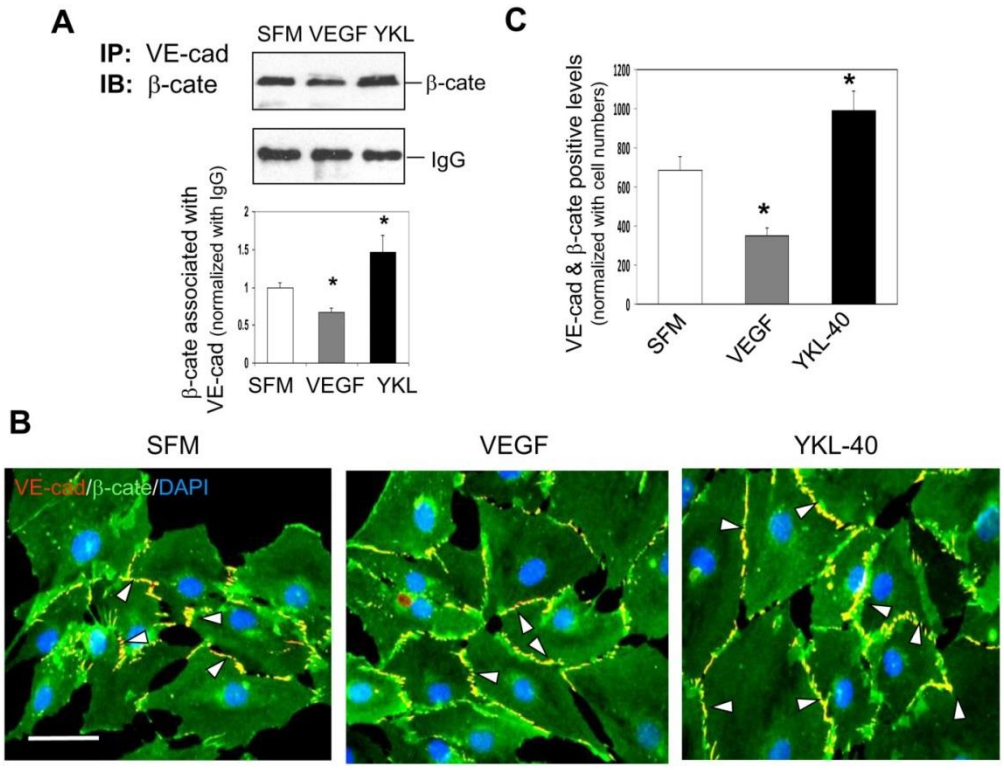

Figure 4.7 YKL-40 enhances interaction of VE-cadherin and β-catenin, but VEGF attenuates the interaction in HMVECs.

A. (Top) HMEVC lysates treated 24 hr with serum-free medium (SFM) with or without 10 ng/mL VEGF, or 200 ng/mL recombinant YKL-40 were immunoprecipated with an anti-VE-cad Ab and probed for β-cate by western blotting. IgG was used as IP control. **(Bottom)** Quantification of the western blots above, normalized to IgG levels. *P<0.05 compared with SFM. n=3. **B.** Representative images of VE-cad (red) and β-cate (green) double stained HMVECs in the presence of either SFM, 10 ng/mL VEGF, or 200 ng/mL for 24 hr. White arrowheads highlight the areas positively co-stained for VE-cad and β-cate (yellow). **C.** Quantification of the VE-cad/β-cate overlap in the images in part C. A bar: 20 μm. N=3, *P≤0.05 compared to control.

4.3.5 YKL-40 expressed by GSDCs mediates the cadherin/catenin complexes in co-culture of GSDCs and HMVECs

To monitor the interaction of cadherin and catenin between endothelial cells and mural cells that may recapitulate their functional relationship in vessels *in vivo*, we undertook an immunocytochemical approach probing the co-localization of either VE-cadherin/β-catenin or N-cadherin/β-catenin in a cell co-culture system with GSDCs and HMVECs. Intense co-staining of VE-cadherin/β-catenin was found in HMVECs mixed with control GSDCs, but this co-localization was decreased by 58% in HMVECs when co-cultured with YKL-40 shRNA GSDCs (Figure 4.8A), in which HMVECs were distinguished from GSDCs by positive staining of VE-cadherin as indicated with white asterisks (Figure 4.8A). This is indicative that YKL-40 expressing cells are crucial to VE-cadherin/β-catenin interaction in HMVECs.

Next, to determine the interaction between the N-cadherin and β-catenin in this co-culture system, we labeled GSDCs only with nuclear staining DAPI prior to mixing with HMVECs, because both cell types express N-cadherin and β-catenin. By this approach, we could discern GSDCs (DAPI-positive) from HMVECs (DAPI-negative), and analyzed individual GSDC-GSDC, HMVEC-HMVEC, and GSDC-HMVEC contacts (Figure 4.8B, top & bottom left). Membrane co-localization of N-cadherin and β-catenin between control GSDCs was found around 38% of GSDC population, but this co-staining between YKL-40 shRNA GSDCs was reduced to 23% (around 40% reduction compared with the control) (Figure 4.8B, bottom right). However, there was no appreciable difference of their co-localizations in other cell types. In line with the findings earlier using the single cell type system, the data suggest that YKL-40 mediates VE-cadherin/β-catenin association in HMVECs and N-cadherin/β-catenin complex in GSDCs.

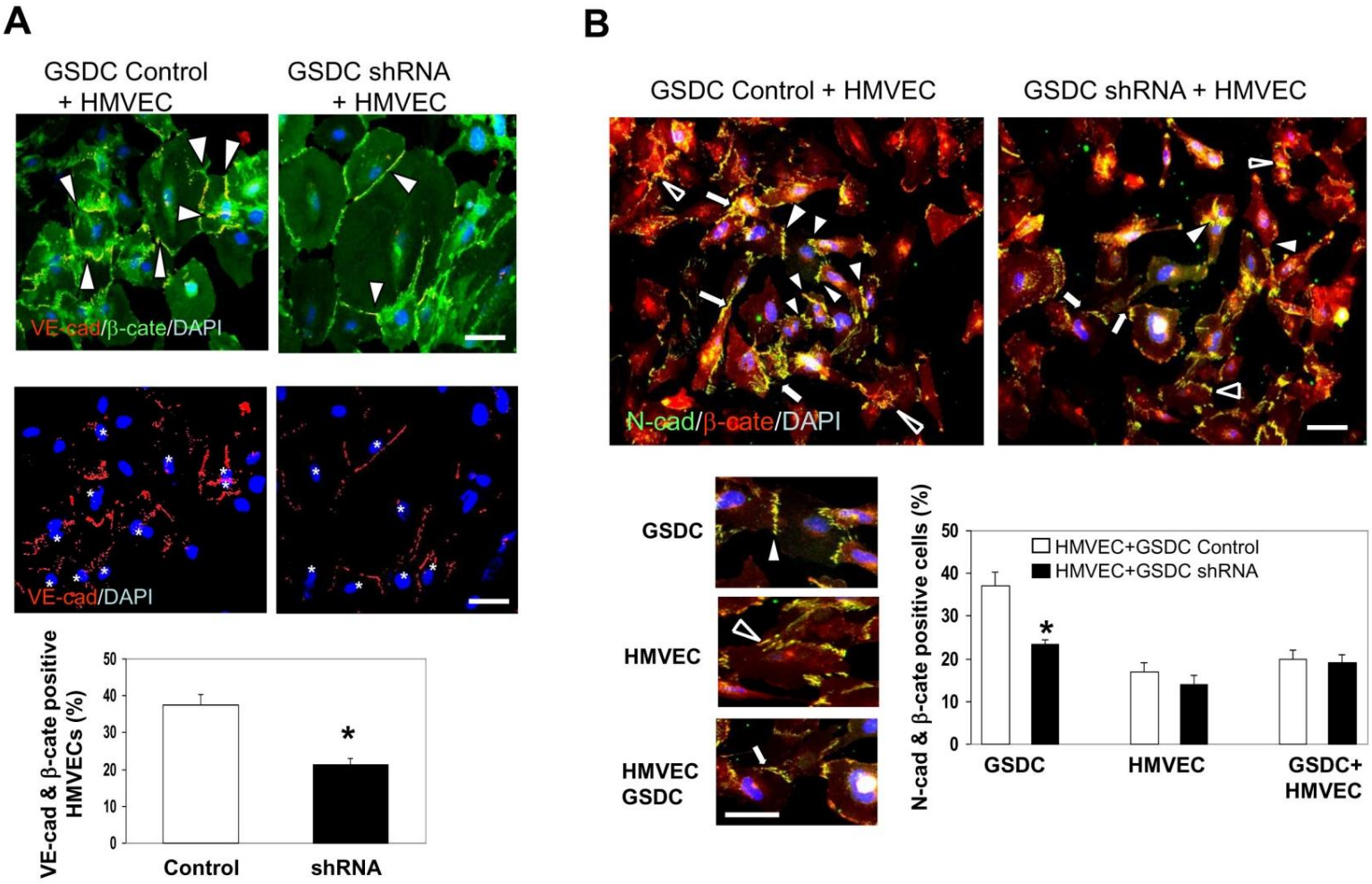
A
GSDC Control
+ HMVEC
GSDC shRNA
+ HMVEC
VE-cad/β-cate/DAPI
VE-cad/DAPI
VE-cad & β-cate positive HMVECs (%)
50
40
30
20
10
0
*
Control
shRNA
B
GSDC Control + HMVEC
GSDC shRNA + HMVEC
N-cad/β-cate/DAPI
GSDC
HMVEC
HMVEC
GSDC
N-cad & β-cate positive cells (%)
HMVEC+GSDC Control
HMVEC+GSDC shRNA
50
40
30
20
10
0
*
GSDC
HMVEC
GSDC+
HMVEC

Figure 4.8 Co-culture of HMVECs and YKL-40-expressing GSDCs displays interaction between cadherin and catenin.

A. (Top) HMVECs cultured with control or YKL-40 shRNA GSDCs were stained for VE-cad (red) and β-cate (green). White arrowheads mark regions of co-localization of VE-cad and β-cate. **(Middle)** VE-cad (red) staining was to show HMVECs distinct from VE-cad-negative GSDCs. White asterisks indicate HMVECs. DAPI (blue) was used as a nuclear stain for all images. **(Bottom)** Quantification of the percentage of HMVECs that have co-expression (yellow) of both VE-cad and β-cate in a total of HMVECs. Bars: 10 μm. N=3, *P≤0.05 compared to control. **B. (Top)** HMVECs and either control or YKL-40 shRNA GSDCs were cultured together and tested for overlapping of N-cad (green) and β-cate (red). DAPI was pre-stained for the nuclei of GSDCs only, but not for HMVECs to discriminate different cell types. **(Bottom, Left)** Representative images of the different types of cell to cell contacts: GSDC-GSDC (white arrowhead), HMVEC-HMVEC (black arrowhead), and HMVEC-GSDC (white arrow). **(Bottom, right)** Quantification of the percentage of cells containing N-cad/β-cate overlapping contacts in a total of individual cell types, displayed by cell contact types. Bars: 10 μm. N=3, *P≤0.05 compared to control.

4.3.6 YKL-40 expression by GSDCs is associated with restricted permeability of HMVECs and GSDCs

To further evaluate permeability of HMVECs and GSDCs, one of the key vascular functions, we utilized a permeability method that assays the ability of cells to be permeable to Dextran conjugated with FITC. First, we treated HMVECs with either conditioned media from control or YKL-40 shRNA GSDCs, and we found that control medium-treated HMVECs restricted the permeability that allowed FITC-Dextran to cross through the cells 30% less than did YKL-40 shRNA medium-treated cells (Figure 4.9A, top graph). In order to verify the functional role of VE-cadherin in HMVEC permeability, we added a VE-cadherin neutralizing antibody to the media. While mIgG, as a control, did not have an impact in the permeability treated with control or YKL-40 shRNA media, a VE-cadherin antibody increased cell permeability in control medium-treated HMVECs (Figure 4.9A, middle graph). However, this VE-cadherin neutralization in YKL-40 shRNA medium-treated cells failed to enhance the permeability induced by YKL-40 shRNA, consistent with HMVEC-HMVEC adhesion found earlier (Figure 4.5E). This implies that VE-cadherin plays a key role in the elevated permeability of HMVECs treated with YKL-40 shRNA media. In order to determine the effect of VEGF on permeability, as VEGF mediated the disassociation of β-catenin from VE-cadherin (Figure 4.5B-D), we treated the HMVECs with an anti-VEGF neutralizing antibody. The anti-VEGF antibody fully reversed the GSDC YKL-40 shRNA medium-induced permeability to the level treated with GSDC control media (Figure 4.9A, bottom graph). As expected, the anti-VEGF antibody did not have effects on the permeability of control medium-treated HMVECs because of the considerably lower level of VEGF in the control media. To validate this endothelial cell permeability restrained by YKL-40, we treated HMVECs with mAY in the presence of GSDC control medium and found that mAY induced HMVEC permeability by 51% (Figure 4.10A). These results suggest that YKL-40 maintains HMVEC

permeability and that YKL-40 blockade destabilizes the permeability probably through VE-cadherin activation.

Next, we assessed impacts of YKL-40 on GSDC permeability. GSDCs expressing YKL-40 shRNA exhibited a much higher permeability than control GSDCs, as the permeability of YKL-40 shRNA GSDCs was increased by up to 58% at 4 hr (Figure 4.9, top graph). Inhibition of N-cadherin using an anti-N-cadherin neutralizing antibody resulted in a 25% and 20% elevation in the permeability of control and YKL-40 shRNA GSDCs, respectively, compared with mIgG treatment over the 4-hr observation (Figure 4.9B, middle graph). Unlike an anti-VE-cadherin antibody in HMVECs (Figure 4.9A, middle panel), blocking N-cadherin in YKL-40 shRNA GSDCs enhanced cell permeability (by 20% compared with YKL-40 shRNA), analogous with the adhesion result (Figure 4.4D), suggesting that other cell adhesion factors, in addition to N-cadherin, may also participate in YKL-40-mediated cell adhesion and permeability. For example, inhibition of integrins αVβ3 or αVβ5 partially increased cell leakage relative to N-cadherin inhibition (Figure 4.10B). To further validate that VEGF contributes to HMVEC, but not GSDC, permeability, we treated GSDCs with an anti-VEGF antibody. As expected, this anti-VEGF antibody failed to have an effect on the permeability of control or YKL-40 shRNA GSDCs that express strong VEGF (Figure 4.9B, bottom graph). These results suggest that YKL-40 stabilizes GSDC permeability in a manner mainly dependent on N-cadherin.

Finally, to evaluate the overall cell permeability mediated by both GSDCs and HMVECs that would be more representative of vessel function in vivo, we loaded either control or shRNA GSDCs first for 2 hours followed by plating HMVECs on the top of the GSDCs, which simulated the vascular orientation from an “endothelial cell to mural cell” layer and encountered penetration of FITC-Dextran. Co-cultured YKL-40 shRNA GSDCs with HMVECs induced the “vascular” permeability by 25% greater than that of the system containing HMVECs and control

GSDCs (Figure 4.10C). To assess the role of VEGF in cell permeability, we treated both cells with an anti-VEGF antibody. Consistent with the results found in the single HMVEC system above, VEGF abrogation suppressed the permeability of HMVECs induced by YKL-40 shRNA GSDCs to the control level (Figure 4.9C). Dual treatment with VE-cadherin and N-cadherin antibodies in HMVECs with either control GSDCs or YKL-40 shRNA GSDCs led to stronger increases in the permeability than that induced by YKL-40 shRNA GSDCs in the presence of mIgG (Figure 4.9D), suggesting that combined activities of VE- and N-cadherin contribute predominantly to the vessel permeability. Collectively, all the data support the notion that YKL-40 controls vascular permeability by regulating VE-cadherin and N-cadherin function in endothelial cells and mural cells, respectively.

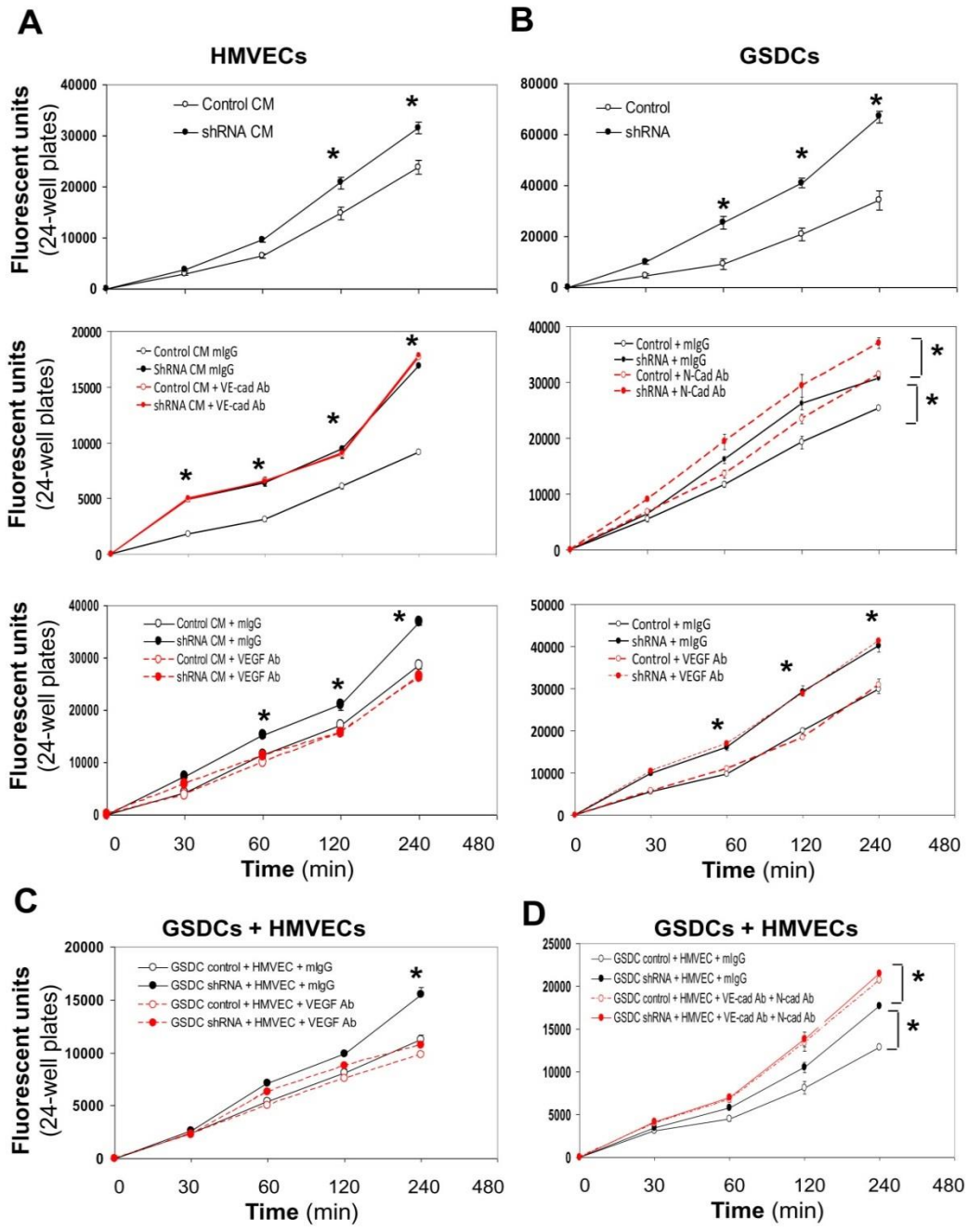
A
HMVECs
Fluorescent units (24-well plates)
Control CM
shRNA CM
Control CM mIgG
ShRNA CM mIgG
Control CM + VE-cad Ab
shRNA CM + VE-cad Ab
Control CM + mIgG
shRNA CM + mIgG
Control CM + VEGF Ab
shRNA CM + VEGF Ab
Time (min)
B
GSDCs
Control
shRNA
Control + mIgG
shRNA + mIgG
Control + N-Cad Ab
shRNA + N-Cad Ab
Control + VEGF Ab
shRNA + VEGF Ab
C
GSDCs + HMVECs
GSDC control + HMVEC + mIgG
GSDC shRNA + HMVEC + mIgG
GSDC control + HMVEC + VEGF Ab
GSDC shRNA + HMVEC + VEGF Ab
D
GSDCs + HMVECs
GSDC control + HMVEC + mIgG
GSDC shRNA + HMVEC + mIgG
GSDC control + HMVEC + VE-cad Ab + N-cad Ab
GSDC shRNA + HMVEC + VE-cad Ab + N-cad Ab

Figure 4.9 YKL-40 decreases permeability of HMVECs, GSDCs, and their combination in a manner dependent on VE-cad or N-cad activity.

A. HMVECs were plated on inserts and allowed to attach and spread. Cells were treated overnight with either GSDC control conditioned media (CM, 24 hr serum-free media) or YKL-40 shRNA CM **(Top)**, control or YKL-40 shRNA CM with mouse IgG or an anti-VE-cad Ab (20 μg/ml) **(Middle)**, or anti-VEGF Ab (100 ng/ml) **(Bottom)**. Cell permeability was then measured using FITC-Dextran as described in the Methods. **B.** GSDC control or YKL-40 shRNA cells were used for the same permeability assay **(Top)** as described in **(A)**, in the presence of an anti-N-cad Ab (50 μg/ml) **(Middle)** or VEGF Ab (100 ng/ml) **(Bottom)**. **C.** GSDC control or YKL-40 shRNA cells were first plated on the insert. 2 hr following attaching and spreading, HMVECs were plated on the top of the GSDCs to form a second layer and allowed to attach and spread in the presence of mIgG or an anti-VEGF Ab (100 ng/ml). The same permeability assay was performed on the next day. **D.** GSDCs were pre-treated with mIgG or an anti-N-cad Ab (50 μg/ml) overnight to exclude the possibility that the top layer of HMVECs prevents the antibody from access to the bottom layer of GSDCs. Then, GSDCs and HMVECs were set up as described in C in the presence of mIgG or an anti-VE-cad Ab (20 μg/ml). The permeability was measured. N=6, *P≤0.05 compared to corresponding controls at the same time points.

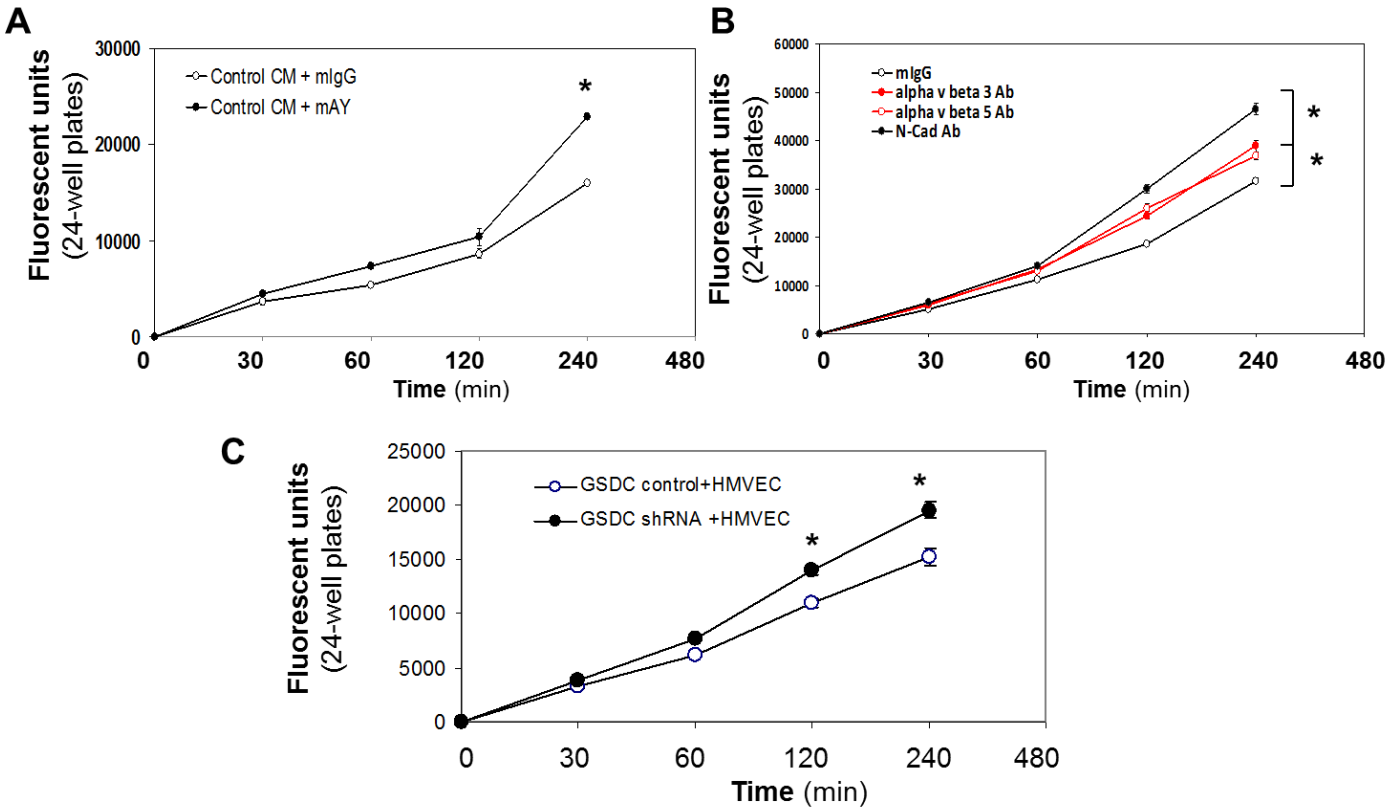

Figure 4.10 Effects of mAY, YKL-40 shRNA, and integrin antibodies on cell permeability.

A. HMVECs were plated in inserts and treated with conditioned medium (CM) of control GSDCs in the presence of mIgG or mAY (10 mg/ml) overnight. Cell permeability was measured. **B.** Control GSDCs were plated in inserts in the presence of anti-N-cadherin (50 mg/ml), integrin avb3, or avb5 antibody (10 mg/ml). Then, cell permeability was determined. **C.** GSDC control or YKL-40 shRNA cells were plated for 2 hr followed by loading HMVECs on the top of the GSDCs. Cell permeability was determined on the next day. N=6, *P<0.05 compared with corresponding controls.

4.3.7 HMVEC-formed tubules are stabilized by GSDCs expressing YKL-40

In an attempt to assess if GSDCs indeed act as mural cells to stabilize endothelial cell vessels, we employed a tube formation assay on Matrigel by co-culturing both HMVECs and GSDCs. HMVECs pre-labeled with Calcein AM (green fluorescence) were mixed with either control or YKL-40 shRNA GSDCs pre-labeled with Calcein red (red fluorescence). Stability of tubules formed by HMVECs and GSDCs was monitored over a 64-hr time course. As shown in Figure 4.11A, HMVECs co-cultured with control GSDCs maintained tubules longer than did HMVECs in the presence of YKL-40 shRNA GSDCs. The breakdowns and gaps in the tube network, indicated by arrows, were significantly less in HMVECs with control GSDCs at 24 hours and 40 hours than corresponding HMVECs co-cultured with YKL-40 shRNA GSDCs (Figure 4.11A + B). HMVECs alone maintained their own tubules only between 24-36 hr (data not shown). To further validate the individual role of VE-cadherin and N-cadherin in vascular stability, we treated this co-culture system with a VE-cadherin or N-cadherin neutralizing antibody. When HMVECs co-cultured with control GSDCs were treated with either cadherin antibody, tubule stability was decreased to the level seen in the co-culture of HMVECs and YKL-40 shRNA GSDCs (Figure 4.11C + Figure 4.12). As expected in the system of HMVECs and YKL-40 shRNA GSDCs, anti-VE-cadherin and N-cadherin antibodies were unable to influence the stability because of impaired activity of VE-cadherin and N-cadherin by YKL-40 gene knockdown. To determine a role of VEGF in the co-culture system, we treated HMVECs and control GSDCs with recombinant VEGF, and we found that the addition of VEGF to the YKL-40-expressing system developed more stabilized tubules than did control counterparts Figure 4.11C + Figure 4.12). The phenotype of elevated tubes is probably due to the synergistic cooperation of these two strong angiogenic factors for the tube generation and stabilization, as the vessel-destabilized property of VEGF may be notably minimized in the presence of YKL-40. An anti-VEGF antibody partially rescued

the tube stability formed by HMVECs and YKL-40 shRNA cells that express a high level of VEGF. Failure of full tubule recovery in the presence of the anti-VEGF antibody is attributed to impaired N-cad function, even when VEGF is inhibited. Thus, these data suggest that the ability of GSDCs to stabilize endothelial cell-based vasculature is reliant on YKL-40 expression that regulates VEGF, VE- and N-cadherin activity. Altogether, in coordination with tumor vasculature found *in vivo*, the *in vitro* system identifying cell-cell contacts/adhesion, permeability, and stability of vascular wall cells have provided the critical mechanisms strengthening our conclusion that YKL-40 plays a central role in mural cell-mediated tumor angiogenesis via autocrine and paracrine loops.

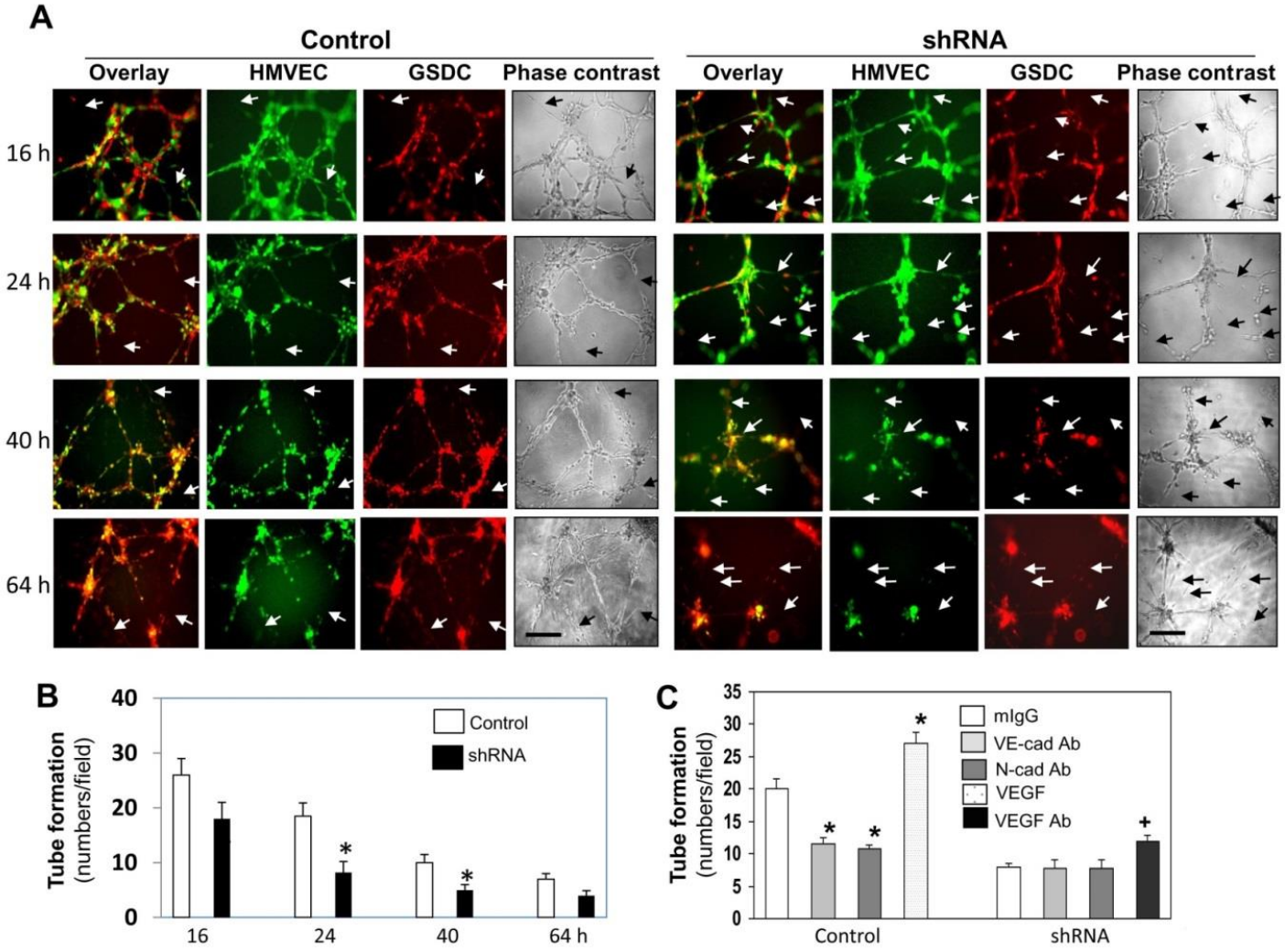
A
Control
shRNA
Overlay
HMVEC
GSDC
Phase contrast
16 h
24 h
40 h
64 h
B
Tube formation
(numbers/field)
Control
shRNA
16
24
40
64 h
C
Tube formation
(numbers/field)
mIgG
VE-cad Ab
N-cad Ab
VEGF
VEGF Ab
Control
shRNA

Figure 4.11 GSDCs expressing YKL-40 stabilize endothelial cell vessels in a manner dependent on VE-cadherin and N-cadherin activity.

A. HMVECs and either control or YKL-40 shRNA GSDCs were pre-stained with Calcein AM (green) and Calcein red, respectively, and plated together on Matrigel. Tube formation was analyzed over a 64-hour time course and representative images were shown at 16, 24, 40, and 64 hr. White arrows demonstrated breaks in the tube networks, while black arrows on the phase contrast images depicted gaps in the corresponding networks. Bars: 100 μm. **B.** Quantification of the tubules formed by HMVECs plus control or YKL-40 shRNA GSDCs. N=3, *P≤0.05 compared to controls. **C.** Same condition as described in A was set up in the presence of recombinant VEGF (10 ng/ml), an anti-VEGF (100 ng/ml), VE-cadherin (20 μg/ml), or N-cadherin antibody (50 μg/ml). 24 hr following incubation, tubules with fluorescence were analyzed and quantified. N=3, *P≤0.05 compared to mIgG.

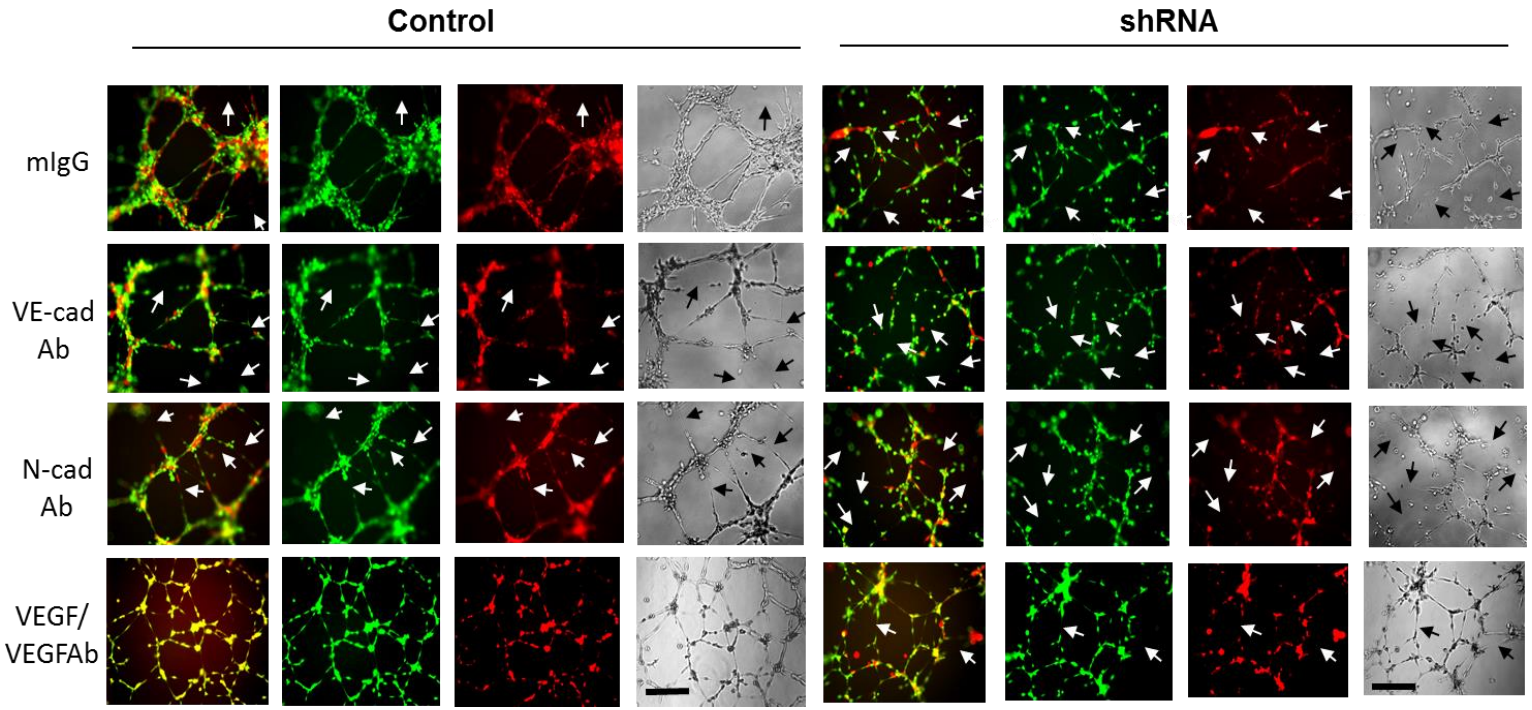

Figure 4.12 Inhibition of VE-cadherin or N-cadherin activity leads to decreases in vascular stability.

HMVECs and either control or YKL-40 shRNA GSDCs were pre-labeled with Calcein AM (green) and Calcein red, respectively, and plated together on Matrigel in the presence of an anti-VE-cadherin (20 mg/ml), anti-N-cadherin (50 mg/ml), or anti-VEGF antibody (100 ng/ml). 24 hr following incubation, tubule images with fluorescence were analyzed. White arrows demonstrated breaks in the tube networks, while black arrows on the phase contrast images depicted gaps in the corresponding networks. Note recombinant VEGF (10 ng/ml) in control and an anti-VEGF Ab in shRNA. Bars: 100 mm.

4.4 Discussion

We previously demonstrated that YKL-40 can induce endothelial cell angiogenesis in tumors (Shao, Hamel, et al. 2009). Here, we have provided substantial evidence using brain tumor-derived mural-like cells to uncover a new angiogenic role of YKL-40 in tumor vascular permeability, stability, and activity characterized by the intimate interaction between endothelial cells and mural cells. This finding was also supported by the identical mural-like characteristics of brain tumor cells from different patients (data not shown). The reason for selecting such mesenchyme-derived mural cells is because a considerable subset of brain tumors (*e.g.* glioblastomas) express strong YKL-40 and demonstrate poorer prognosis with a mesenchymal phenotype and vigorous vascularization (R. Francescone, S. Scully, et al. 2011, Phillips, et al. 2006). In addition, the vasculature of the central nervous system is typically covered with abundant mural cells in angiogenesis (Armulik, Genové and Betsholtz 2011). Thus, the current study has advanced our knowledge about YKL-40 in both mesenchymal mural cell and vascular endothelial cell biology during tumor vascularization. Furthermore, understanding the regulation of the intercellular junctions that mediate the interaction between endothelial cells and mural cells, rather than focusing on endothelial cells alone, has offered additional mechanistic insights into the entity of the angiogenic process induced by YKL-40 in tumor microenvironment.

In physiological angiogenesis, bone marrow-derived progenitor cells or myofibroblastic precursors are appreciated as the primary mesenchymal origin capable of differentiating into mural cells that involve vessel maturation (Chambers, et al. 2003, Tomasek, et al. 2002, Elenbaas and Weinberg 2001). However, in tumor angiogenesis, transplanted tumor cells expressing mesenchymal markers YKL-40, SMa, and vimentin were found to serve as a major component of mesenchymal mural cells. This is the first time in our knowledge to provide evidence indicating

that tumor-derived mural-like cells may functionally substitute host-derived mesenchymal mural cells that are presumably deregulated in the scenario of highly vascular proliferation. Therefore, the evidence enhances our understanding of potential functional and genetic differences in different mural cell identities such as mesenchymal tumor-derived mural cells *vs.* host mesenchyme-differentiated mural cells. YKL-40 supports vessel stability and maintains vascular integrity mainly through activation of the N-cadherin/β-catenin/SMa and VE-cadherin/β-catenin/Actin pathway in mural-to-mural cell and endothelial-to-endothelial cell contacts, respectively. YKL-40 gene knockdown impaired these junctions, leading to vessel collapse and leakage, as a schematic model is illustrated in Figure 4.13. To further support this model, an additional study *in vivo* assaying vessel perfusion and oxygenation by injection of a hypoxia probe will be essential. By this approach, dysfunction of tumor perfusion and oxygenation ascribed to YKL-40 gene knockdown can be visualized. Thus, the characterization of tumor vascular development *in vivo*, in context with the present findings from vascular permeability and stability models using the co-culture systems, demonstrates that elevated YKL-40 mediates vascular mural cell coverage, stability, and angiogenesis; ultimately fostering tumor cell proliferation. These findings underscore a key role of YKL-40 in the establishment of tumor angiogenesis mediated by the coordination of mural cells with endothelial cells. Indeed, focusing on mural cell-mediated vessel coverage and stabilization has recently received significant attention in tumor neo-vascularization, the event that renders tumor cells evasive during the conventional anti-angiogenic therapy. For example, melanoma deficient of mural cells exhibited a leakier vascular phenotype and were more sensitive to an anti-VEGF drug Bevacizumab than the tumors that harbored mural cell-covered vessels (Helfrich, et al. 2010), highlighting a protective role of mural cells in exposure to an anti-angiogenic drug. Whether or not YKL-40-stabilized vessels play the identical role in the drug resistance remains to be clarified,

as it may hold therapeutic promise in patients who do not respond to angiogenesis-blocking agents.

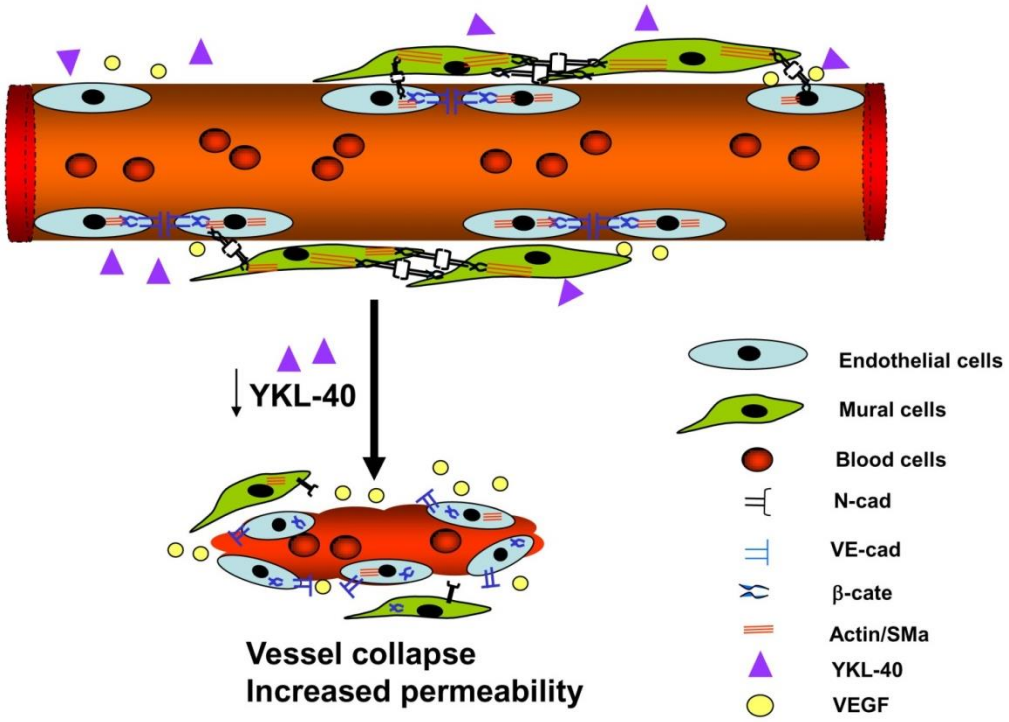

Figure 4.13 A hypothetical model of vessel stability and angiogenesis mediated by YKL-40-expressing mural cells.

A tumor blood vessel is covered with mural cells that express high YKL-40 levels. YKL-40 promotes cell-cell contacts of mural cells via enhanced N-cadherin/β-catenin interaction and downstream effector SMa in an autocrine manner. In addition, YKL-40 also induces VE-cadherin/β-catenin/actin association in endothelial cells in a paracrine loop. Once expression of YKL-40 is inhibited, both mural cell and endothelial cell contacts are disrupted, which impairs vascular permeability and stability. As a result, the diminished angiogenesis restricts nutrients and oxygen delivery to the tumors, impeding the tumor growth.

VEGF, a strong permeability factor, stimulates angiogenesis and tumor growth through enhancing endothelial cell migration, proliferation, survival as well as vessel permeability or destabilization of endothelial-to-endothelial cell contacts (Chen, et al. 2012, Ferrara and Kerbel 2005). VEGF-induced vessel permeability is associated with VE-cadherin tyrosine phosphorylation and degradation. VEGF binds its membrane tyrosine kinase receptor 2 (Flk-1) and induces Flk-1 tyrosine phosphorylation and activity that can activate VE-cadherin by Src-dependent tyrosine phosphorylation (Lambeng, et al. 2005, Nakamura, et al. 2008, Lin, et al. 2007). Subsequently, the activated VE-cadherin disassociates from Flk-1 and β-catenin, and is internalized to the cytoplasm where it is degraded. Thus, VE-cadherin phosphorylation leads to the loss of cell-cell junctions and the increase in cell permeability (Shrivastava-Ranjan, Rollin and Spiropoulou 2010, Gorbunova, Gavrilovskaya and Mackow 2010, Shay-Salit, et al. 2002). Our current studies have provided multiple relevant results supporting this mechanism. For example, stimulation of endothelial cells with VEGF reduced the association between VE-cadherin and β-catenin, and treatment with an anti-VEGF antibody in YKL-40 shRNA cells over-expressing VEGF facilitated the interaction of VE-cadherin with β-catenin. VE-cadherin blockade led to increased endothelial cell permeability, the effect identical to treatment of these cells with YKL-40 shRNA medium expressing high levels of VEGF. In addition, this VE-cadherin neutralization failed to enhance endothelial cell permeability induced by YKL-40 shRNA medium, suggesting that functional loss of VE-cadherin mediates VEGF-induced cell permeability. It is emerging that VEGF exhibits distinct impacts on endothelial cells and mural cells. Although we did not find effects of VEGF on GSDC permeability, there is evidence demonstrating inhibitory effects of VEGF on mural cell coverage of the vessels, thereby suppressing tumor development (Greenberg, et al. 2008, Stockmann, et al. 2008). We also interestingly found that expression of β-catenin and SMa, in contrast to VEGF, was down-regulated in YKL-40 shRNA cells, suggesting

that YKL-40 differentially regulates their expressions. Intracellular pathways mediating SMa and VEGF expression involve PI3K and/or MAPK signaling, as a PI3K inhibitor Wortmannin or MAPK inhibitor PD98059 blocked their expression in GSDCs (Figure 4.14). This finding is consistent with our previous reports that PI3K-Akt and MAPK Erk-1 and Erk-2 mediate YKL-40 signaling in the regulation of angiogenesis and cell survival in U87 cells and GSDCs (R. Francescone, S. Scully, et al. 2011, R. Francescone, S. Scully, et al. 2012, Faibish, et al. 2011). It will also be interesting to interrogate if a membrane receptor specific for YKL-40 mediates the activation and expression of these molecules, as it is likely that the YKL-40 receptor interacts and coordinates with its adjacent cadherins to induce intracellular signaling pathways.

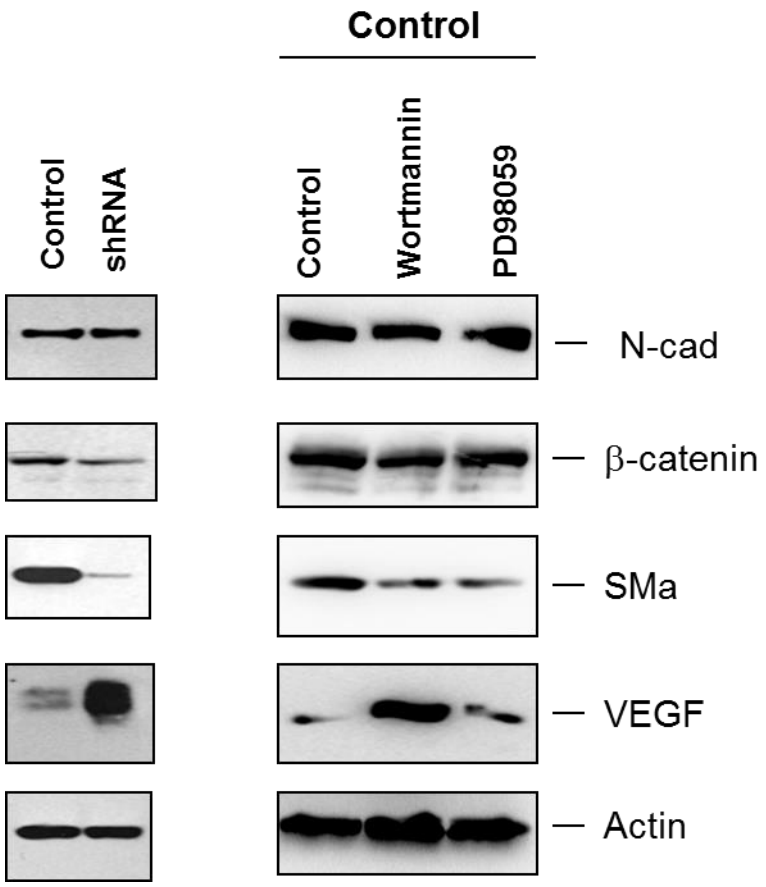

Figure 4.14 PI3K and MAPK signaling pathways mediate expression of SMa and VEGF in GSDCs.

GSDCs were treated with PI3K inhibitor Wortmannin (10 nM) and MAPK inhibitor PD98059 (10 mM) overnight. Cell lysates and media were collected to test N-cad, b-catenin, SMa, and VEGF in immunoblotting. Actin was a control.

We utilized GSDCs derived from a glioblastoma patient and found this population participates in the vascular stability and permeability, functioning as mural cells. YKL-40 shRNA led to induction of VEGF, which seems to conflict with our previous findings in which YKL-40 up-regulates VEGF in glioblastoma cells U87, a commercially available tumor cell line (R. Francescone, S. Scully, et al. 2011). A number of possibilities might account for this discrepancy observed in the different studies. First, the heterogeneity of tumor could contribute to the difference of VEGF expression and its regulation by YKL-40, as glioblastomas contain several cell subpopulations such as astrocytes, neurons, and oligodendrocytes, in addition to other vascular cells and immune cells. Expression of VEGF is higher in U87 cells than that in GSDCs and another glioblastoma cell line SNB-75 (data not shown). Indeed, YKL-40 and VEGF expression vary in individual glioblastoma patients (R. Francescone, S. Scully, et al. 2011). Second, the elevation of VEGF in GSDCs expressing YKL-40 shRNA may represent a compensating effect in angiogenic responses during a chronic course of YKL-40 blockade, the event resembling the neutralization of VEGF in U87 cells that also increased YKL-40 expression (R. Francescone, S. Scully, et al. 2011). Neutralizing VEGF in YKL-40 shRNA GSDCs led to induction of VEGF expression, although the neutralized VEGF is not functional, supporting the compensating responses of the cells to their severely impaired angiogenic activities. Thus, those two vascular promoting factors coordinate and regulate each other to render tumors vascularized. Supporting this speculation, VEGF induced by YKL-40 in U87 cells stimulated endothelial cell tube formation, while in this study we primarily focused on VEGF in endothelial cell permeability, these different events cooperative for angiogenesis. In addition, adding VEGF to the co-culture system of YKL-40-expressing control GSDCs and HMVECs induced and stabilized vascular tubes (Figure 4.11C). It is currently unknown which factor expressed differentially by U87 and GSDCs plays a key role in the regulation of VEGF that divergently induces angiogenesis through the different cells. HIF-1α is

not a core factor to contribute to the differential expression of VEGF in both cells (data not shown). Finally, even though it is currently unknown if U87 cells also mediate vascular stability via VEGF expression controlled by YKL-40, it is conceivable that multiple molecular mechanisms are involved in YKL-40-induced vascular stability and integrity, not limited to VEGF only. In the present study, we found that vascular stability contributed by GSDCs is dependent on N-cadherin, in contrast to endothelial cell-mediated permeability that depends on activation of VEGF-VE-cad. Therefore, the regulation between YKL-40 and VEGF in tumor vascularization relies on the function of individual cell populations that orchestrate tumor mass, vascular endothelium, and/or mural cell (vessel supporting) network.

Recent pre-clinical and clinical trials have established a therapeutic paradigm complementary to the conventional vessel-blocking regimen, in which normalization of tumor vascular abnormalities impedes tumor development (Carmeliet and Jain 2011). Depletion of mural cells in animal tumor models led to diminished blood vessels, increased tumor hypoxia, and restrained tumor growth (Huang, et al. 2010). PDGF over-expression in patients was found to be associated with metastasis (Liu, et al. 2011) and PDGF blockade that impairs mural cell recruitment was reported to improve drug delivery and chemotherapy (Jayson, et al. 2005, Hellberg, Ostman and Heldin 2010). It is also noteworthy that delivery of drugs targeting both endothelial cells (*e.g.* VEGFR inhibitor) and mural cells (*e.g.* PDGFRβ inhibitor) was more effective than individual anti-angiogenic drugs, because destabilizing vessels by inhibition of mural cell function rendered endothelial cells more susceptible to endothelial cell blockers (Erber, et al. 2004, Bergers, Song, et al. 2003). Despite these promising data, conflicting evidence was also documented from several animal settings and clinical trials. For instance, deletion of mural cells promotes metastasis probably due to lack of a barrier preventing tumor

cells from dissemination into the circulation system (Gerhardt and Semb, Pericytes: gatekeepers in tumour cell metastasis? 2008). Analogous with these findings, decreased mural cell coverage around vessels in patients is correlated with cancer metastasis (Yonenaga, et al. 2005). Although the molecular mechanisms underlying these distinct outcomes remain to be deciphered, the data suggest that multiple regulatory pathways be involved in the formation of tumor vascular network that demonstrates spatial-temporal deregulation of the interaction between endothelial cells and mural cells. Therefore, in the evaluation of drug delivery and therapy, several important factors mediating vascular maturation and normalization should be taken into account, such as vessel coverage, permeability and stability, interstitial fluid pressure, oxygen delivery, and local blood perfusion. Nevertheless, our current findings on YKL-40 in tumor angiogenesis characterized by coupling of mural cells to endothelial cells have demonstrated a potential therapeutic target in treatment of cancer patients that produce high levels of YKL-40.

4.5 Methods

4.5.1 Cell Culture

GSDCs established previously were grown in DMEM supplemented with 10% FBS and penicillin/streptomycin (39). HMVECs were grown in EBM-2 (Lonza, Allendale, NJ) supplemented with 5 μg/ml hydrocortisone, 10 ng/ml hEGF, 10% FBS, and penicillin/streptomycin.

4.5.2 YKL-40 Gene knockdown

DNA oligos (19 bp) specifically targeting N-terminal (siRNA 1) or C-terminal (siRNA 2) region of YKL-40, were selected and then templates (64 oligo nucleotides) containing these oligos were

subcloned into a retroviral pSUPER-puro-vector (OligoEngine, Seattle, WA) (40). 293T retroviral packaging cells were transfected with pSUPER siRNA constructs in the presence of pCL 10A1 vector using Fugene 6 (Roche, Indianapolis, IN). Forty-eight hours after transfection, the supernatant was harvested and filtered through 0.45-μm pore size filter and then the viral medium was used to infect targeted cells. Selection with 1 μg/ml of puromycin was started 48 hr after infection and the puromycin-resistant cell populations were used for subsequent studies.

4.5.3 Immunoprecipitation and immunoblotting

Cell lysate samples were processed as described previously (Yan, Bentley and Shao, Distinct angiogenic mediators are required for basic fibroblast growth factor- and vascular endothelial growth factor-induced angiogenesis: the role of cytoplasmic tyrosine kinase c-Abl in tumor angiogenesis 2008). Samples were subjected to running SDS-PAGE and PVDF membranes were incubated with one of a series of primary antibodies against N-cadherin, VE-cadherin (Invitrogen, Carlsbad, CA), β-catenin (Santa Cruz Biotechnology, Santa Cruz, CA), YKL-40 (our lab), VEGF (Sigma, St. Louis, MO), SMa (Abcam, Cambridge, MA), and actin (Sigma). Membranes were then incubated with goat anti-mouse or anti-rabbit secondary antibodies (Jackson Lab, Bar Harbor, Maine). Specific signals were detected by enhanced chemiluminescence (VWR, Rockford, IL). For immunoprecipitation, cell lysates were incubated with either an anti-VE-cadherin, N-cadherin, or β-catenin antibody at 4^0C overnight followed by incubation with protein G Sepharose 4 Fast Flow beads at 4^0C for 4 hr. The immunocomplex was extensively washed and the samples were run for immunoblotting as described earlier.

4.5.4 RT-PCR

Total RNA from cells was extracted with Tri-reagent (Molecular Research Inc, Cincinnati, OH). RNA concentration and purity were determined spectrophotometrically ($A_{260/280}$). cDNAs with poly A tails were subsequently synthesized through a reverse transcriptional reaction in the presence of 15-oligo (dT) (Promega, Madison, WI). A fragment of VEGF and GAPDH DNA was synthesized by a polymerase chain reaction with sense primer 5'-CTTTCTGCTGTCTTGGGTGC-3' and antisense primer 5'- GTGCTGTAGGAAGCTCATCTCTCC-3', and sense primer 5'-ATGGGGAAGGTGAAGGTCGGA-3' and antisense primer 5'-CTCCTTGGAGGCCATGT-3', respectively.

4.5.5 MTS Assay

Cellular proliferation was measured using Cell Titer 96 Aqueous Nonradioactive Cell Proliferation Assay Kit (Promega, Madison, WI) per the manufacturer's instructions. Briefly, GSDCs ($2x10^3$ cells) were plated onto a 96 well plate and allowed to grow overnight. The next day, the MTS reagent was added to the cells and incubated at 37° C for 1 hour. The plate was read at 490 nm absorbance to determine cell proliferation.

4.5.6 Cell permeability

HMVECs or GSDCs (2×10^5cells) were loaded onto 0.4-μm 24-transwells pre-coated with 100 μg/ml collagen IV overnight. For cell co-culture, GSDCs (1×10^5cells) were loaded for 2 hr prior to HMVECs (1×10^5cells). 24 hr later, Dextran conjugated with FITC (0.4 mg/ml, Invitrogen) was added on the top of the wells for 4 hr. At various time points, an aliquot from the bottom of the wells was measured for absorbance at 485 μm.

4.5.7 Immunocytochemistry

The method was described previously (Yan, Cao, et al. 2010). Briefly, cells were grown to sub-confluence and fixed with 4% paraformaldehyde for 5 min. After permeabilization with Triton 100X, the cells were incubated with an anti-N-cadherin or VE-cadherin monoclonal antibody (1:100, Invitrogen) at 4^0C overnight followed by incubation with a secondary anti-mouse or rabbit Alexa Fluor 488 or Alxa Fluor 555 antibody (1:1000, Invitrogen) for 2 hr. Cell nuclei were stained with DAPI. For dual staining, after incubation of the first antibody, the samples were then incubated with a polyclonal anti-β-catenin (1:100, Santa Cruz) or SMa antibody (1:100, Abcam) as described earlier. Positive staining in a single cell was defined based on each cell recognized by nuclear staining of DAPI. The positive signal from a viewed field was quantified with software ImageJ and then normalized with total cell numbers positive for DAPI. In some of dual-cell culture staining analyses, in addition to nuclear DAPI counted for cell number, a specific cell marker (*e.g.* VE-cad for endothelial cells) was also used to distinguish marker-positive cells from marker-negative cells. Images were analyzed using a Nikon TE2000U inverted fluorescent microscope.

4.5.8 Tube formation

HMVECs (2 x 10^4cells) were transferred onto 96-well Matrigel (BD Bioscience, San Jose, CA). After 16 hours of incubation, tube-forming structures were analyzed. Images were analyzed with an inverted microscope. Averages of tubules were calculated from three fields in each sample. For the vascular stability assay, HMVECs (2 x 10^4cells) and GSDCs (2 x 10^3cells) pre-labeled with Calcein AM and Calcein Red (5 μg/ml, Invitrogen), respectively, were mixed and loaded onto 96-well Matrigel over 64 hours. Tubules with fluorescence were imaged and quantified at various time points.

4.5.9 Cell aggregation

GSDCs or HMVECs ($2x10^6$) were re-suspended in 1 mL of serum-free media containing 1mM $CaCl_2$ and transferred to a 2-mL Eppendorf tube. The tube was placed in a shaker at 90 rpm at 37°C for 1 hour. Finally, cells were transferred to a cell culture dish for phase contrast imaging of cell aggregation. Aggregates were counted as colonies of 10 cells or more.

4.5.10 Scratch wound migration

GSDCs were plated at 95% confluency on a 24-well plate and allowed to grow overnight. A sterile 200 µL tip was then used to make a scratch through the middle of the well. The wells were washed gently twice with PBS to remove floating cells. Images were taken at time points 0 and 24 hr and the number of cells that migrated into the scratch was quantified.

4.5.11 Tumor xenografts in mice

All animal experiments were performed under the approval of Institutional Animal Care and Use Committee of the University of Massachusetts. GSDCs expressing control vector or YKL-40 shRNA (1.5×10^5) cells in 10 µl of PBS were injected into right striatum of SCID/Beige mice. Mice were sacrificed when mice displayed decreased locomotion.

4.5.12 Immunohistochemistry and immunofluorescence

Paraffin-embedded or frozen tumor tissue were cut to 6 µm thickness and processed for immunohistochemical analysis. In brief, samples were incubated with 3% H_2O_2 for 30 min to block endogenous peroxidase activity, followed by incubation with blocking buffer containing 10% goat serum for 1 hr. The samples then were incubated at room temperature for 2 hr with a rabbit polyclonal anti-Ki67 antibody (1:100, Invitrogen). A goat anti-rabbit secondary antibody (1: 100, Dako Inc, Carpinteria, CA) conjugated to HRP was added for one hr. Finally, DAB

substrate (Dako Inc) was introduced for several minutes and after washing, methyl green was used for counterstaining. For a single and dual immunofluorescent staining, tumor specimens were incubated with a rat anti-CD31 (1: 50, BD Pharmingen, San Diego, CA) antibody for 2 hr followed by incubation with a goat anti-rat Alexa Fluor 555 secondary antibody (1: 250) for 1 hr. Then the samples were similarly incubated with a mouse anti-SMa (1:500, Dako Inc) or rabbit anti-fibrinogen antibody (1: 100, Dako Inc) followed by incubation with a goat anti-mouse or rabbit Alexa Fluor 488 antibody (1: 250) for 1 hr. Finally, DAPI was added to stain nucleus. NIH ImageJ software was used to quantify vessel density in the single staining of CD31, individual density of SMa, CD31, and fibrinogen in dual staining.

4.5.13 Statistics:

Data are expressed as mean ± SE and n refers to the numbers of individual experiments performed. Differences among groups were determined using one-way ANOVA analysis followed by the Newman-Keuls test. The 0.05 level of probability was used as the criterion of significance.

CHAPTER 5

FUTURE DIRECTIONS

5.1 Search for the YKL-40 Receptor

While we have uncovered multiple roles for YKL-40 in tumor progression, with a particular emphasis on the molecular mechanisms of tumor vasculature (Shao, et al. 2009, R. Francescone, et al. 2011, Faibish, et al. 2011, Francescone, Ngernyuang, et al. 2013), how YKL-40 initiates these signaling cascades still remains unknown. The identification and characterization of the potential receptor of YKL-40 is therefore a vital avenue to pursue for two major reasons. First, we would gain insight into how YKL-40 works at the membrane to initiate the activation of downstream signaling pathways. Second, and most importantly, the discovery of the YKL-40 receptor would offer another therapeutic target for pharmaceutical development. Inhibition of the membrane receptor could result in more potent suppression of tumor progression, as small molecule drugs could also be developed for membrane proteins.

5.2 Validation Combination Therapy that includes Anti-YKL-40 treatment *in vivo*:

YKL-40 undoubtedly plays an important role in conferring radioresistance to glioblastoma cells, especially *in vitro* (Pelloski, et al. 2005) (R. Francescone, et al. 2011) (Junker, et al. 2005). However, it is not clear whether anti-YKL-40 therapy, in conjunction with radiation, chemotherapy, and anti-angiogenic therapy would be well tolerated by the patient. Therefore, it is of the utmost importance that more studies are done *in vivo* to determine the efficacy and safety of adding an anti-YKL-40 regimen to the current “standard of care” for glioblastoma. This would ultimately have direct clinical applications and could lead to clinical trials in humans for the treatment of GBM.

5.3 Summary

Vasculature is a vital source of nutrients and oxygen for an expanding tumor, and is often considered the rate limiting step in tumor progression. Glioblastoma (GBM) is characterized by extremely high amounts of vasculature, whether it is host or tumor derived. It remains a key target in cancer therapy, although most treatments rely on blocking angiogenesis, leaving all other types of vasculature unscathed. In addition, these types of therapies tend to increase the invasion of glioblastoma cells into the normal brain, which is detrimental to patient survival. Thus, new molecular targets unique to glioblastoma must be uncovered, and their mechanisms fully defined, in order to develop more effective therapies. One exciting biomarker and putative therapeutic target is the secreted glycoprotein YKL-40. It is highly expressed in the serum of many high grade cancers and is correlated with short survival and resistance to therapies, and this is especially true in glioblastoma. In chapter 2, I discussed work that was done in our lab that unveiled the signaling pathways involved with YKL-40 mediated angiogenesis in glioblastoma. In addition, we showed its ability to confer radioresistance to GBM cells. Overall, blockade of YKL-40 prolonged the survival of mice in two distinct models, demonstrating the therapeutic value of inhibiting YKL-40.

In chapter 3, I presented a study that illustrated the plasticity of GBM tumor cells. The stem-like cells from a human patient with GBM could be differentiated into mural-like cells that could form vasculature independent of endothelial cells, referred to as vasculogenic mimicry (VM). In addition, these cells where functionally dependent on the protein Flk-1, which is the major receptor to vascular endothelial growth factor (VEGF). On the other hand, the formation of VM was independent of VEGF, which is important to note because most therapies target VEGF mediated angiogenesis, highlighting the significance of inhibiting other forms of vasculature in GBM. All in all, this study was novel and of great consequence because we established the first

molecular mechanisms of VM formation in glioblastoma, and developed a great model system to study the impact of mural-like tumor cells in vasculature formation in relation to other players, including YKL-40.

As outlined in chapter 4, using the mural-like tumor cell model developed in chapter 3, and the knowledge gained about the role of YKL-40 in angiogenesis in chapter 2, we wanted to explore whether YKL-40 played a part in the mural-like cell function to support or create vasculature. What was unveiled was that YKL-40 does indeed control mural-like cell function through cell to cell contacts of tumor derived mural-like cells and host endothelial cells. This cell contacts were critical for vessel integrity and permeability in tumor xenograft mouse models. *In vitro* analysis revealed that the cadherin/catenin/actin pathway was a major component in the adhesion of cells, and that the presence of YKL-40 was necessary to maintain cell to cell contacts through this pathway. In sum, YKL-40 allowed rapid tumor development, by maintaining vessel stability and a constant blood supply network within the tumor. Inhibition of YKL-40 created hyperpermeable vessels that stunted tumor growth, prolonging mouse survival.

It is my hope that the work presented in this dissertation will provide the foundation for future studies into the role of YKL-40 in GBM, and demonstrate the therapeutic value of targeting YKL-40. Therefore, we can add another weapon to our arsenal in the fight to cure this horrible disease and improve the quality of like for patients.

APPENDICES

APPENDIX A

ROLE OF YKL-40 IN THE ANGIOGENESIS, RADIORESISTANCE, AND PROGRESSION OF GLIOBLASTOMA

This is an original research article by: Francescone RA, Scully S, Faibish M, Taylor SL, Oh D, Moral L, Yan W, Bentley B, Shao R.
Published in *The Journal of Biological Chemistry.2011. April 29;286(17):15332-43.*

THE JOURNAL OF BIOLOGICAL CHEMISTRY VOL. 286, NO. 17, pp. 15332–15343, April 29, 2011

Role of YKL-40 in the Angiogenesis, Radioresistance, and Progression of Glioblastoma*[S]

Received for publication, December 14, 2010, and in revised form, February 28, 2011 Published, JBC Papers in Press, March 8, 2011, DOI 10.1074/jbc.M110.212514

Ralph A. Francescone[‡], Steve Scully[‡§], Michael Faibish[‡], Sherry L. Taylor[¶], Dennis Oh[¶], Luis Moral[‖], Wei Yan[‡], Brooke Bentley[§], and Rong Shao[‡§1]**

*From the [‡]Molecular and Cellular Biology Program, Morrill Science Center, and the **Department of Veterinary and Animal Sciences, University of Massachusetts, Amherst, Massachusetts 01003, the [§]Pioneer Valley Life Sciences Institute, University of Massachusetts Amherst, Springfield, Massachusetts 01107, and the Departments of [¶]Neurosurgery and [‖]Pathology, Baystate Medical Center, Tufts University, Springfield, Massachusetts 01199*

Glioblastoma is one of the most fatal cancers, characterized by a strong vascularized phenotype. YKL-40, a secreted glycoprotein, is overexpressed in patients with glioblastomas and has potential as a novel tumor biomarker. The molecular mechanisms of YKL-40 in glioblastoma development, however, are poorly understood. Here, we aimed to elucidate the role YKL-40 plays in the regulation of VEGF expression, tumor angiogenesis, and radioresistance. YKL-40 up-regulated VEGF expression in glioblastoma cell line U87, and both YKL-40 and VEGF synergistically promote endothelial cell angiogenesis. Interestingly, long term inhibition of VEGF up-regulated YKL-40. YKL-40 induced coordination of membrane receptor syndecan-1 and integrin $\alpha v\beta 5$, and triggered a signaling cascade through FAK^{397} to ERK-1 and ERK-2, leading to elevated VEGF and enhanced angiogenesis. In addition, γ-irradiation of U87 cells increased YKL-40 expression that protects cell death through AKT activation and also enhances endothelial cell angiogenesis. Blockade of YKL-40 activity or expression decreased tumor growth, angiogenesis, and metastasis in xenografted animals. Immunohistochemical analysis of human glioblastomas revealed a correlation between YKL-40, VEGF, and patient survival. These findings have shed light on the mechanisms by which YKL-40 promotes tumor angiogenesis and malignancy, and thus provide a therapeutic target for tumor treatment.

Tumor angiogenesis, a process of new vasculature formation, is of paramount importance in solid tumor development (1). The supply of new blood vessels in tumors not only supports autonomous tumor proliferation but also aids in removing accumulated waste from extensive metabolism that would normally induce necrosis. A number of angiogenic factors such as VEGF, bFGF, and a recently identified secreted glycoprotein YKL-40 (also known as human cartilage glycoprotein-39) have been known to play critical roles in the development of the tumor vasculature (2–4). Thus, they presumably function through synergistic action to give rise to a robust angiogenic phenotype.

YKL-40, a member of the chitinase-like glycoprotein family, was first identified from the medium of human osteosarcoma cell line MG-63 (5). Structural analysis has demonstrated that YKL-40 contains highly conserved chitin-binding domains; however, it functionally lacks the ability to act as a chitinase because of a mutation of an essential glutamic acid residue to leucine in the chitinase-3-like catalytic domain (6, 7). Although the physiological role of YKL-40 is not completely understood, it is conceivable that YKL-40 is linked with proliferation of connective tissues and activation of vascular endothelial cells (8–10). Growing clinical evidence has indicated that aberrant expression of YKL-40 is largely associated with the pathogenesis of a variety of human diseases. For example, YKL-40 levels are elevated in the blood serum of patients with chronic inflammatory diseases such as rheumatoid- and osteoarthritis, hepatic fibrosis, and asthma (11–15), which is suggestive of its pathological function associated with extracellular matrix remodeling. Over the past decade, mounting clinical studies have demonstrated a correlation of elevated serum levels of YKL-40 with aggressive cancers and poorer survival in carcinomas of the breast, colon, ovary, and brain (16–22), suggesting that serum levels of YKL-40 serve as a diagnostic and prognostic biomarker. Recently, we found that YKL-40 is capable of stimulating angiogenesis of microvascular endothelial cells in breast cancer (2). In addition, YKL-40-induced angiogenesis is dependent on the interaction between membrane receptors syndecan-1 (Syn-1)[2] and integrin $\alpha v\beta 3$. These findings have shed light onto the mechanisms through which YKL-40 prompts breast cancer development.

Vascular endothelial growth factor (VEGF) is believed to be a primary promoter of angiogenesis (23). VEGF binds to two tyrosine kinase membrane receptors, VEGFR-1 (known as Flt-1) and VEGFR-2 (also named as Flk-1). Flk-1 acts as a primary receptor mediating VEGF-induced angiogenesis (24–26). Upon binding of VEGF, Flk-1 is activated by autophosphorylation of specific tyrosine residues, followed by binding and activation of Src or proteins containing a Src homology domain 2 (27). Consequently, these mediators activate multiple downstream effectors, including FAK and MAPK (28, 29). Clinic evidence shows that elevated serum levels of VEGF are related to

* This work was supported, in whole or in part, by National Institutes of Health Grant R01 CA120659 from the NCI (to R. S.).

[S] The on-line version of this article (available at http://www.jbc.org) contains supplemental Figs. S1–S3.

[1] To whom correspondence should be addressed: Pioneer Valley Life Sciences Institute, University of Massachusetts Amherst, Springfield, MA 01107. Fax: 413-794-0857; E-mail: rong.shao@bhs.org.

[2] The abbreviations used are: Syn-1, syndecan-1; HMVECs, human microvascular endothelial cells; mAY, monoclonal anti-YKL-40 antibody; IHC, immunohistochemistry; Gy, gray.

APPENDIX B

A YKL-40-NEUTRALIZING ANTIBODY BLOCKS TUMOR ANGIOGENESIS AND PROGRESSION: A POTENTIAL THERAPEUTIC AGENT IN CANCERS

This is an original research article by:
Faibish M, Francescone R, Bentley B, Yan W, Shao R
Published in *Molecular Cancer Therapeutics. 2011. May;10(5):742-51.*

Published OnlineFirst February 25, 2011; DOI: 10.1158/1535-7163.MCT-10-0868

Molecular Cancer Therapeutics

Therapeutic Discovery

A YKL-40–Neutralizing Antibody Blocks Tumor Angiogenesis and Progression: A Potential Therapeutic Agent in Cancers

Michael Faibish[1], Ralph Francescone[1], Brooke Bentley[3], Wei Yan[2], and Rong Shao[1,2,3]

Abstract

Accumulating evidence has indicated that expression levels of YKL-40, a secreted glycoprotein, were elevated in multiple advanced human cancers. Recently, we have identified an angiogenic role of YKL-40 in cancer development. However, blockade of the function of YKL-40, which implicates therapeutic value, has not been explored yet. Our current study sought to establish a monoclonal anti–YKL-40 antibody as a neutralizing antibody for the purpose of blocking tumor angiogenesis and metastasis. A mouse monoclonal anti–YKL-40 antibody (mAY) exhibited specific binding with recombinant YKL-40 and with YKL-40 secreted from osteoblastoma cells MG-63 and brain tumor cells U87. In the functional analysis, we found that mAY inhibited tube formation of microvascular endothelial cells in Matrigel induced by conditioned medium of MG-63 and U87 cells, as well as recombinant YKL-40. mAY also abolished YKL-40–induced activation of the membrane receptor VEGF receptor 2 (Flk-1/KDR) and intracellular signaling mitogen-activated protein (MAP) kinase extracellular signal–regulated kinase (Erk) 1 and Erk 2. In addition, mAY enhanced cell death response of U87 line to γ-irradiation through decreased expression of pAKT and AKT and accordingly, abrogated angiogenesis induced by the conditioned medium of U87 cells in which YKL-40 levels were elevated by treatment with γ-irradiation. Furthermore, treatment of xenografted tumor mice with mAY restrained tumor growth, angiogenesis, and progression. Taken together, this study has shown the therapeutic use for the mAY in treatment of tumor angiogenesis and metastasis. *Mol Cancer Ther; 10(5); 742–51. ©2011 AACR.*

Introduction

The human cartilage glycoprotein-39 (YKL-40) is a secreted glycoprotein originally identified from the medium of a human osteosarcoma cell line, MG-63 (1). Structural analyses of this 40-kDa molecule have revealed that YKL-40 is a highly phylogenetically conserved chitin-binding glycoprotein, classifying it in the family of chitinase-like proteins. However, YKL-40 lacks chitinase/hydrolase activity due to mutation of an essential glutamic acid to leucine in the chitinase-3–like catalytic domain (2, 3). Whereas the biophysiologic activity of YKL-40 is poorly understood, it is believed to be associated with proliferation of connective tissue cells (4, 5) and activation of vascular endothelial cells (6). Accumulating evidence has shown that serum levels of YKL-40 were elevated in a variety of chronic inflammatory diseases (7, 8), suggestive of its pathologic function being connected with the process of extracellular matrix remodeling (9, 10).

Over the last decade, particular attention has been paid to the pathologic role of YKL-40 in development of a broad type of human cancers. For instance, the database of gene microarray analyses and serial analysis of gene expression (SAGE) shows significantly higher expression levels of YKL-40 in carcinoma tissues from ovary, brain, and breast than those expressed in adjacent normal tissues (11, 12). Furthermore, a multitude of clinical studies have found that high serum levels of YKL-40 were associated with metastasis and short survival in a number of human cancers, such as breast, colorectal, ovarian, leukemia, and brain carcinoma (13–18), indicating that serum levels of YKL-40 may serve as a new cancer biomarker. Although there is mounting evidence showing elevated expression of YKL-40 in human cancers, little is known regarding its mechanisms underlying cancer progression and metastasis. Recently, we have identified YKL-40 as a tumor angiogenic factor capable of stimulating angiogenesis of microvascular endothelial cells in culture as well as in xenograft models (19). Furthermore, the expression levels of YKL-40 in human breast cancer were found to positively correlate with blood vessel formation. These findings have markedly enhanced our understanding of the molecular

Authors' Affiliations: [1]Molecular and Cellular Biology Program, Morrill Science Center, [2]Department of Veterinary and Animal Sciences, University of Massachusetts, Amherst; and [3]Pioneer Valley Life Sciences Institute, Springfield, Massachusetts

Note: Supplementary material for this article is available at Molecular Cancer Therapeutics Online (http://mct.aacrjournals.org/).

Corresponding Author: R. Shao, Pioneer Valley Life Sciences Institute, 3601 Main Street Springfield, MA 01199. Phone: 413-794-9568; Fax: 413-794-0857. E-mail: rong.shao@bhs.org

doi: 10.1158/1535-7163.MCT-10-0868

APPENDIX C

A MATRIGEL-BASED TUBE FORMATION ASSAY TO ASSESS THE VASCULOGENIC ACTIVITY OF TUMOR CELLS.

An original research article by:
Francescone RA 3rd, Faibish M, Shao R.
Published in *The Journal of Visualized Experiments. 2011 Sep 7;(55).*

A Matrigel-Based Tube Formation Assay to Assess the Vasculogenic Activity of Tumor Cells

Ralph A. Francescone III[1], Michael Faibish[2], Rong Shao[1,2,3]

[1]Molecular and Cellular Biology Program, Morrill Science Center, **University of Massachusetts**, [2]Pioneer Valley Life Sciences Institute, **University of Massachusetts**, [3]Department of Veterinary and Animal Sciences, **University of Massachusetts**

Video Article Chapters

Related Videos


An Orthotopic B
Tumor Model an
the...
Published 7/28/2


Isolation, Enrich
and Maintenanc
Published 9/01/2


Microtiter Dish E
Formation Assa
Published 1/30/2


Quantitative, Re
Analysis of Basa
Excision ...
Published 8/06/2

Cite this Article

Francescone III, R. A., Faibish, M., Shao, R. A Matrigel-Based Tube Formation Assay to Assess the Vasculogenic Activity of Tumor Cells. *J. Vis. Exp.* (55), e3040, doi:10.3791/3040 (2011).

Abstract

Over the past several decades, a tube formation assay using growth factor-reduced Matrigel has been typically employed to demonstrate the angiogenic activity of vascular endothelial cells *in vitro*[1-5]. However, recently growing evidence has shown that this assay is not limited to test vascular behavior for endothelial cells. Instead, it also has been used to test the ability of a number of tumor cells to develop a vascular phenotype[6-8]. This capability was consistent with their vasculogenic behavior identified in xenotransplanted animals, a process known as vasculogenic mimicry (VM)[9]. There is a multitude of evidence demonstrating that tumor cell-mediated VM plays a vital role in the tumor development, independent of endothelial cell angiogenesis[6, 10-13]. For example, tumor cells were found to participate in the blood perfused, vascular channel formation in tissue samples from melanoma and glioblastoma patients[8, 10, 11]. Here, we described this tubular network assay as a useful tool in evaluation of vasculogenic activity of tumor cells. We found that some tumor cell lines such as melanoma B16F1 cells, glioblastoma U87 cells, and breast cancer MDA-MB-435 cells are able to form vascular tubules; but some do not such as colon cancer HCT116 cells. Furthermore, this vascular phenotype is dependent on cell numbers plated on the Matrigel. Therefore, this assay may serve as powerful utility to screen the vascular potential of a variety of cell types including vascular cells, tumor cells as well as other cells.

Download

RIS EndNote, RefWorks, Refe
Manager, ProCite

Materials List

XML File

Information

Date Published	9/07/2011
JoVE Section	General
JoVE Issue	55
Comments	0 Comment
View Count	17,462 (Deta
DOI	doi:10.3791/

Keywords

Cancer Biology, Issue 55, tumor,
vascular, endothelial, tube forma
Matrigel, in vitro

APPENDIX D

GLIOBLASTOMA-DERIVED TUMOR CELLS INDUCE VASCULOGENIC MIMICRY THROUGH FLK-1 PROTEIN ACTIVATION.

An original research article by:
Francescone R, Scully S, Bentley B, Yan W, Taylor SL, Oh D, Moral L, Shao R.
Published in *The Journal of Biological Chemistry. 2012 Jul 13;287(29):24821-31.*

THE JOURNAL OF BIOLOGICAL CHEMISTRY VOL. 287, NO. 29, pp. 24821–24831, July 13, 2012

Glioblastoma-derived Tumor Cells Induce Vasculogenic Mimicry through Flk-1 Protein Activation*[S]

Received for publication, December 15, 2011, and in revised form, May 30, 2012 Published, JBC Papers in Press, May 31, 2012, DOI 10.1074/jbc.M111.334540

Ralph Francescone[‡1], Steve Scully[‡1], Brooke Bentley[§], Wei Yan[§], Sherry L. Taylor[¶], Dennis Oh[¶], Luis Moral[‖], and Rong Shao[‡§2]**

*From the [‡]Molecular and Cellular Biology Program, Morrill Science Center, University of Massachusetts, Amherst, Massachusetts 01003, the [§]Pioneer Valley Life Sciences Institute, Springfield, Massachusetts 01199, the Departments of [¶]Neurosurgery and [‖]Pathology, Baystate Medical Center, Tufts University, Springfield, Massachusetts 01199, and the **Department of Veterinary and Animal Sciences, University of Massachusetts, Amherst, Massachusetts 01003*

Background: The malignancy of glioblastoma is characterized by strong vascularization, including vasculogenic mimicry and angiogenesis.
Results: Glioblastoma cells promote vasculogenic mimicry and tumor development via Flk-1 activation.
Conclusion: Glioblastoma cells display the ability to constitute vascular channels.
Significance: Identification of Flk-1 as a key factor regulating vasculogenic mimicry could offer a novel therapeutic target for patient treatment.

Glioblastoma (GBM) is extremely aggressive and essentially incurable. Its malignancy is characterized by vigorous microvascular proliferations. Recent evidence has shown that tumor cells display the ability to drive blood-perfused vasculogenic mimicry (VM), an alternative microvascular circulation independent of endothelial cell angiogenesis. However, molecular mechanisms underlying this vascular pathogenesis are poorly understood. Here, we found that vascular channels of VM in GBM were composed of mural-like tumor cells that strongly express VEGF receptor 2 (Flk-1). To explore a potential role of Flk-1 in the vasculogenesis, we investigated two glioblastoma cell lines U87 and GSDC, both of which express Flk-1 and exhibit a vascular phenotype on Matrigel. Treatment of both cell lines with either *Flk-1* gene knockdown or Flk-1 kinase inhibitor SU1498 abrogated Flk-1 activity and impaired vascular function. Furthermore, inhibition of Flk-1 activity suppressed intracellular signaling cascades, including focal adhesion kinase and mitogen-activated protein kinase ERK1/2. In contrast, blockade of VEGF activity by the neutralizing antibody Bevacizumab failed to recapitulate the impact of SU1498, suggesting that Flk-1-mediated VM is independent of VEGF. Xenotransplantation of SCID/Beige mice with U87 cells and GSDCs gave rise to tumors harboring robust mural cell-associated vascular channels. *Flk-1* shRNA restrained VM in tumors and subsequently inhibited tumor development. Collectively, all the data demonstrate a central role of Flk-1 in the formation of VM in GBM. This study has shed light on molecular mechanisms mediating tumor aggressiveness and also provided a therapeutic target for patient treatment.

Glioblastoma (GBM)[3] is an extremely aggressive brain tumor with a median survival of ~12 months, irrespective of surgical resection and post-operative adjuvant radio/chemotherapy (1). More than 70% of patients with GBM succumb to the disease in 2 years, and fewer than 10% are alive 5 years following the initial diagnosis (2). The aggressiveness of this disease is characterized by strong vascular proliferation that is highly correlated with the malignancy of GBM. Thus, most of the current chemotherapies against GBM aim at vascular endothelial cells that orchestrate a significant component of blood vessels (3). However, it has been increasingly documented that an anti-angiogenic monotherapy did not give rise to a promise for improvement of patient overall survival, as drug resistance or angiogenic rebound occurs once the treatment is terminated (4, 5). For example, clinical trials using a neutralizing anti-VEGF antibody (Bevacizumab, also named Avastin) in recurrent GBMs revealed minimal benefit to patient survival (4, 6, 7). Consistent with clinical evidence, the anti-angiogenic preclinical studies using animal models reported conflicting outcomes in which malignant tumors unexpectedly developed (8, 9), implicating that escape mechanisms may account for the malignancy.

Recently, a number of research groups have demonstrated that vasculogenic mimicry (VM), an alternative vascular mechanism, contributes a central role to the vascularization of GBM in which tumor cells participate (10–12). Growing evidence suggests that this matrix-embedded, blood-perfused microvasculature renders tumor progression independent of endothelial cell angiogenesis (13, 14). In addition, this VM is believed to be at least partially ascribed to the multipotency of glioblastoma stem cells (GSCs) capable of transdifferentiation into vascular nonendothelial cells (15, 16). Furthermore, these studies suggest that transdifferentiation of GSCs into mural-like tumor

* This work was supported, in whole or in part, by National Institutes of Health Grant R01 CA120659 from NCI (to R. S.).
[S] This article contains supplemental Figs. 1–3.
[1] Both authors contributed equally to this work.
[2] To whom correspondence should be addressed. Fax: 413-794-0857; E-mail: rong.shao@bhs.org.

[3] The abbreviations used are: GBM, glioblastoma; VM, vasculogenic mimicry; Flk-1, VEGF receptor 2; Sma, smooth muscle α-actin; HMVEC, human microvascular endothelial cells; FAK, focal adhesion kinase; IHC, immunohistochemistry; PDGFR, platelet-derived growth factor receptor; PAS, periodic acid-Schiff; GSC, glioblastoma stem cell; h, human; cad, cadherin.

APPENDIX E

TRANSDIFFERENTIATION OF GLIOBLASTOMA STEM-LIKE CELLS INTO MURAL CELLS DRIVES VASCULOGENIC MIMICRY IN GLIOBLASTOMAS

This an original research article by:
Scully S, Francescone R, Faibish M, Bentley B, Taylor SL, Oh D, Schapiro R, Moral L, Yan W, Shao R.
Published in *The Journal of Neuroscience. 2012 Sep 12;32(37):12950-60.*

Neurobiology of Disease

Transdifferentiation of Glioblastoma Stem-Like Cells into Mural Cells Drives Vasculogenic Mimicry in Glioblastomas

Steve Scully,[1,2] Ralph Francescone,[2] Michael Faibish,[2] Brooke Bentley,[1] Sherry L. Taylor,[4] Dennis Oh,[4] Robert Schapiro,[4] Luis Moral,[5] Wei Yan,[1] and Rong Shao[1,2,3]

[1]Pioneer Valley Life Sciences Institute, University of Massachusetts, Amherst, Springfield, Massachusetts 01107, [2]Molecular and Cellular Biology Program, Morrill Science Center, and [3]Department of Veterinary and Animal Sciences, University of Massachusetts, Amherst, Amherst, Massachusetts 01003, and Departments of [4]Neurosurgery and [5]Pathology, Baystate Medical Center, Tufts University, Springfield, Massachusetts 01199

Recent evidence has shown that glioblastoma stem-like cells (GSCs) can transdifferentiate into endothelial cells and vascular-like tumor cells. The latter pattern of vascularization indicates an alternative microvascular circulation known as vasculogenic mimicry (VM). However, it remains to be clarified how the GSC-driven VM makes a significant contribution to tumor vasculature. Here, we investigated 11 cases of glioblastomas and found that most of them consisted of blood-perfused vascular channels that coexpress mural cell markers smooth muscle α-actin and platelet-derived growth factor receptor β, epidermal growth factor receptor, and vascular endothelial growth factor receptor 2 (Flk-1), but not CD31 or VE-cadherin. This microvasculature coexisted with endothelial cell-associated vessels. GSCs derived from patients with glioblastomas developed vigorous mural cell-associated vascular channels but few endothelial cell vessels in orthotopic animal models. Suppression of Flk-1 activity and gene expression abrogated GSC transdifferentiation and vascularization *in vitro*, and inhibited VM in animal models. This study establishes mural-like tumor cells differentiated from GSCs as a significant contributor to microvasculature of glioblastoma and points to Flk-1 as a potential target for therapeutic intervention that could complement current anti-angiogenic treatment.

Introduction

Tumor vasculature is typically assumed to arise from endothelial cell origin (Folkman, 1971). However, recent discoveries suggest an alternative mechanism whereby microvascular circulation is derived from tumor cells through a process known as vasculogenic mimicry (VM) (Maniotis et al., 1999). Evidence suggests that this matrix-embedded, blood-perfused microvasculature plays a vital role in tumor development, independent of endothelial cell angiogenesis. For example, highly aggressive melanoma cells generate numerous matrix-rich patterned channels containing blood cells, and the formation of these channels positively correlates with a worse prognosis for patients (Hendrix et al., 2003; Folberg et al., 2006). A mosaic model consisting both of tumor cell and endothelial cell-integrated networks was also described in the development of colon cancer (Chang et al., 2000). The presence of tumor-derived vasculatures highlights the plasticity of tumor cells and suggests involvement of cancer stem cells.

Received April 26, 2012; revised July 5, 2012; accepted July 25, 2012.

Author contributions: R.F. and R. Shao designed research; S.S., R.F., M.F., B.B., W.Y., and R. Shao performed research; S.S., R.F., S.L.T., D.O., R. Schapiro, L.M., and R. Shao analyzed data; R. Shao wrote the paper.

This work was partially supported by National Cancer Institute Grant R01 CA120659 (R. Shao). We are grateful to Drs. Mary Hendrix, Alonzo Ross, D. Joseph Jerry, Lawrence Schwartz, and Lisa Minter for their critical comments. We also thank Dr. Geet de Vries for help of intracranial injection and Narvis Handford, RN, for her assistance in patients' consenting in the sample collection.

The authors declare no competing financial interests.

Correspondence should be addressed to Rong Shao, Pioneer Valley Life Sciences Institute, University of Massachusetts, Amherst, 3601 Main Street, Springfield, MA 01199. E-mail: rong.shao@bhs.org.

DOI:10.1523/JNEUROSCI.2017-12.2012

 0270-6474/12/3212950-11$15.00/0

Glioblastomas, the most lethal primary brain tumor, display an extensive vasculature phenotype which is highly correlated with aggressiveness (Wen and Kesari, 2008). Glioblastoma stem cells (GSCs) that possess self-renewing and differentiation properties have been found to be associated with malignancy of this disease (Singh et al., 2004; Beier et al., 2007). Furthermore, GSCs are capable of transdifferentiation into vascular endothelial cells that participate in angiogenesis (Ricci-Vitiani et al., 2010; Wang et al., 2010) and vessel-like tumor cells that also involve VM (El Hallani et al., 2010). However, it has not been thoroughly characterized whether this GSC-derived VM represents a significant component of microvasculature, and how GSCs transdifferentiate into vessel-like cells that mediate vasculogenesis of glioblastomas. Thus, it is emerging that elucidation of these vascularized events will offer new mechanistic insights into the malignancy of glioblastomas that are commonly characterized by tumor angiogenesis. In addition, it is noteworthy that recent clinical trials have demonstrated a minimal overall benefit of anti-angiogenic monotherapy (e.g., an anti-VEGF antibody bevacizumab) to patient survival (Bergers and Hanahan, 2008; Verhoeff et al., 2009). Therefore, investigation of GSC-derived VM will complement current therapeutic strategies that mainly focus on inhibition of endothelial cell angiogenesis. Here, we discovered that GSCs primarily transdifferentiate into vascular mural-like cells, to develop VM, a process dependent on VEGF receptor 2 (Flk-1).

Materials and Methods

Neurospheres. Tumor samples were obtained from consenting patients with glioblastoma as approved by Baystate Medical Center Institutional

APPENDIX F

TUMOR-DERIVED MURAL-LIKE CELLS COORDINATE WITH ENDOTHELIAL CELLS: ROLE OF YKL-40 IN MURAL CELL-MEDIATED ANGIOGENESIS

This is an original research article by:
Francescone R, Ngernyuang N, Yan W, Bentley B, Shao R.
Published in *Oncogene. 2013 May 13. Epub.*

Oncogene (2013), 1–13

www.nature.com/onc

ORIGINAL ARTICLE

Tumor-derived mural-like cells coordinate with endothelial cells: role of YKL-40 in mural cell-mediated angiogenesis

R Francescone[1], N Ngemyuang[2], W Yan[3], B Bentley[3] and R Shao[1,3,4]

Tumor neo-vasculature is characterized by spatial coordination of endothelial cells with mural cells, which delivers oxygen and nutrients. Here, we explored a key role of the secreted glycoprotein YKL-40, a mesenchymal marker, in the interaction between endothelial cells and mesenchymal mural-like cells for tumor angiogenesis. Xenotransplantation of tumor-derived mural-like cells (GSDCs) expressing YKL-40 in mice developed extensive and stable blood vessels covered with more GSDCs than those in YKL-40 gene knockdown tumors. YKL-40 expressed by GSDCs was associated with increased interaction of neural cadherin/β-catenin/smooth muscle alpha actin; thus, mediating cell-cell adhesion and permeability. YKL-40 also induced the interaction of vascular endothelial cadherin/β-catenin/actin in endothelial cells (HMVECs). In cell co-culture systems, YKL-40 enhanced both GSDC and HMVEC contacts, restricted vascular leakage, and stabilized vascular networks. Collectively, the data inform new mechanistic insights into the cooperation of mural cells with endothelial cells induced by YKL-40 during tumor angiogenesis, and also enhance our understanding of YKL-40 in both mural and endothelial cell biology.

Oncogene advance online publication, 13 May 2013; doi:10.1038/onc.2013.160

Keywords: YKL-40; cadherins; vessel permeability; mural cells; tumor angiogenesis; VEGF

INTRODUCTION

Neo-vascular networks function to deliver nutrients, oxygen, and other molecules to developmental tissue or pathologic lesion, the process known to mediate vasculogenesis and angiogenesis.[1,2] The key step of this event involves the formation of the neo-vasculature wall that is primarily composed of both endothelial cells and mesenchyme-derived mural cells including smooth muscle cells and/or pericytes.[3] In physiological angiogenesis (e.g. wound healing), endothelial cells initially sprout to form neo-vessels followed by recruitment of mural cells in a paracrine manner dependent on PDGFB-PDGFRβ and angiopoietin-1-Tie-2 reciprocal activation.[4,5] It is acknowledged that vasculature in the central nervous system contains the highest amount of mural cell coverage.[6]

Once mural cells are recruited onto the abluminal surface of endothelial cell-based vessels, intercellular junctions between endothelial cells, mural cells, and/or endothelial-mural cells act as a central factor to render the vascular network mature and stable. A number of intercellular adhesion molecules are appreciated to regulate vessel fenestration, permeability, and stability. For instance, vascular endothelial cadherin (VE-cadherin) plays an important role in controlling endothelial-to-endothelial cell contacts,[7–9] while neural cadherin (N-cadherin) mediates endothelial-to-mural cell and mural-to-mural cell communication.[10–12] A key intracellular mediator of the cadherin-associated cell-to-cell contacts is β-catenin that acts as a physical link to the cytoskeleton assembly including actin.[13,14] Disruption of the complex between cadherins and β-catenin results in decreased cell-cell interactions and increased cell permeability. Other gap junction proteins such as claudins, occludin, and connexins also participate in distinct intercellular interactions.[3,6] The spatial cooperation and regulation of these cell-cell tight contacts commit endothelial cells and mural cells to orchestrate the vessel wall, which offers adequate nutrients and oxygen for tissue proliferation.

Although it remains to be clarified if different identities and/or functions of mural cells exist between tumor and normal vessels, chaotic vasculature with either abundant or insufficient coverage of mural cells is frequently observed during tumor angiogenesis.[15] Deletion of mural cells in tumor-bearing mice exhibited an impaired vascular phenotype with diminished mature vessel formation and increased vessel permeability, thus retarding tumor progression.[16,17] As the most potent angiogenic factor, vascular endothelial growth factor (VEGF), also known as a vascular permeability factor, promotes endothelial permeability and destabilizes vascular integrity via interrupting VE-cadherin function in endothelial cells.[18,19] In light of VEGF activity in mural cell coverage of tumor vessels, there is strong evidence indicating that ablation of myeloid cell-derived VEGF in mice led to increased mural cell coverage of the vessels and acceleration of tumorigenesis. These findings unveil a new pathologic signature of VEGF in functional inhibition of mural cell-associated vessels.[20,21]

YKL-40 (human cartilage glycoprotein-39 or chitinase-3-like-1) is a secreted glycoprotein that was originally identified from culture medium of a human osteosarcoma cell line MG-63.[22] Human YKL-40 protein contains an open reading frame of 383 amino acids with a molecular mass of 40 kDa and it is a member of glycoside hydrolase family 18 that contains chitinases. But YKL-40 can only bind chitin-like oligosaccharides and does not have chitinase/hydrolase activity because of the substitution of an essential glutamic acid with leucine in the chitinase-3-like catalytic

[1]Molecular and Cellular Biology Program, Morrill Science Center, University of Massachusetts, Amherst, MA, USA; [2]Graduate School, Khon Khaen University, Khon Khaen, Thailand; [3]Pioneer Valley Life Sciences Institute, Springfield, MA, USA and [4]Department of Veterinary and Animal Sciences, University of Massachusetts, Amherst, MA, USA. Correspondence: Professor R Shao, Pioneer Valley Life Sciences Institute, University of Massachusetts Amherst, Springfield, MA 01107, USA.
E-mail: rong.shao@bhs.org
Received 4 October 2012; revised 8 March 2013; accepted 14 March 2013

BIBLIOGRAPHY

Abedi, H, and I Zachary. "Vascular Endothelial Growth Factor Stimulates Tyrosine Phosphorylation and Recruitment to New Focal Adhesions of Focal Adhesion Kinase and Paxillin in Endothelial Cells." *J Biol Chem*, 1997: 15442-15451.

Abramsson, A, P Lindblom, and C Betsholtz. "Endothelial and nonendothelial sources of PDGF-B regulate pericyte recruitment and influence vascular pattern formation in tumors." *J Clin Invest*, 2003: 1142-1151.

Armulik, A, G Genové, and C Betsholtz. "Pericytes: developmental, physiological, and pathological perspectives, problems, and promises." *Dev Cell*, 2011: 193-215.

Bao, S, et al. "Stem cell-like glioma cells promote tumor angiogenesis through vascular endothelial growth factor." *Cancer Res*, 2006: 7843-7846.

Basu, GD, et al. "A novel role for cyclooxygenase-2 in regulating vascular channel formation by human breast cancer cells." *Breast Cancer Res*, 2006: epub.

Batchelor, TT, et al. "AZD2171, a pan-VEGF receptor tyrosine kinase inhibitor, normalizes tumor vasculature and alleviates edema in glioblastoma patients." *Cancer Cell*, 2011: 83-95.

Bazzoni, G, and E Dejana. "Endothelial cell-to-cell junctions: molecular organization and role in vascular homeostasis." *Physiol Rev*, 2004: 869-901.

Bergers, G, and D Hanahan. "Modes of resistance to anti-angiogenic therapy." *Nat Rev Cancer*, 2008: 592-603.

Bergers, G, and LE Benjamin. "Tumorigenesis and the Angiogenic Switch." *Nat Rev:Can*, 2003: 401-410.

Bergers, G, S Song, N Meyer-Morse, E Bergsland, and D Hanahan. "Benefits of targeting both pericytes and endothelial cells in the tumor vasculature with kinase inhibitors." *J Clin Invest*, 2003: 1287-1295.

Bergmann, OJ, et al. "High serum concentration of YKL-40 is associated with short survival in patients with acute myeloid leukemia." *Clin Cancer Res*, 2005: 8644-8652.

Bloch, W, et al. "The angiogenesis inhibitor endostatin impairs blood vessel maturation during wound healing." *FASEB J*, 2000: 2373-2376.

Borges, E, Y Jan, and E Ruoslahti. "Platelet-derived growth factor receptor beta and vascular endothelial growth factor receptor 2 bind to the beta 3 integrin through its extracellular domain." *J Biol Chem*, 2000: 39867-39873.

Brem, S, R Cotran, and J Folkman. "Tumor angiogenesis: a quantitative method for histologic grading." *J Natl Cancer Inst*, 1972: 347–356.

Carmeliet P, Lampugnani MG, Moons L, et al. "Targeted deficiency or cytosolic truncation of the VE-cadherin gene in mice impairs VEGF-mediated endothelial survival and angiogenesis." *Cell*, 1999: 147-157.

Carmeliet, P. "Mechanisms of angiogenesis and arteriogenesis." *Nat Med*, 2000: 389–395.

Carmeliet, P, and RK Jain. "Molecular mechanisms and clinical applications of angiogenesis." *Nature*, 2011: 298-307.

Carmeliet, P, and RK Jain. "Principles and mechanisms of vessel normalization for cancer and other angiogenic diseases." *Nat Rev Drug Discov*, 2011: 417-427.

Carro, MS, et al. "The transcriptional network for mesenchymal transformation of brain tumours." *Nature*, 2010: 318-325.

Casanovas, O, DJ Hicklin, G Bergers, and D Hanahan. "Drug resistance by evasion of antiangiogenic targeting of VEGF signaling in late-stage pancreatic islet tumors." *Cancer Cell*, 2005: 299-309.

Cavallaro, U, and E Dejana. "Adhesion molecule signalling: not always a sticky business." *Nat Rev Mol Cell Biol*, 2011: 189-197.

Chambers, RC, P Leoni, N Kaminski, GJ Laurent, and RA Heller. "Global expression profiling of fibroblast responses to transforming growth factor-beta1 reveals the induction of inhibitor of differentiation-1 and provides evidence of smooth muscle cell phenotypic switching." *Am J Pathol*, 2003: 533-546.

Chang, YS, E di Tomaso, DM McDonald, R Jones, RK Jain, and LL Munn. "Mosaic blood vessels in tumors: frequency of cancer cells in contact with flowing blood." *Proc Natl Acad Sci U S A*, 2000: 14608-14613.

Chen, XL, et al. "VEGF-induced vascular permeability is mediated by FAK." *Dev Cell*, 2012: 146-157.

Chen, Y, et al. "Vasculogenic mimicry-potential target for glioblastoma therapy: an in vitro and in vivo study." *Med Oncol*, 2012: 324-331.

Chetty, C, SS Lakka, P Bhoopathi, and JS Rao. "MMP-2 alters VEGF expression via alphaVbeta3 integrin-mediated PI3K/AKT signaling in A549 lung cancer cells." *Int J Cancer*, 2010: 1081-1095.

Cintin, C, JS Johansen, IJ Christensen, PA Price, S Sørensen, and HJ and Nielsen. "Serum YKL-40 and colorectal cancer." *Br J Cancer*, 1999: 1494–1499.

Cintin, C, JS Johansen, IJ Christensen, PA Price, S Sørensen, and HJ Nielsen. "High serum YKL-40 level after surgery for colorectal carcinoma is related to short survival." *Cancer*, 2002: 267-274.

De Ceuninck, F., S. Gaufillier, A. Bonnaud, M. Sabatini, C. Lesur, and P Pastoureau. "YKL-40 (Cartilage gp-39) Induces Proliferative Events in Cultured Chondrocytes and Synoviocytes and Increases Glycosaminoglycan Synthesis in Chondrocytes ." *Biochemical and Biophysical Research Communications*, 2001: 926-931.

de Groot, JF, et al. "Tumor invasion after treatment of glioblastoma with bevacizumab: radiographic and pathologic correlation in humans and mice." *Neuro Oncol*, 2010: 233-42.

Dejana, E. "Endothelial cell-cell junctions: happy together." *Nat Rev Mol Cell Biol*, 2004: 261-270.

Dejana, E, E Tournier-Lasserve, and BM Weinstein. "The control of vascular integrity by endothelial cell junctions: molecular basis and pathological implications." *Dev Cell*, 2009: 209-221.

Dejana, E, F Orsenigo, and MG Lampugnani. "The role of adherens junctions and VE-cadherin in the control of vascular permeability." *J Cell Sci*, 2008: 2115-2122.

di Tomaso, E, et al. "Glioblastoma recurrence after cediranib therapy in patients: lack of "rebound" revascularization as mode of escape." *Cancer Res*, 2011: 19-28.

di Tomaso, E, et al. "Mosaic tumor vessels: cellular basis and ultrastructure of focal regions lacking endothelial cell markers." *Cancer Res*, 2005: 5740-5749.

Döme, B, MJ Hendrix, S Paku, J Tóvári, and J Tímár. "Alternative vascularization mechanisms in cancer: Pathology and therapeutic implications." *Am J Pathol*, 2007: 1-15.

Dong, J, et al. "Glioma stem/progenitor cells contribute to neovascularization via transdifferentiation." *Stem Cell Rev*, 2011: 141-152.

Dreyfuss, JM, MD Johnson, and PJ Park. "Meta-analysis of glioblastoma multiforme versus anaplastic astrocytoma identifies robust gene markers." *Mol Cancer*, 2009: 1-10.

Ebos, JM, CR Lee, W Cruz-Munoz, GA Bjarnason, JG Christensen, and RS Kerbel. "Accelerated metastasis after short-term treatment with a potent inhibitor of tumor angiogenesis." *Cancer Cell*, 2009: 232-239.

Eichmann, A, C Corbel, V Nataf, P Vaigot, C Bréant, and NM Le Douarin. "Ligand-dependent development of the endothelial and hemopoietic lineages from embryonic mesodermal cells expressing vascular endothelial growth factor receptor 2." *Proc Natl Acad Sci U S A*, 1997: 5141-5146.

El Hallani, S, et al. "A new alternative mechanism in glioblastoma vascularization: tubular vasculogenic mimicry." *Brain*, 2010: 973-982.

Elenbaas, B, and RA Weinberg. "Heterotypic signaling between epithelial tumor cells and fibroblasts in carcinoma formation." *Exp Cell Res*, 2001: 169-184.

Eliceiri, BP. "Integrin and growth factor receptor crosstalk." *Circ Res*, 2001: 1104-1110.

Ellis, LM, and DJ Hicklin. "VEGF-targeted therapy: mechanisms of anti-tumour activity." *Nat Rev Cancer*, 2008: 579-591.

Erber, R, et al. "Combined inhibition of VEGF and PDGF signaling enforces tumor vessel regression by interfering with pericyte-mediated endothelial cell survival mechanisms." *FASEB J*, 2004: 338-340.

Faibish, M, R Francescone, B Bentley, W Yan, and R Shao. "A YKL-40-neutralizing antibody blocks tumor angiogenesis and progression: a potential therapeutic agent in cancers." *Mol Cancer Ther*, 2011: 742-751.

Ferrara, N, and RS Kerbel. "Angiogenesis as a therapeutic target." *Nature*, 2005: 967-974.

Folberg, R, and AJ Maniotis. "Vasculogenic mimicry." *APMIS*, 2004: 508-525.

Folberg, R, et al. "Tumor cell plasticity in uveal melanoma: microenvironment directed dampening of the invasive and metastatic genotype and phenotype accompanies the generation of vasculogenic mimicry patterns." *Am J Pathol*, 2006: 1376-1389.

Folberg, R, MJ Hendrix, and AJ Maniotis. "Vasculogenic mimicry and tumor angiogenesis." *Am J Pathol*, 2000: 361-381.

Folkman, J. "Tumor angiogenesis: therapeutic implications." *N Engl J Med*, 1971: 1182-1186.

Folkman, J, and M Klagsbrun. "Angiogenic factors." *Science*, 1987: 442-447.

Fong, GH, J Rossant, M Gertsenstein, and ML Breitman. "Role of the Flt-1 receptor tyrosine kinase in regulating the assembly of vascular endothelium." *Nature*, 1995: 66-70.

Francescone, R, et al. "Glioblastoma-derived tumor cells induce vasculogenic mimicry through Flk-1 protein activation." *J Biol Chem*, 2012: 24821-24831.

Francescone, R, N Ngernyuang, W Yan, B Bentley, and R Shao. "Tumor-derived mural-like cells coordinate with endothelial cells: role of YKL-40 in mural cell-mediated angiogenesis." *Oncogene*, 2013 : In Press.

Francescone, RA, et al. "Role of YKL-40 in the angiogenesis, radioresistance, and progression of glioblastoma." *J Biol Chem*, 2011: 15332-15343.

Francescone, RA, M Faibish, and R Shao. "A Matrigel-based tube formation assay to assess the vasculogenic activity of tumor cells." *J Vis Exp*, 2011: epub.

Furnari, FB, et al. "Malignant astrocytic glioma: genetics, biology, and paths to treatment." *Genes Dev*, 2007: 2683-2710.

Fusetti, F, T Pijning, KH Kalk, E Bos, and W Dijkstra. "Crystal structure and carbohydrate-binding properties of the human cartilage glycoprotein-39." *J Biol Chem*, 2003: 37753–37760.

Gavard, J, and JS Gutkind. "VEGF controls endothelial-cell permeability by promoting the beta-arrestin-dependent endocytosis of VE-cadherin." *Nat Cell Biol*, 2006: 1223-1234.

Gerhardt, H, and H Semb. "Pericytes: gatekeepers in tumour cell metastasis?" *J Mol Med*, 2008: 135-144.

Gerhardt, H, H Wolburg, and C Redies. "N-cadherin mediates pericytic-endothelial interaction during brain angiogenesis in the chicken." *Dev Dyn*, 2000: 472-479.

Gorbunova, E, IN Gavrilovskaya, and ER Mackow. "Pathogenic hantaviruses Andes virus and Hantaan virus induce adherens junction disassembly by directing vascular endothelial cadherin internalization in human endothelial cells." *J Virol*, 2010: 7405-7411.

Greenberg, JI, et al. "A role for VEGF as a negative regulator of pericyte function and vessel maturation." *Nature*, 2008: 809-813.

Guo, D, Q Jia, HY Song, RS Warren, and DB Donner. "Vascular endothelial cell growth factor promotes tyrosine phosphorylation of mediators of signal transduction that contain SH2 domains. Association with endothelial cell proliferation." *J Biol Chem*, 1995: 6729-6733.

Hanahan, D. "Signaling vascular morphogenesis and maintenance." *Science*, 1997: 48-50.

Hanahan, D, and J Folkman. "Patterns and emerging mechanisms of the angiogenic switch during tumorigenesis." *Cell*, 1996: 353-364.

Hardee, ME, and D Zagzag. "Mechanisms of glioma-associated neovascularization." *Am J Pathol*, 2012: 1126-1141.

Helfrich, I, et al. "Resistance to antiangiogenic therapy is directed by vascular phenotype, vessel stabilization, and maturation in malignant melanoma." *J Exp Med*, 2010: 491-503.

Hellberg, C, A Ostman, and CH Heldin. "PDGF and vessel maturation." *Recent Results Cancer Res*, 2010: 103-114.

Hellström, M, et al. "Lack of pericytes leads to endothelial hyperplasia and abnormal vascular morphogenesis." *J Cell Biol*, 2001: 543-553.

Hendrix, MJ, EA Seftor, AR Hess, and RE and Seftor. "Vasculogenic mimicry and tumour-cell plasticity: lessons from melanoma." *Nat Rev Can*, 2003: 411-421.

Hofman, FM, and TC Chen. "The Basic Science of Avastin (Bevacizumab) Therapy." *Controversies in Neuro-Oncology*, 2010 : epub.

Hogdall, EV, et al. "High plasma YKL-40 level in patients with ovarian cancer stage III is related to shorter survival." *Oncol Reports*, 2003: 1535-1538.

Holash, J, et al. "Vessel cooption, regression, and growth in tumors mediated by angiopoietins and VEGF." *Science*, 1999: 1994–1998.

Hood, JD, R Frausto, WB Kiosses, MA Schwartz, and DA Cheresh. "Differential alphav integrin-mediated Ras-ERK signaling during two pathways of angiogenesis." *J Cell Biol*, 2003: 933-943.

Hormigo, A, et al. "YKL-40 and matrix metalloproteinase-9 as potential serum biomarkers for patients with high-grade gliomas." *Clin Cancer Res*, 2006: 5698-5704.

Hottinger, AF, et al. "YKL-40 and MMP-9 as serum markers for patients with primary central nervous system lymphoma." *Ann Neurol*, 2011: 163-169.

Hu, B, K Trinh, WF Figueira, and PA Price. "Isolation and sequence of a novel human chondrocyte protein related to mammalian members of the chitinase protein family." *J Biol Chem*, 1996: 19415-19420.

Huang, FJ, WK You, P Bonaldo, TN Seyfried, EB Pasquale, and WB Stallcup. "Pericyte deficiencies lead to aberrant tumor vascularizaton in the brain of the NG2 null mouse." *Dev Biol*, 2010: 1035-1046.

Hurwitz, H, et al. "Bevacizumab plus irinotecan, fluorouracil, and leucovorin for metastatic colorectal cancer." *N Engl J Med*, 2004: 2335-2342.

Ido, K, T Nakagawa, T Sakuma, H Takeuchi, K Sato, and T Kubota. "Expression of vascular endothelial growth factor-A and mRNA stability factor HuR in human astrocytic tumors." *Neuropathology*, 2008: 604-611.

Ilhan, A, et al. "Angiogenic factors in plasma of brain tumour patients." *Anticancer Res*, 2009: 731-736.

Inoue, T, and T Meyer. "Synthetic activation of endogenous PI3K and Rac identifies an AND-gate switch for cell polarization and migration." *PLoS One*, 2008: 1-10.

Jain, RK. "Molecular regulation of vessel maturation." *Nat Med*, 2003: 685-693.

Jayson, GC, et al. "Blockade of platelet-derived growth factor receptor-beta by CDP860, a humanized, PEGylated di-Fab', leads to fluid accumulation and is associated with increased tumor vascularized volume." *J Clin Oncol*, 2005: 973-981.

Jensen, BV, JS Johansen, and PA Price. "High levels of serum HER-2/neu and YKL-40 independently reflect aggressiveness of metastatic breast cancer." *Clin Cancer Res*, 2003: 4423-4434.

Johansen, JS, et al. "High serum YKL-40 levels in patients with primary breast cancer is related to short recurrence free survival." *Breast Cancer Res Treat*, 2003: 15-21.

Johansen, JS, et al. "Serum YKL-40 is increased in patients with hepatic fibrosis." *J Hepatol*, 2000: 911-920.

Johansen, JS, et al. "YKL-40 in giant cells and macrophages from patients with giant cell arteritis." *Arthritis Rheum*, 1999: 2624-2630.

Johansen, JS, MK Williamson, JS Rice, and PA Price. "Identification of proteins secreted by human osteoblastic cells in culture." *J Bone Miner Res*, 1992: 501-512.

Johansen, JS, PE Høyer, LA Larsen, PA Price, and K Møllgård. "YKL-40 protein expression in the early developing human musculoskeletal system." *J Histochem Cytochem*, 2007: 1213-1228.

Junker, N, JS Johansen, CB Andersen, and PE Kristjansen. "Expression of YKL-40 by peritumoral macrophages in human small cell lung cancer." *Lung Cancer*, 2005: 223-231.

Junker, N, JS Johansen, LT Hansen, EL Lund, and PE Kristjansen. "Regulation of YKL-40 expression during genotoxic or microenvironmental stress in human glioblastoma cells." *Cancer Sci*, 2005: 183-190.

Kalluri, R. "Basement Membranes: Structure, Assembly and Role in Tumor Angiogenesis." *Nat Rev: Can*, 2003: 422-433.

Kamoun, WS, et al. "Edema control by cediranib, a vascular endothelial growth factor receptor-targeted kinase inhibitor, prolongs survival despite persistent brain tumor growth in mice." *J Clin Oncol*, 2009: 2542-2552.

Keunen, O, et al. "Anti-VEGF treatment reduces blood supply and increases tumor cell invasion in glioblastoma." *Proc Natl Acad Sci U S A*, 2011: 3749-3754.

Kirkpatrick, RB, JG Emery, JR Connor, R Dodds, PG Lysko, and M Rosenberg. "Induction and expression of human cartilage glycoprotein 39 in rheumatoid inflammatory and peripheral blood monocyte-derived macrophages." *Exp Cell Res*, 1997: 46-54.

Kozin, SV, Y Boucher, DJ Hicklin, P Bohlen, RK Jain, and HD Suit. "Vascular endothelial growth factor receptor-2-blocking antibody potentiates radiation-induced long-term control of human tumor xenografts." *Cancer Res*, 2001: 39-44.

Kreisl, TN, et al. "Phase II trial of single-agent bevacizumab followed by bevacizumab plus irinotecan at tumor progression in recurrent glioblastoma." *J Clin Oncol*, 2009: 740-745.

Kzhyshkowska, J, A Gratchev, and S Goerdt. "Human chitinases and chitinase-like proteins as indicators for inflammation and cancer." *Biomark Insights*, 2007: 128-146.

Lal, A, et al. "A public database for gene expression in human cancers." *Cancer Res*, 1999: 5403-5407.

Lambeng, N, et al. "Vascular endothelial-cadherin tyrosine phosphorylation in angiogenic and quiescent adult tissues." *Circ Res*, 2005: 384-391.

Lee, CG, and JA Elias. "Role of breast regression protein-39/YKL-40 in asthma and allergic responses." *Allergy Asthma Immunol Res*, 2010: 20-27.

Lee, CG, et al. "Role of breast regression protein 39 (BRP-39)/chitinase 3-like-1 in Th2 and IL-13–induced tissue responses and apoptosis." *J Exp Med*, 2009: 1149-1166.
Lee, J, et al. "Tumor stem cells derived from glioblastomas cultured in bFGF and EGF more closely mirror the phenotype and genotype of primary tumors than do serum-cultured cell lines." *Cancer Cell*, 2006: 391-403.
Létuvé, S, et al. "YKL-40 is elevated in patients with chronic obstructive pulmonary disease and activates alveolar macrophages." *J Immunol*, 2008: 5167-5173.
Li, HF, JS Kim, and T Waldman. "Radiation-induced Akt activation modulates radioresistance in human glioblastoma cells." *Radiat Oncol*, 2009: 1-10.
Lin, MI, J Yu, Murata T, and WC Sessa. "Caveolin-1-deficient mice have increased tumor microvascular permeability, angiogenesis, and growth." *Cancer Res*, 2007: 2849-2856.
Liu, C, et al. "Prostate-specific membrane antigen directed selective thrombotic infarction of tumors." *Cancer Res*, 2002: 5470-5475.
Liu, J, et al. "PDGF-D improves drug delivery and efficacy via vascular normalization, but promotes lymphatic metastasis by activating CXCR4 in breast cancer." *Clin Cancer Res*, 2011: 3638-3648.
Liu, XM, et al. "Clinical significance of vasculogenic mimicry in human gliomas." *J Neurooncol*, 2011: 173-179.
Lorger, M, JS Krueger, M O'Neal, K Staflin, and B Felding-Habermann. "Activation of tumor cell integrin alphavbeta3 controls angiogenesis and metastatic growth in the brain." *Proc Natl Acad Sci U S A*, 2009: 10666-10671.
Luo, Y, FA High, JA Epstein, and GL Radice. "N-cadherin is required for neural crest remodeling of the cardiac outflow tract." *Dev Biol*, 2006: 517-528.
Malinda, KM, L Ponce, HK Kleinman, LM Shackelton, and AJ Millis. "Gp38k, a protein synthesized by vascular smooth muscle cells, stimulates directional migration of human umbilical vein endothelial cells." *Exp Cell Res*, 1999: 168-173.
Mancuso, MR, et al. "Rapid vascular regrowth in tumors after reversal of VEGF inhibition." *J Clin Invest*, 2006: 2610-2621.
Manegold, C. "Bevacizumab for the treatment of advanced non-small-cell lung cancer." *Expert Rev Anticancer Ther*, 2008: 689-699.
Maniotis, AJ, et al. "Vascular channel formation by human melanoma cells in vivo and in vitro: vasculogenic mimicry." *American Journal of Pathology*, 1999: 739-752.
Matsuura, H, et al. "Role of breast regression protein-39 in the pathogenesis of cigarette smoke-induced inflammation and emphysema." *Am J Respir Cell Mol Biol*, 2011: 777-786.
Millauer, B, et al. "Dominant-negative inhibition of Flk-1 suppresses the growth of many tumor types in vivo." *Cancer Res*, 1996: 1615-1620.
Miller, K, et al. "Paclitaxel plus bevacizumab versus paclitaxel alone for metastatic breast cancer." *N Engl J Med*, 2007: 2666-2676.
Minn, AJ, et al. "Genes that mediate breast cancer metastasis to lung." *Nature*, 2005: 518-524.
Nakamura, Y, et al. "Role of protein tyrosine phosphatase 1B in vascular endothelial growth factor signaling and cell-cell adhesions in endothelial cells." *Circ Res*, 2008: 1182-1191.
Neufeld, G, T Cohen, S Gengrinovitch, and Z Poltorak. "Vascular endothelial growth factor (VEGF) and its receptors." *FASEB J*, 1999: 9-22.
Nghiemphu, PL, et al. "Bevacizumab and chemotherapy for recurrent glioblastoma: a single-institution experience." *Neurology*, 2009: 1217-1222.
Nigro, JM, et al. "Integrated array-comparative genomic hybridization and expression array profiles identify clinically relevant molecular subtypes of glioblastoma." *Cancer Res*, 2005: 1678-86.

Norden, AD, et al. "Bevacizumab for recurrent malignant gliomas: efficacy, toxicity, and patterns of recurrence." *Neurology*, 2008: 779-787.

Norden, AD, J Drappatz, and PY Wen. "Antiangiogenic therapies for high-grade glioma." *Nat Rev Neurol*, 2009: 610-620.

Nyirkos, P, and EE Golds. "Human synovial cells secrete a 39 kDa protein similar to a bovine mammary protein expressed during the non-lactating period." *Biochem J*, 1990: 265-268.

Orlova, VV, M Economopoulou, F Lupu, S Santoso, and T Chavakis. "Junctional adhesion molecule-C regulates vascular endothelial permeability by modulating VE-cadherin-mediated cell-cell contacts." *J Exp Med*, 2006: 2703-2714.

Pàez-Ribes, M, et al. "Antiangiogenic therapy elicits malignant progression of tumors to increased local invasion and distant metastasis." *Cancer Cell*, 2009: 220-231.

Paik, JH, et al. "Sphingosine 1-phosphate receptor regulation of N-cadherin mediates vascular stabilization." *Genes Dev*, 2004: 2392-2403.

Pelloski, CE, et al. "Prognostic associations of activated mitogen-activated protein kinase and Akt pathways in glioblastoma." *Clin Cancer Res*, 2006: 3935-3941.

Pelloski, CE, et al. "YKL-40 expression is associated with poorer response to radiation and shorter overall survival in glioblastoma." *Clin Cancer Res*, 2005: 3326–3334.

Pettersson, A, et al. "Heterogeneity of the angiogenic response induced in different normal adult tissues by vascular permeability factor/vascular endothelial growth factor." *Lab Invest*, 2000: 99-115.

Phillips, HS, et al. "Molecular subclasses of high-grade glioma predict prognosis, delineate a pattern of disease progression, and resemble stages in neurogenesis." *Cancer Cell*, 2006: 157-173.

Ping, YF, and XW Bian. "Consice review: Contribution of cancer stem cells to neovascularization." *Stem Cells*, 2011: 888-894.

Prewett, M, et al. "Antivascular endothelial growth factor receptor (fetal liver kinase 1) monoclonal antibody inhibits tumor angiogenesis and growth of several mouse and human tumors." *Cancer Res*, 1999: 5209-5218.

Quadri, SK. "Cross talk between focal adhesion kinase and cadherins: role in regulating endothelial barrier function." *Microvasc Res*, 2012: 3-11.

Rathcke, CN, I Raymond, C Kistorp, P Hildebrandt, J Faber, and H Vestergaard. "Low grade inflammation as measured by levels of YKL-40: association with an increased overall and cardiovascular mortality rate in an elderly population." *Int J Cardiol*, 2010: 35-42.

Rathcke, CN, JS Johansen, and H Vestergaard. "YKL-40, a biomarker of inflammation, is elevated in patients with type 2 diabetes and is related to insulin resistance." *Inflamm Res*, 2006: 53-59.

Recklies, AD, C White, and H Ling. "The chitinase 3-like protein human cartilage glycoprotein 39 (HC-gp39) stimulates proliferation of human connective-tissue cells and activates both extracellular signal-regulated kinase- and protein kinase B-mediated signalling pathways." *Biochem J*, 2002: 119–126.

Rehli, M, SW Krause, and R Andreesen. "Molecular characterization of the gene for human cartilage gp-39 (CHI3L1), a member of the chitinase protein family and marker for late stages of macrophage differentiation." *Genomics*, 1997: 221-225.

Renkema, GH, et al. "Chitotriosidase, a chitinase, and the 39-kDa human cartilage glycoprotein, a chitin-binding lectin, are homologues of family 18 glycosyl hydrolases secreted by human macrophages." *Eur J Biochem*, 1998: 504-509.

Ricci-Vitiani, L, et al. "Tumour vascularization via endothelial differentiation of glioblastoma stem-like cells." *Nature*, 2010: 824-828.
Richert, MM, et al. "Metastasis of hormone-independent breast cancer to lung and bone is decreased by alpha-difluoromethylornithine treatment." *Breast Cancer Res*, 2005: 819-827.
Ringsholt, M, EV Høgdall, JS Johansen, PA Price, and LH Christensen. "YKL-40 protein expression in normal adult human tissues--an immunohistochemical study." *J Mol Histol*, 2007: 33-43.
Saidi, A, et al. "Experimental anti-angiogenesis causes upregulation of genes associated with poor survival in glioblastoma." *Int J Cancer*, 2008: 2187-2198.
Sandler, A, et al. "Paclitaxel–Carboplatin Alone or with Bevacizumab for Non–Small-Cell Lung Cancer." *N Engl J Med* , 2006: 2542-2550.
Schultz, NA, and J Johansen. "YKL-40—A Protein in the Field of Translational Medicine: A Role as a Biomarker in Cancer Patients? ." *Cancers*, 2010: 1453-1491.
Scully, S, et al. "Transdifferentiation of glioblastoma stem-like cells into mural cells drives vasculogenic mimicry in glioblastomas." *J Neurosci*, 2012: 12950-12960.
Shackelton, LM, DM Mann, and AJT Millis. "Identification of a 38-kDa heparin- binding glycoprotein (gp38k) in differentiating vascular smooth muscle cells as a member of a group of proteins associated with tissue remodelling." *J Biol Chem*, 1995: 13076-13083.
Shalaby, F, et al. "Failure of blood-island formation and vasculogenesis in Flk-1-deficient mice." *Nature*, 1995: 62-66.
Shao, R, and X Guo. "Human microvascular endothelial cells immortalized with human telomerase catalytic protein: a model for the study of in vitro angiogenesis." *Biochem Biophys Res Commun*, 2004: 788-794.
Shao, R, et al. "YKL-40, a secreted glycoprotein, promotes tumor angiogenesis." *Oncogene*, 2009: 4456-4468.
Sharif, M, R Granell, J Johansen, S Clarke, C Elson, and JR Kirwan. "Serum cartilage oligomeric matrix protein and other biomarker profiles in tibiofemoral and patellofemoral osteoarthritis of the knee." *Rheumatology*, 2006: 522-526.
Shay-Salit, A, et al. "VEGF receptor 2 and the adherens junction as a mechanical transducer in vascular endothelial cells." *Proc Natl Acad Sci U S A*, 2002: 9462-9467.
Shrivastava-Ranjan, P, PE Rollin, and CF Spiropoulou. "Andes virus disrupts the endothelial cell barrier by induction of vascular endothelial growth factor and downregulation of VE-cadherin." *J Virol*, 2010: 11227-11234.
Soda, Y, et al. "Transdifferentiation of glioblastoma cells into vascular endothelial cells." *Proc Natl Acad Sci U S A*, 2011: 4274-4280.
Sood, AK, et al. "The clinical significance of tumor cell-lined vasculature in ovarian carcinoma: implications for anti-vasculogenic therapy." *Cancer Biol Ther*, 2002: 661-664.
Sottoriva, A, et al. "Intratumor heterogeneity in human glioblastoma reflects cancer evolutionary dynamics." *Proc Natl Acad Sci U S A*, 2013: 4009-4014.
Stockmann, C, et al. "Deletion of vascular endothelial growth factor in myeloid cells accelerates tumorigenesis." *Nature*, 2008: 814-818.
Sun, J, et al. "Inhibiting angiogenesis and tumorigenesis by a synthetic molecule that blocks binding of both VEGF and PDGF to their receptors." *Oncogene*, 2005: 4701-4709.
Tanwar, MK, MR Gilbert, and EC Holland. "Gene expression microarray analysis reveals YKL-40 to be a potential serum marker for malignant character in human glioma." *Cancer Res*, 2002: 4364-4368.

Taura, D, et al. "Induction and isolation of vascular cells from human induced pluripotent stem cells--brief report." *Arterioscler Thromb Vasc Biol*, 2009: 1100-1103.
Timke, C, et al. "Combination of vascular endothelial growth factor receptor/platelet-derived growth factor receptor inhibition markedly improves radiation tumor therapy." *Clin Cancer Res*, 2008: 2210-2219.
Tomasek, JJ, G Gabbiani, B Hinz, C Chaponnier, and RA Brown. "Myofibroblasts and mechano-regulation of connective tissue remodelling." *Nat Rev Mol Cell Biol*, 2002: 349-363.
Van Meir, EG, CG Hadjipanayis, AD Norden, H Shu, PY Wen, and JJ Olson. "Exciting New Advances in Neuro-Oncology: The Avenue to a Cure for Malignant Glioma." *CA Cancer J Clin*, 2010: 166–193.
Verhaak, RG, KA Hoadley, E Purdom, and et al. "Integrated genomic analysis identifies clinically relevant subtypes of glioblastoma characterized by abnormalities in PDGFRA, IDH1, EGFR, and NF1." *Cancer Cell*, 2010: 98-110.
Verhoeff, JJ, et al. "Concerns about anti-angiogenic treatment in patients with glioblastoma multiforme." *BMC Cancer*, 2009: 1-9.
Vestweber, D. "VE-cadherin: the major endothelial adhesion molecule controlling cellular junctions and blood vessel formation." *Arterioscler Thromb Vasc Biol*, 2008: 223-232.
Volck, B, et al. "Studies on YKL-40 in knee joints of patients with rheumatoid arthritis and osteoarthritis. Involvement of YKL-40 in the joint pathology." *Osteoarthritis Cartilage*, 2001: 203-214.
Volck, B, et al. "YKL-40, a mammalian member of the chitinase family, is a matrix protein of specific granules in human neutrophils." *Proc Assoc Am Physicians*, 1998: 351-360.
Volck, B, K Ostergaard, JS Johansen, C Garbarsch, and PA Price. "The distribution of YKL-40 in osteoarthritic and normal human articular cartilage." *Scand J Rheumatol*, 1999: 171-179.
Wang, R, et al. "Glioblastoma stem-like cells give rise to tumour endothelium." *Nature*, 2010: 829-833.
Weis, S, J Cui, L Barnes, and D Cheresh. "Endothelial barrier disruption by VEGF-mediated Src activity potentiates tumor cell extravasation and metastasis." *J Cell Biol*, 2004: 223-229.
Wen, PY, and S Kesari. "Malignant gliomas in adults." *N Engl J Med*, 2008: 492-507.
Wheeler-Jones, C, R Abu-Ghazaleh, R Cospedal, RA Houliston, J Martin, and I Zachary. "Vascular endothelial growth factor stimulates prostacyclin production and activation of cytosolic phospholipase A2 in endothelial cells via p42/p44 mitogen-activated protein kinase." *FEBS Lett*, 1997: 28-32.
Wick, W, M Weller, M van den Bent, and R Stupp. "Bevacizumab and Recurrent Malignant Gliomas: A European Perspective." *J Clin Oncol*, 2010: 188-199.
Wijelath, ES, et al. "Novel vascular endothelial growth factor binding domains of fibronectin enhance vascular endothelial growth factor biological activity." *Circ Res*, 2002: 25-31.
Winkler, F, et al. "Kinetics of vascular normalization by VEGFR2 blockade governs brain tumor response to radiation: role of oxygenation, angiopoietin-1, and matrix metalloproteinases." *Cancer Cell*, 2004: 553-563.
Wurmser, AE, et al. "Cell fusion-independent differentiation of neural stem cells to the endothelial lineage." *Nature*, 2004: 350-356.
Yamashita J, Itoh, H, et al. "Flk1-positive cells derived from embryonic stem cells serve as vascular progenitors." *Nature*, 2000: 92-96.
Yan, W, and R Shao. "Transduction of a mesenchyme-specific gene periostin into 293T cells induces cell invasive activity through epithelial-mesenchymal transformation." *J Biol Chem*, 2006: 19700-19708.

Yan, W, B Bentley, and R Shao. "Distinct angiogenic mediators are required for basic fibroblast growth factor- and vascular endothelial growth factor-induced angiogenesis: the role of cytoplasmic tyrosine kinase c-Abl in tumor angiogenesis." *Mol Biol Cell*, 2008: 2278-2288.

Yan, W, QJ Cao, RB Arenas, B Bentley, and R Shao. "GATA3 inhibits breast cancer metastasis through the reversal of epithelial-mesenchymal transition." *J Biol Chem*, 2010: 14042-14051.

Yancopoulos, GD, M Klagsbrun, and J Folkman. "Vasculogenesis, angiogenesis, and growth factors: ephrins enter the fray at the border." *Cell*, 1998: 661-664.

Yancopoulos, GD, S Davis, NW Gale, JS Rudge, SJ Wiegand, and J Holash. "Vascular-specific growth factors and blood vessel formation." *Nature*, 2000: 242-248.

Yang L, Soonpaa MH, Adler ED, Roepke TK, Kattman SJ, Kennedy M, Henckaerts E, Bonham K, Abbott GW, Linden RM, Field LJ, Keller GM. "Human cardiovascular progenitor cells develop from a KDR+ embryonic-stem-cell-derived population." *Nature*, 2008: 524-528.

Yonenaga, Y, et al. "Absence of smooth muscle actin-positive pericyte coverage of tumor vessels correlates with hematogenous metastasis and prognosis of colorectal cancer patients." *Oncology*, 2005: 159-166.

Yue, WY, and ZP Chen. "Does vasculogenic mimicry exist in astrocytoma?" *J Histochem Cytochem*, 2005: 997-1002.

Zhang, Z, KG Neiva, MW Lingen, LM Ellis, and JE Nör. "VEGF-dependent tumor angiogenesis requires inverse and reciprocal regulation of VEGFR1 and VEGFR2." *Cell Death Differ*, 2010: 499-512.

Zhao, J, F Yan, H Ju, J Tang, and J Qin. "Correlation between serum vascular endothelial growth factor and endostatin levels in patients with breast cancer." *Cancer Lett*, 2004: 87-95.